Supercapacitor Electrodes, Life Cycle Assessment of lithium-ion and sodium-ion battery packs
Innovation report

Jonathan Wellings

Doctor of Engineering in Sustainable Materials

WMG
University of Warwick
CDT for Sustainable Materials and Manufacturing

Ricardo PLC

30/09/2021

Executive summary

Transport sits as an essential industry within modern human society, both for industry and communities, although it also sits as one of the greatest contributors to global environmental impacts, which fuels to disastrous changes in our climate. This has encouraged the development of electric vehicles to replace the petrol and diesel vehicles that currently populate the globe's roads. While this can only be part of a greater effort to reduce emissions from the transport sector, many of the critical technologies used in electric vehicles can also be applicable in other applications, such as with trains and other public transport solutions, alongside stationary energy storage units.

One such technology is the energy storage device used in electric vehicles, with both batteries and supercapacitors being examined in this report, driven by industrial interest from the two sponsor companies of this EngD, Johnson Matthey Plc and Ricardo Plc. While batteries offer high energy capacities but low power outputs within energy storage solutions, supercapacitors offer high power outputs but at the cost of smaller energy capacities in comparison to batteries.

Working with the supercapacitors, different attributes of the electrodes were examined to see how different elements affected their performance, with the binders used, mixing methodologies of the inks and electrode wet thicknesses being looked at in a large number of lab scale tests. This was motivated by the desire of sponsor Johnson Matthey to examine supercapacitor materials and production methods for new innovations. Over 100 cells were made and tested to look at these different attributes. This testing showing that a mixture of Carboxy-Methyl Cellulose (CMC) and Styrene–Butadiene Rubber (SBR) binders offered better specific capacity compared with Poly-Vinylidene DiFluoride (PVDF) binders within an active carbon-based electrode.

The mixing methodologies differed, with one method using a high-speed dispersion mixer and the other using a high torque kneader mixer, with the two methods offered a mix of results. Both varied in how they affected the supercapacitor performance, with one offering benefits over the other depending on the wet thicknesses of each electrode, with the high torque mixing methodology showing better performance at the lower wet thicknesses. The wet thickness investigations suggested there was minimal benefit to increasing wet

thicknesses due to the minimal increase in capacity retention compared with the increase in required electrode material. This is also an issue given the higher failure rates the higher thicknesses suffered during testing in comparison to the lower thicknesses. SEM examination eventually determined this was likely due to binder pooling on the surface of the thicker electrodes.

The direction of the degree ultimately led away from supercapacitor research and into research on battery production, with an area of interest being the environmental impacts their production had and how different battery chemistries influenced these impacts. To examine the environmental impacts of different battery chemistries, two models were constructed within openLCA, a dedicated life cycle assessment (LCA) software package for life cycle assessments. One of these models examined a lithium-ion battery pack and the other examined a sodium-ion pack, using information on the production of these packs from literature and including all the processes to produce a 60-kWh capacity pack for use in electric vehicles. The models were encouraged by this project's sponsor Ricardo PLC, who showed interest in this area and the data that came from these models, which could benefit their operations.

These models showed that the sodium-ion battery packs produced higher environmental impacts than their lithium-ion counterparts, with between 18-65% increases over lithium-ion depending on the impact category, with sodium-ion's lower specific capacity being a primary cause of this.

Producing these models did show issues in the use of the openLCA software, such as complex navigation to find certain values within the model and complexity of exported data, with queries raised on how to improve the user experience within this software. This led to the development of three tools, two which modified the lithium-ion model to allow for different scenarios to be examined, while the other processes the data produced by the model and presented it in a clean and readable manner. This not only needed an understanding of programming languages, with Python ultimately being used, needed to produce the tools but also a wide understanding of the battery manufacturing process, with processes and sources of materials being among the most vital areas to examine. This led to the gathering of a wide set of data, which covered active material inputs, national electricity

generation mixes and locations of material production among some of the relevant areas, all of which were needed to fuel the functions of the tools.

These tools offered a range of functions, including changes to distance, electricity and battery chemistry data within the model, alongside data processing of the final data on environmental impacts. These were useful for working with the model and improved how a user interacted with it and its data. They allowed for several beneficial comparisons between changes to the lithium-ion battery model and their impacts, including re-location of key material or production location, as well as changes to the cathode active material. They also improved the speed of locating key impact data for comparisons like these. They also open the door for further tools and improvements, such as operation with other LCA software and an expansion of the databases the tools use.

Acknowledgments

I have been supported by a wide range of people across the course of the EngD and I absolutely must thank them for their assistance for the past four or so years.

Firstly, I must thank my supervisors Stuart Coles, David Greenwood, Kerry Kirwan, Julian Dunn, Leon Rosario, and James Cookson for their support at different stages of my EngD and MSc, providing me with guidance across both degrees. I feel that I have genuinely improved my professionalism and mindset thanks to their help and advice, which will help me in the future in opportunities in academia and industry. I would also like to thank Alex Roberts, Rohit Bhagat, and Jenny Mash for the work I conducted on supercapacitors with them and its contribution to my EngD. I would also like to thank the companies Johnson Matthey and Ricardo PLC, for their financial support of this project and the support of their employees as my industrial supervisors. For their support of me during some of the toughest parts of my EngD, I must also thank Sue Gibson and Helen Luckhurst from their positions as the administrators of the Centre for Doctoral Training. Their support and encouragement were exactly what I needed at those points in my degree, and I cannot thank them enough.

My families support for me has been unmatched throughout this degree, with my parents Richard and Deborah giving me the best encouragement anyone could ask for. My brother Adam has also been an excellent help, offering a new perspective within engineering on some of my work helping me move forward. My sister Bryony has also been a massive help, supporting me during this degree. I would also like to thank both my grandparents Michael and Ann for their support, as well as my uncles and aunts, Marian, Andrea, and Alan for their encouragement during the degree.

During my time at the Centre for Doctoral Training, I was also supported by several veteran EngD and PhD researchers and staff, with Lavinia, Christina, Dan, Ronny, Felipe, Pete, Victoria, Joko, and Romeo being some of the researchers that greatly helped me during my EngD, both as colleagues and friends. I would also like to thank the wide range of other EngD and PhD students that joined the CDT and worked with me during my EngD. They were of immense help and their support helped me through my EngD. So, in no particular order, I would like to thank Sam, Adam, Konstantinos, Martin, Chris, Craig, Evé, Keiron, Mike,

Michael, Dave, Matt, and Shaf as some of the many people who helped me throughout this degree, as both friends and colleagues throughout my EngD and MSc.

This degree has been the most difficult point in my life so far, even excluding the global pandemic the occurred part way through it. Despite its difficulty, I have greatly enjoyed my time completing the degree and I look forward to the future challenges I may face in work or in life.

Thank you for taking your time to read this report.

Jonathan Wellings

Author declaration

I declare that the work presented is my own and has not been submitted for any other award. All sources of published information have been acknowledged in the text using references and bibliography.

Jonathan Wellings

Publications

Wellings, J, Greenwood, D, Coles, S, 2021, Understanding the future impact of electric vehicles on society, Vehicles, 3, pp851-871, Available from: https://doi.org/10.3390/vehicles3040051

Table of contents

List of figures

List of tables

Definitions and Abbreviations

BMS – Battery Management System

CDT – Centre for Doctoral Training

CMC – Carboxy-Methyl Cellulose

DRC – Democratic Republic of the Congo

EngD – Engineering Doctorate

EPSRC – Engineering and Physical Sciences Research Council

FE-SEM – Field Emission Scanning Electron Microscope

Hydro – Hydroelectric energy generation

IHP – Inner Helmholtz Plane

LCA – Life Cycle Assessment

LiNMC – Lithium Nickel-Manganese-Cobalt Oxide

NMP - *N*-Methyl-2-Pyrrollidone

OHP – Outer Helmholtz Plane

PAA – Poly-Acrylic Acid

PLC – Public Limited Company

PVDF – Poly-Vinylidene DiFluoride

SBR – Styrene–Butadiene Rubber

SEM – Scanning Electron Microscope

UK – United Kingdom

WMG – Warwick Manufacturing Group

1. Introduction

1.1 Project motivation

Electrical storage devices are becoming increasingly prevalent within various industries, but especially within the automotive industry as increasing numbers of manufacturers begin production of electric vehicles. With sales of electric vehicles rising considerably over the last decade, this has created significant interest in development of new and improved energy storage methods, with batteries and supercapacitors being among the most promising (International Energy Agency (IEA), 2020b). Two companies that have shown interest in these areas are Johnson Matthey, a chemical production company, and Ricardo PLC, an engineering consultancy company. Within energy storage solutions, Johnson Matthey produces key material used in different energy storage units, while Ricardo PLC has designs and simulates batteries within the automotive industry (Ricardo PLC, 2021) (Johnson Matthey, 2021). Johnson Matthey showed interest in gaining new technologies relating to supercapacitors, with variations on the material used and methods of producing supercapacitors being of particular interest. Meanwhile, Ricardo PLC showed interest in new means to examine battery packs and how they impacted the environment, with simulations of these impacts being of interest to provide knowledge to assist their consultancy work.

This EngD has developed as two distinct parts, with the degree initially examining supercapacitors with assistance from Johnson Matthey, which was intended to be the focus for the entire degree. By the end of the initial year of the degree, Johnson Matthey chose to withdraw support over the increased pace of development for supercapacitors, with an EngD degree being unable to keep pace with the developments in Industrial laboratories. Ricardo PLC agreed to step in as a new sponsor company to examine the related but new area within energy storage solutions, to examine battery packs and their environmental impacts through life cycle assessments.

1.2 Structure of the EngD

Within these stipulations set by the sponsor companies, the first stage was to conduct literature reviews to examine where innovation could be produced from industrial need or

holes in the understanding of the relevant areas. The first literature review examined supercapacitors, along with their composition and different variations within industry. This revealed a lack of information on how different aspects of the electrode production affected the supercapacitor's performance, from ingredients to production methods being included among these. This led to an examination of binders, mixing methods and electrode thicknesses being conducted, as these areas had less information on them compared with other aspects, such as active materials.

After the change in research area, as detailed above in section 1.1, a second literature review was undertaken, to examine life cycle assessment methodologies, along with related impacts in the electric vehicle market. This revealed the need to further examine battery packs and their impacts though life cycle assessments but also highlighted some issues with the dedicated software that can be used to produce them. With many of them being complex and requiring extensive training to use, there was a clear gap in the market for a means to better interact with the software and improve the user experience, which should assist in convincing companies to adopt LCA methodologies.

These literature review led to a range of smaller projects undertaken as part of the EngD degree this innovation report will cover. These include:

1) Production and comparison of supercapacitors, with variable binders, wet thicknesses, and mixing methods. Discovering an optimal electrode composition and how certain conditions affect the electrodes would be beneficial to industry.

2) Production of lithium-ion and sodium-ion battery pack life cycle assessment models for comparison with each other and literature data on their environmental impacts. Models for battery pack productions would not only provide essential data but also allow for a breakdown of the processes to examine where certain impacts are produced throughout the manufacturing process.

3) Development of Python based tools to modify life cycle assessment models, allowing for locations of key materials and the manufacturing centre for the battery pack to be changed when needed, as well as another tool for modifying battery chemistry. This would work to improve the user experience of working with life cycle assessment

models, making LCA work more cost effective by reducing time, as well as expanding the groups that could work with LCA models.

4) Development of a Python based tool to process exported LCA data from the models and present it in an easier to understand format. As with the modification tools, this would improve the value of LCA software by reducing the time needed to process the data, along with giving users a base to present data to inform their decisions and convince others within industry.

From these projects, several submissions were produced, with figure 1.1 displaying them and how they fit into the overall portfolio of this EngD:

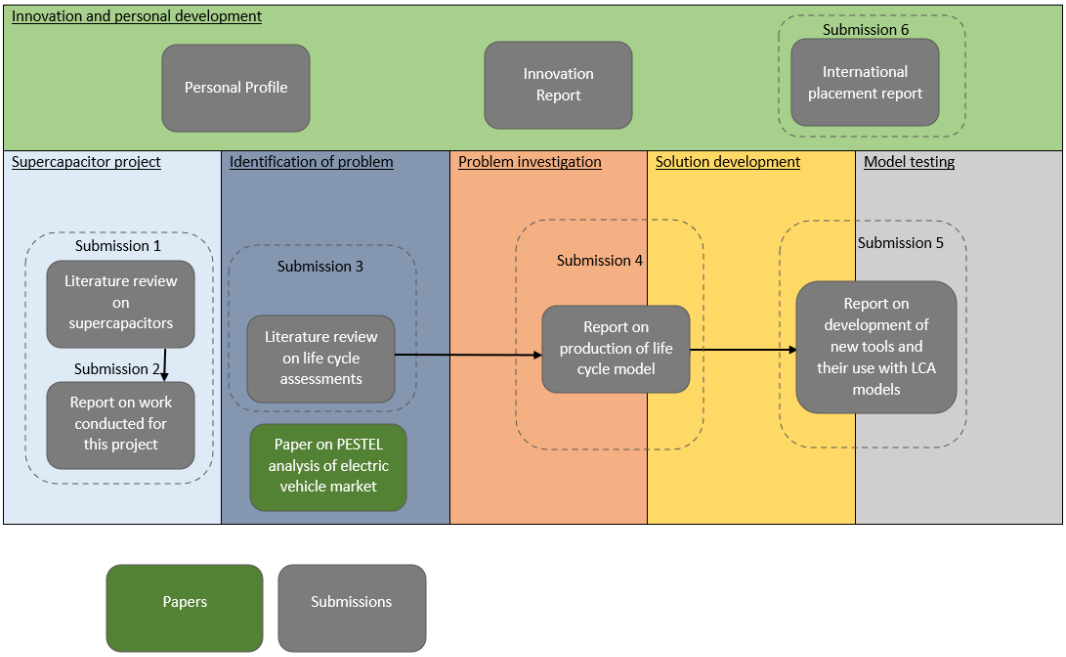

Figure 1.1: Overview of EngD portfolio, showing development of the projects and the placement of each submission within the portfolio

1.3 Importance of sustainability

Rapid changes in climate around the globe have spurred the nations of the world to begin to tackle the impacts they produce, particularly carbon dioxide emissions. This has been supported by the Paris agreement, signed in 2015 to set targets for nations to achieve, which includes global emissions being carbon neutral by 2050 (United Nations (UN), 2019).

This is in order to limit global temperature rises to below 2 ^{o}C above pre-industrial levels (United Nations (UN), 2019). These targets can be achieved by the nations of the world, with the agreement setting out frameworks to assist them, including financial assistance and development of technology. This helps promote sustainability within many nations, some of whom currently lack the means to re-structure their nations to achieve these goals.

With ever increasing concerns on the impact humanity has on the environment, examining new technologies and methodologies to lessen, or even reverse, these impacts are paramount to reduce these concerns and tackle the issues that drive them. Modern manufacturing of goods is currently highly reliant on virgin materials and increasing demand from both developed and developing economies for goods such as electronic and vehicles only exacerbates the issues that reliance on a finite supply of virgin materials has. The finite amount of these virgin materials inherently means not only a large environmental cost from producing them from their base materials, such as metal ores, but also climbing economic costs as supplies of these materials are depleted. Coupled with many of the major production centres for a substantial number of these materials being dependent on fossil fuels, and you see an escalating rate of emissions into the environment, along with the devastating impacts these emissions have globally. The recent deluge of floods, heatwaves, and thawing tundra have been increasing in severity due to the environmental emissions of human society (United Nations (UN), 2021). While cycles of global warming and cooling can be seen by studying fossil records, the current evidence shows that humanity has accelerated the rate of climate change substantially (Masson-Delmotte et al., 2021).

Therefore, reducing dependence on virgin materials and rebuilding business and economic models to minimise environmental impacts where they can in their life cycle is a crucial set of policies that should be implemented. This would allow for nation to meet some of the sustainability needs of their people, which can be defined as “meeting the needs of the present without compromising the ability of future generations to meet their own needs” as defined by the UN Brundtland Commission (United Nations (UN), n.d.). A reduction of virgin materials would also assist in shifting businesses into circular economies, by reducing a group’(Kirchherr, Reike and Hekkert, 2017)

Unfortunately, many of these policies run into opposition within businesses, with concerns about cost to change their practices with few opportunities to economically benefit in the

short term, along with engrained mentalities on how businesses are run. This is partly as many policies are focused purely on environmental sustainability, although this is perfectly understandable given the urgent nature of climate change. A newer way of thinking on sustainability in business, developed within the last few decades, which includes three major pillars of sustainability, often referred to as the triple bottom line (Elkingson, 1997):

1) Environmental sustainability, to ensure that a process conserves natural resources and protects ecosystems around the globe. One means that can achieve this is by working to eliminate or reduce the impacts the production of a product or providing of a service has on the environment, by reducing waste emissions of a process or eliminating the need for finite resources from it. This also works towards some of the 17 goals for sustainable development set out by the United Nations in 2015, with climate action, life on land and below water being covered by environmental sustainability (United Nations (UN), 2022).

2) Economic sustainability, that a process can sustain economic success and bring profits into the business and market. It is one of the important, if not the most important, aspect of a successful business, although in sustainable business it cannot stand above the other two pillars of sustainability. As with environmental sustainability, multiple goals of the UN's sustainable development programs contribute to economic sustainability, including Industry, innovation and infrastructure, along with Decent work and economic growth (United Nations (UN), 2022)

3) Social sustainability, although more difficult to measure as it challenging to quantify it, often examines how the society and individuals benefit from the business. This can range from a supply of jobs a business provides to a community, to a product supply chain avoiding socially unacceptable practices. Within the UN's sustainable development goals, social sustainability can be covered by several of the statements set out, including quality education, gender equality, along with peace, justice and strong institutions (United Nations (UN), 2022)

Within this definition, economic sustainability is well understood. As mentioned, it is the backbone of any successful business and can be easily quantified with various measures, such as profits and investments into the business or other areas. Social and environmental sustainability are less well understood, with there being uncertainty on how to define social

sustainability. Efforts are being made through corporate social responsibility (CSR) reports being produced by several companies to communicate their social responsibility, which help manage their socially responsible activities and identifying future risks and opportunities in this area (Moravcikova, Stefanikova and Rypakova, 2015). Alongside CSR reporting, there has also been a push for the publication of Environmental, Social and Governance (ESG) scores of companies, although this has resulted in many different methodologies being used by companies to calculate these scores (Yoo and Managi, 2022). This can lead to misleading implications, especially when some companies focus on ESG information, while others focus on their activities and consequences(Yoo and Managi, 2022)

Environmental sustainability is better understood, although still struggles to be accepted into many businesses, sometimes due to the business's reliance on unsustainable resources and products, such as crude oil extraction. Innovations can be provided to improve the standing and applicability of environmental sustainability, while also minimising the negative impacts, or even adding bonuses, to the economic and social sustainability of a business. Circular economy is one such innovative concept that seeks to address some of these issues, with the retention of materials within industry through reuse and recycling offering potential economic and environmental benefits by reducing a reliance on raw materials (Martins-Rodrigues et al., 2020). It currently has several issues relating to industry, including the technical and economic viability of several recycling processes for key materials, such as lithium (Martins-Rodrigues et al., 2020).

Within current processes, including ones looking to transition to circular economy, there is a need to understand the magnitude of their impacts, as well as where they come from. Within production electric vehicle, one of the areas of most concern with environmental sustainability is the production of battery packs, which use a wide range of virgin materials and produce a variety of waste products. Examining the impacts these battery pack produce would be beneficial, especially with the rising demand for electric vehicles worldwide, which was part of the work conducted with Ricardo PLC. There were various parameters of interest in measuring how the battery production impacted the environment, including global warming potential (GWP), terrestrial acidification, fossil fuel depletion and metal depletion. Alongside this, to work to reduce these embedded emissions in battery packs,

industry needs accurate, reliable, and user-friendly software and tools to quantify these impacts. This led to further work to develop these tools in conjunction with Ricardo PLC.

1.4 Batteries, supercapacitors, and Life Cycle Assessment

Within the automotive industry, electric vehicles are increasingly becoming an important sector, with sales rising year upon year globally (International Energy Agency (IEA), 2020a). Innovations within the automotive industry are responsible for this area of the market existing and growing to the size it is today. Within this sector, energy storage is extremely important, as it determines the range, acceleration, cost, and recharging times of the vehicle. This has traditionally used lithium-ion batteries, due to their high energy density but recently newer developments have brought supercapacitors to be of greater interest to industry (Dutta et al., 2022). This is in part due to them promising a greater power output than the batteries, which could be useful in electric vehicles (Dutta et al., 2022)This has led them to be proposed to be integrated into electric vehicles with specific purposes, such as reclaiming energy during braking or granting extra power to the engine during acceleration (Horn et al., 2019). Some companies, such as the Aowei development company, have been supplying supercapacitors for transport solutions, demonstrating that there is industrial interest in supercapacitors in the EV industry (Horn et al., 2019).

Along with improvements to the energy storage methods of electric vehicles, there have also been innovations within how to assess the environmental impact they have, with LCA increasingly becoming a desirable method of assessment. There is a notable concern on how battery packs influence the overall impact the production of electric vehicles has, with their demand for difficult to produce and high purity materials being a major factor in this (Xu et al., 2020). Compared with vehicles that use internal combustion engines, while overall impacts tend to be lower for battery electric vehicles, their production creates larger impacts than internal combustion vehicles, with the battery production being a major contributor to this (European Environment Agency, 2018). Determining the values of key impacts in understandable units, including the carbon dioxide produced by the manufacturing process, is vital to inform policy makers on how to structure their policies and put in practical measures to counter or prevent these impacts.

1.4.1 Supercapacitors

Supercapacitors are a relatively new energy storage solution, with the technology often being considered as a mid-point between batteries and capacitors. This is due to them offering better power density, but lower energy storage compared with batteries of the same size, while offering the inverse compared with capacitors(Dutta et al., 2022) Supercapacitors are also a fairly young technology, especially when compared with batteries and capacitors, with the first patent appearing in 1957 (Samantara and Ratha, 2018). Supercapacitors comprise two electrodes separated by a porous material, placed in a cell with an appropriate electrolyte. The charged supercapacitors often rely on a phenomenon known as the electrochemical double layer, which uses the charged ions within the electrolyte to store energy along the electrode surfaces (González et al., 2016), with figure 1.2 displaying three models for this mechanism:

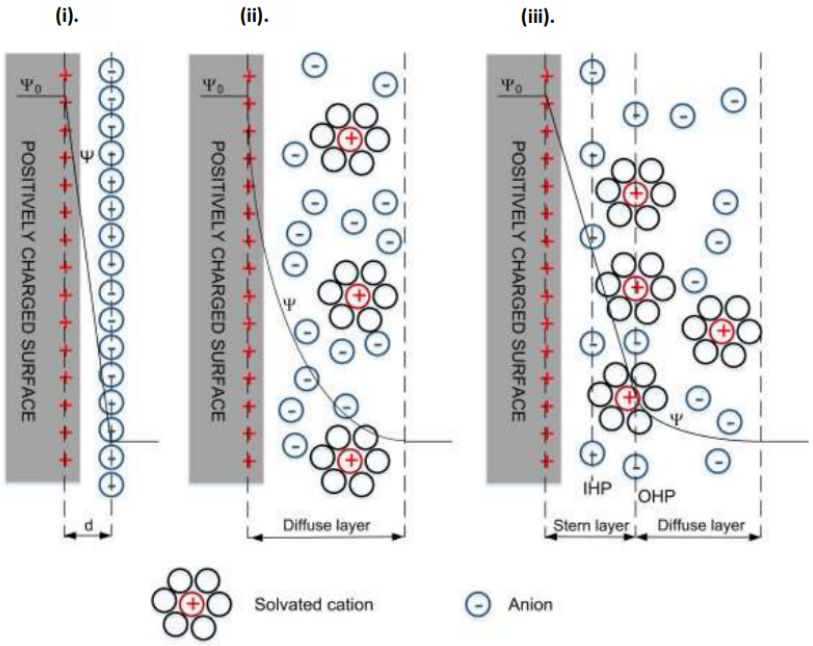

Figure 1.2: Diagrams of the three model for electrochemical double layer (i). Helmholtz model, (ii). Gouy-Chapman model, (iii). Stern Modification model (González et al., 2016)

As can be seen with figure 1.2, the Helmholtz model is the simplest of the three displayed, with the charged ion aligning parallel to the surface of the oppositely charged electrode at a set distance (González et al., 2016). The Gouy-Chapman model was developed later, which

includes a mix of charged ions the collect loosely to the electrode in an area known as the diffuse layer. The lack of a defined distance the layer exists at, as seen in the Helmholtz model, does present an issue for the Gouy-Chapman model, as it assumed the ions are points of energy (González et al., 2016). This would allow the impossibility of the ion centre to touch the electrode surface, which leads to the model overestimating the capacity. The Stern Modification offers an improvement to the Gouy-Chapman model, with elements of the Helmholtz model incorporated to solve the issue with the other model (González et al., 2016). This model includes the Diffuse lays, but also adds in the Stern layer comprising of the Inner Helmholtz Plane (IHP), which operates similarly to the layer described in the Helmholtz model, and Outer Helmholtz Plane (OHP), which has a mix of positively and negatively charged ions. The capacity of these models can be calculated with a set of equations shown below, with equation 1 representing the capacity of the Helmholtz model, equation 2 representing the Gouy-Chapman model and equation 3 the Stern modification (González et al., 2016):

$$C_H = \frac{\varepsilon_r \varepsilon_0}{d} \qquad \text{(Equation 1)}$$

$$C_{GC} = \frac{d\sigma_M}{d\varphi_0} = \sqrt{\frac{2z^2 e^2 n_i^0 \varepsilon_r \varepsilon_0}{kT}} \cosh\left(\frac{ze_0}{2kT}\right) \qquad \text{(Equation 2)}$$

$$\frac{1}{C_S} = \frac{1}{C_H} + \frac{1}{C_{GC}} \qquad \text{(Equation 3)}$$

The C units represent the capacity values for the various models, with ε_r representing the relative permittivity of the electrolyte, ε_0 the relative permittivity of a vacuum and d being the thickness of the layer, as seen in figure 1.2. For equation 2, z represents the ions charge, e the charge of the unit, n_i^0 represents the ions concentration in the electrolyte, T being the absolute temperature, k the Boltzmann constant, σ_M the charge density of the diffuse layer and φ_0 the potential of the electrode (González et al., 2016).

While these models give a good idea of the basic mechanisms of the electrochemical double layer, they assume a perfectly smooth electrode surface, which is simply not present in the electrodes produced for supercapacitors, which often use a range of porous materials (Heimböckel, Hoffmann and Fröba, 2019). There is a general idea available for how the double layer acts within the pores, although there does not appear to be a consensus on how it acts within micropores, which appears to be due to a lack of appropriate evidence to support one theory over another(Heimböckel, Hoffmann and Fröba, 2019)The general mechanism seems to be applicable to the pores as well, although testing has shown a non-linear relationship between the electrode surface area and the capacity of the electrode, which it is suggested is due to the limited space capable of storing the charged ions(Heimböckel, Hoffmann and Fröba, 2019) Figure 1.3 displays how the mechanism may function:

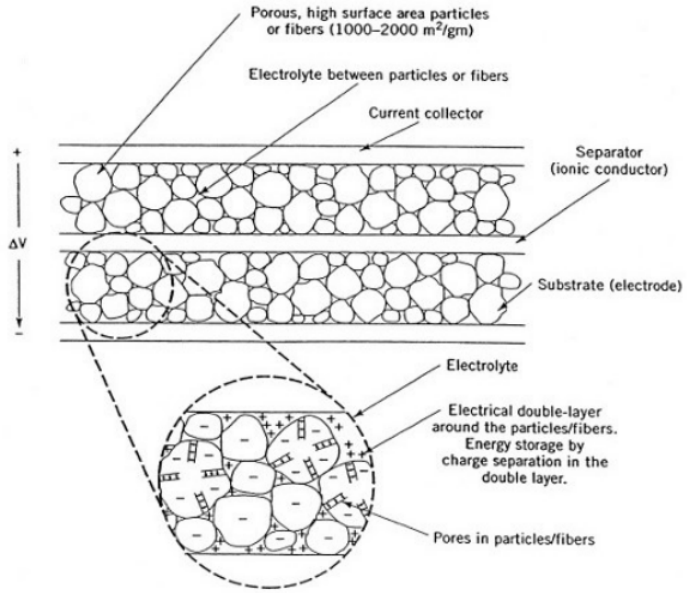

Figure 1.3: Diagram of supercapacitor electrodes and a close-up view of porous particle in the electrode (Lu and Dai, 2010)

An alternate mechanism used in energy storage for supercapacitor is pseudo-capacitance, which uses fast and reversible reactions on the electrode surfaces to store charge (Wang et al., 2017). Within pseudo-capacitance, three different mechanisms can be used, which includes underpotential deposition, redox pseudo-capacitance, and intercalation pseudo-

capacitance (Wang et al., 2017). The underpotential deposition relies on metal ions forming a charged monolayer on the surface of a metal electrode, while redox pseudo-capacitance utilises redox reactions between the electrode surface and a charged ion, such as H^+ (Wang et al., 2017). Intercalation pseudo-capacitance operates with charged ions entering the pores of an electrode materials (Augustyn, Simon and Dunn, 2014). These three mechanisms can be seen in figure 1.4:

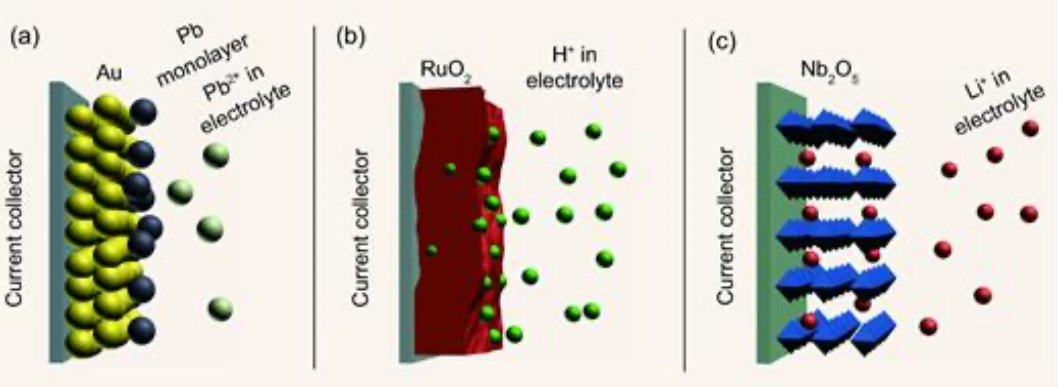

Figure 1.4: Diagrams of Pseudo-capacitance mechanisms, with (a) displaying underpotential deposition, (b) exhibiting redox pseudo-capacitance and (c) demonstrating intercalation pseudo-capacitance (Wang et al., 2017)

These mechanisms are used in some supercapacitor applications, as the supercapacitors that rely on the double layer mechanism cannot be used with alternating current, along with other issues. Pseudo capacitance supercapacitors do have their own weaknesses compared with their double layer counterparts, such as worse mechanical stability (Wu et al., 2017).

Supercapacitors comprise of two electrodes, a separator, and electrolyte contained in a packaging material (Wu, Feng and Cheng, 2014). Carbon based electrodes primarily use the electric double-layer mechanism to store energy, with the electrodes being mounted on metal current collectors (Wu, Feng and Cheng, 2014). Within the electrodes, graphite a common active material coupled with binders to hold the electrode together. As part of this, there potentially lies innovation within the electrode production, both in the methods of

production and the materials used in producing them, and how this affects the key attributes of the supercapacitors. The electrode inks offer an effective manufacturing method for large scale production. Within this several different opportunities lie that are worth exploring to advance knowledge and innovation within this area.

1.4.2 Batteries

Batteries within electric vehicles have come a long way since the 1890s when they were first used (Shahan, 2015). Within the last few decades there has been a shift to lithium-ion based batteries over lead acid batteries that had been common in electric vehicles before, with the TESLA Roadster being the first to make the shift at its launch in 2008 (Shahan, 2015). These battery packs also incorporate multiple individual cells to provide a desired capacity, along with cooling and management systems to keep the packs operating optimally, as well as packaging to keep all the components together.

The battery cells, like the supercapacitor cells, comprise of two electrodes, an electrolyte, a separator, and packaging, with the major differences being the different mechanics used in storing energy and that the electrodes are structurally different (Balasubramaniam et al., 2020). The electrodes are split between an anode and a cathode, which draw lithium ions from each other to store or discharge energy, with the cathode losing ions to the anode during charging and gaining them during discharging. This is displayed in figure 1.5:

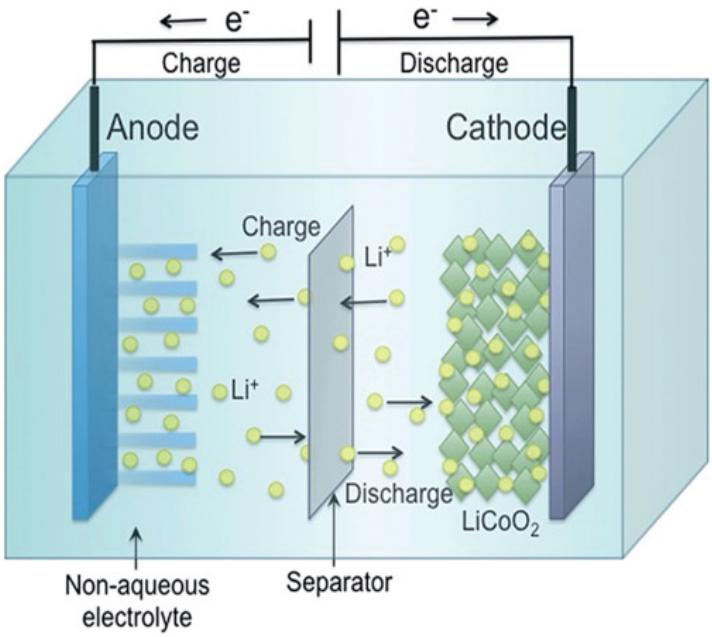

Figure 1.5: Lithium-ion battery charge mechanisms (Balasubramaniam et al., 2020)

Both the anode and cathode require active materials within them to accommodate the mechanics that allow the battery to store energy, with graphite being a common active material within the anode. The cathode active material for lithium-ion batteries varies depending on the exact chemistry of the reactions that occur at the cathode surfaces, with variations of Lithium Nickel Manganese Cobalt Oxide (LiNMC) being used in several different batteries. Alongside this are several other battery chemistries, including lithium cobalt oxide (LCO), lithium manganese oxide (LMO), and Lithium Iron Phosphate (LFP) (Mishra et al., 2018).

While lithium-ion chemistries are currently the most used type in the electric vehicle market, concerns over the impacts of lithium extraction have encouraged investigations into other battery chemistries. One that has shown a lot of promise is sodium-ion batteries, many of which can be manufactured similar production processes as lithium-ion batteries, reducing possible costs for changing from lithium-ion. Sodium is also considerably more available than lithium as a raw material, which could also reduce impacts derived from its extraction. Lithium rarity has also brough the economic sustainability of lithium-ion battery production into question, with lithium prices climbing to around £17,200 per tonne in 2017, although this dropped to around £8,600 in 2019 (Huisman et al., 2020). This is in contrast to sodium, which offers a low-cost alternative (Wu et al., 2022). There is also interest in sodium-ion chemistries as they can offer a means to eliminate cobalt from the battery production

process, which(Wu et al., 2022)ing concentrated in a few nations (Wu et al., 2022). Once again, sodium's abundance and ease of access to many nations(Wu et al., 2022)Many current sodium-ion chemistries use similar cathode active materials to lithium-ion, with a more recent development being O3 type sodium active materials, which utilises a range of transitional metals to produce a high-capacity material (Yao et al., 2017).

1.4.3 Life cycle assessment

Life cycle assessments examine the life cycle of a product or service and the impacts it has across the desired period. These impacts focus on the environmental aspects of products or services within using a life cycle assessment to examine them, with other methodologies used to examine the other pillars of sustainability. A range of environmental impacts can be examined by this methodology, which can be broken up into categories, with these being distributed between endpoint and midpoint categories. Endpoint categories are often quantified representation of changes in the environment, providing a simple view of the complex systems influencing the environment (Jolliet et al., 2003). These endpoint categories are often unitless and include resource depletion, human health and climate change (Jolliet et al., 2003). Midpoint categories are often based on specific themes or groups of emissions that have a toxic effect on the environment (Jolliet et al., 2003). These do often have specific units, such as Global Warming Potential being measured in equivalent emissions of CO_2 (kg CO_2 eq) (Jolliet et al., 2003). This measurement does include other emissions that have a similar impact on the environment, such as CH_4 and N_2O, measured in their equivalent mass of CO2 by the impacts they have on the environment (Jolliet et al., 2003). Figure 1.6 displays a diagram breaking down these impact categories:

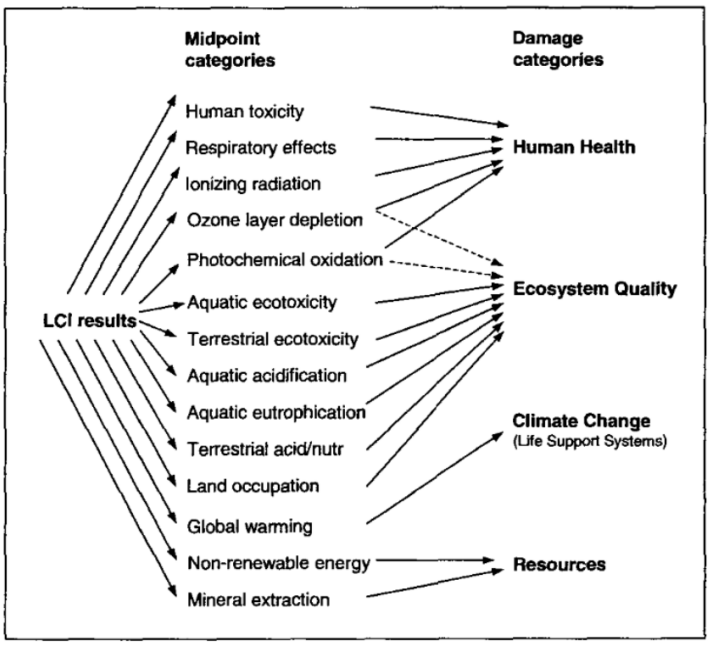

Figure 1.6: Framework of endpoint and midpoint categories in LCA (Jolliet et al., 2003)

For a product, this often focuses on the three key parts of the product's life, its manufacture, use and disposal phases. Each of these stages can be examined separately or as part of the entire life cycle of the product or service. Figure 1.7 displays the structure of life cycle assessments, as detailed in ISO 14040 and ISO 14044 (International Organization for Standardization, 2006), the standards used in LCA methodology worldwide:

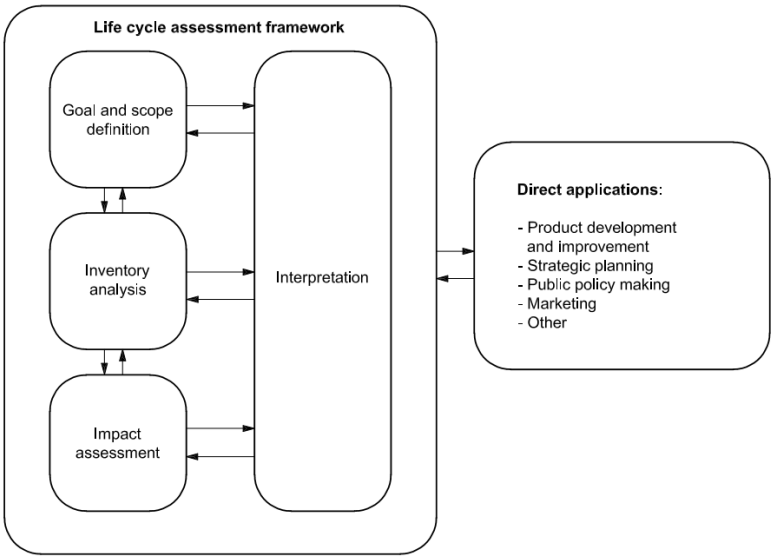

Figure 1.7: LCA framework (International Organization for Standardization, 2006)

Life cycle assessments have changed over the years, with initial variations excluding the goal and scope definition shown above (Curran, 2017). Within these variations, two groups have emerged, with retrospective and prospective life cycle assessment being conducted by many practitioners (Ekvall, Tillman and Molander, 2005). Retrospective methodologies focus on the flow of materials, both inputs and outputs, as well as the processes that use them. Prospective methodologies examine how these materials change will change with modifications are made to the processes. Both can be utilised to examine different systems and the changes made to them, providing a range of options for examine the environmental impact something has. Retrospective examines the impacts of a process, while prospective examines how changes to the process affect these impacts.

Life cycle assessments have been used by a variety of groups, with both journalistic papers and business reports, such as ones produced by Polestar, have been used to examine various industries (Røynem and Bolin, 2021). Within the electric vehicle market, various companies have become interested in life cycle assessments for a variety of reasons. Some of them are concerns over the impacts their products within the electric vehicle market have on the environment, along with public demands for transparency from customers and stakeholders(Røynem and Bolin, 2021) Life cycle assessments also offer the comparison between electric vehicles and their internal combustion counterparts, along with how changes in industry, such as (Røynem and Bolin, 2021)

1.5 Issues present in industry and potential innovations

From examining various literature sources and through work with life cycle assessments and supercapacitor production, several issues within these areas came to light and prompted investigation for potential innovations.

1.5.1. Issues facing LCA, energy storage and electric vehicles

Regulations for vehicles have tended to focus on the use phase of the vehicles

Regulations for road vehicles have been implemented to tackle the environmental impacts they produce(UK Department of Transport, 2020) The Road Vehicle Emission Performance Standards (Cars and Vans) (Amendment) (EU Exit) Regulations 2019 being one set of regulations, covering the emissions for new vehicles after they are produced or registered in the UK (UK Department of Transport, 2020). Similar regulations are present in the EU as well, with regulation 2019/631 establishing similar restrictions on emissions as the UK regulations, as the UK law is partially derived from the EU regulation(UK Department of Transport, 2020)(European Environment Agency, 2019).

Along with this, while they have significantly lower environmental emissions in their use phase compared with petrol/diesel vehicles, their production produces a significant number of emissions, especially from the manufacture of their batteries. A lot of public perception on the environmental impacts of electric vehicles comes from the focus on the substantially lower emissions through general use of them compared with their combustion engine counterparts. There are concerns about the carbon intensity of the electricity used to power their electric vehicles, as while they have zero tail-pipe emissions, impacts are generated by the power plants generating the electricity used by the vehicles, with GWP being a key impact. However, this is often misplaced as electricity generation offers better efficient over combustion engines, with well to wheel energy efficiency of between 53-77% for optimum electric vehicles verse 13-20% for petrol vehicles (Helmers and Marx, 2012). Concerns have also been raised over the production impacts of the vehicle, although these are relatively muted compared with the concerns over use phase emissions. However, over the entire lifetime of a vehicle, electric vehicles still produce less pollution compared with their

combustion engine equivalents, although this is dependent on the energy generation method, with coal reducing the improvements over petrol vehicles (McLaren et al., 2016). This difference between electric and petrol vehicles of similar sizes is shown in the comparison found in Figure 1.8, displaying the global warming potential over the vehicles life, with figure 1.9 displaying the boundaries of the life cycle comparison of both:

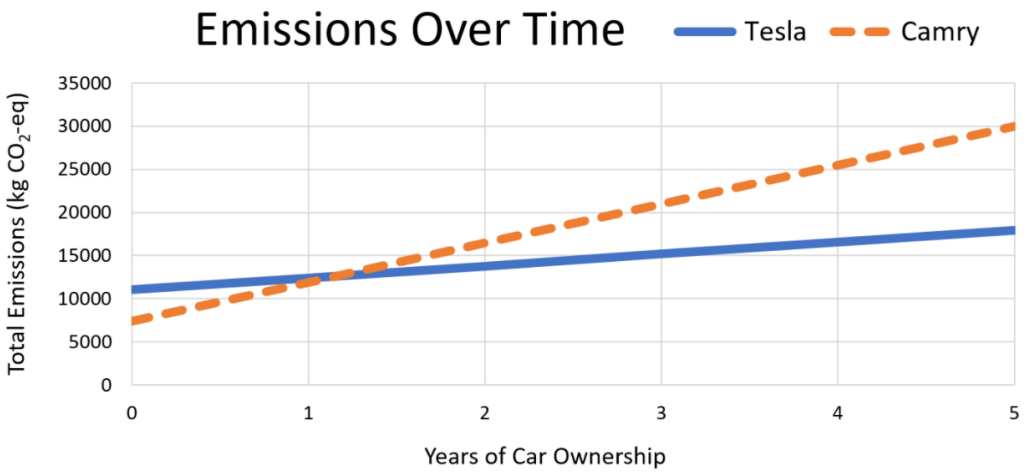

Figure 1.8: Global Warming Potential over time comparison between an electric vehicle (EV) (Tesla Model 3) and an internal combustion engine vehicle (ICEV) (Toyota Camry) (Young-Saver, 2021)

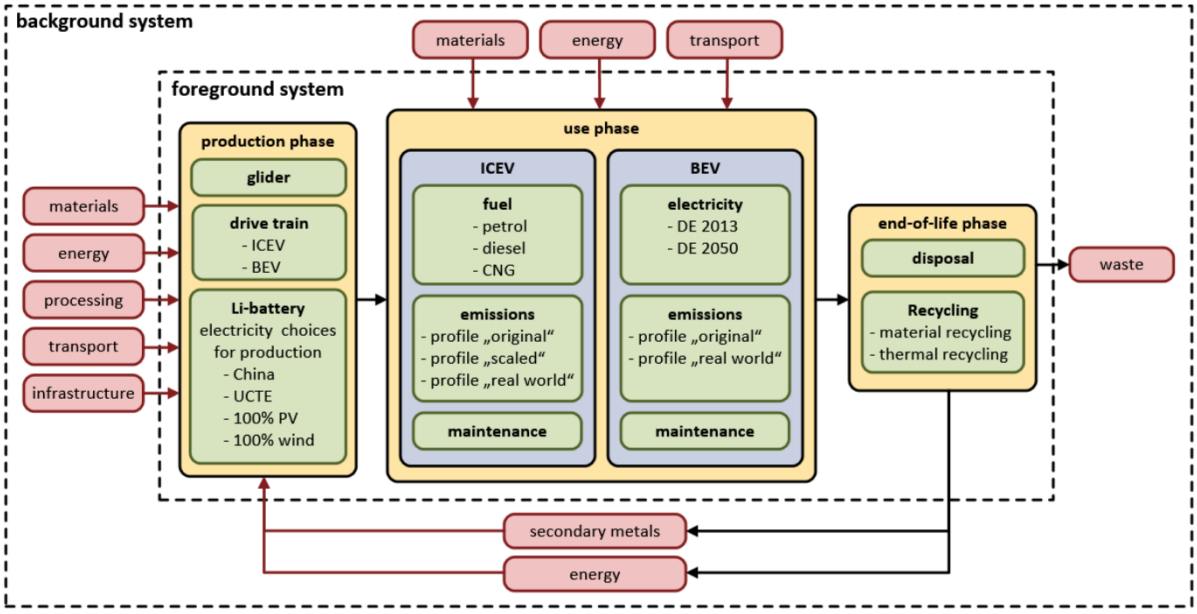

Figure 1.9: EV and IECV LCA boundaries for total life cycle (Helmers, Dietz and Weiss, 2020)

While this offers benefits in the long term, the ever-increasing demand for electric vehicles may cause an initial increase in the transport sectors emissions. Therefore, further awareness and assessments of the manufacturing stages emissions would be beneficial to developing strategies to reduce these initial emissions.

Life cycle assessments have limited data for battery production processes and the software is difficult to use for un-trained users

Life cycle assessments have been conducted before for multiple battery packs before with the resultant data being published (L.A.-W. Ellingsen et al., 2014)(Majeau-Bettez, Hawkins and Strømman, 2011). However, there is often a lack of information on exactly what material and processes are used to construct a battery pack, data which is vital to produce a life cycle assessment. There are also concerns on the quality of this data, as many of these data sources often merge processes to cover general steps, removing detail and granularity in breaking down which processes are producing key impacts. Another issue is that much of the data is quickly out of date, due to rapidly changing battery technologies and improvements, such as new efficiencies in battery production or the adoption of a new battery chemistry. This not only covers process inputs and output but other vital

information, such as the sources of materials used in battery manufacture at different stage of production. This requires an extensive literature search if data is not available from battery manufacturers, with WMG's unique position giving access to a variety of different data sets on the different processes, materials and equipment used in production of battery packs. It was also beneficial due to WMG's access to their own dedicated cell manufacturing facilities, giving a direct insight on processes used in their production and the data related to them.

While dedicated software for LCA has emerged in the last few decades and has been useful in simplifying the process of producing an assessment by automating the maths required to calculate emissions, many of them are difficult to use initially. Given that for some tools, such as openLCA, to change values in an established process involves an often-slow search of the process database to manually change one value. This is coupled with how complex some of the model developed within openLCA can get, with some utilising 400+ processes, most of which connect to multiple different processes either by requiring an input from one process or by producing an output required by another process. Even for individuals that have extensively used these programs, these models often become cumbersome and difficult to change if required, such as introducing new battery chemistries.

1.5.2. Innovations to address these issues

Further studies and comparisons between battery manufacturing life cycle assessments

With new battery chemistries being developed regularly, producing life cycle assessments on the batteries they produce and comparing them to current and other potential chemistries is a worthwhile pursuit. Showing the production emissions of a new battery technology can not only assist in their development by showing where they excel or fall short environmentally in their production phase but can also be used in showing the benefits of a new technology. With increasing concerns globally of industries impacts on the environment, showing a technologies environmental benefits compared with its competition may work to bring in investors for further development or adoption by a company. Sodium-ion batteries are one technology that show promise and a comparison with current lithium-ion batteries would be beneficial, with consistent and repeatable

methods of analysis to demonstrate the merits of LCA over focus on tailpipe. This can also be true when making policies, which may not fully account for the insights that life cycle assessments can bring.

Development of assistive tools for LCA software

While the construction of a LCA model will always be a complex endeavour to produce the data desired, steps can be taken to decrease the time required to perform certain tasks. Developing new tools to interact with the produced model can simplify the process of making changes to the model to examine different scenarios the model may undertake, while retaining the ability to return the model to its original set-up consistently. Working to improve the user experience would not only help improve the quality of models, as it would leave more time for the core attributes of the model rather than having to work around the software but may also bring in more users with a wide range of expertise, which would help improve LCA practices.

1.6 Supercapacitor issues and potential innovations

1.6.1 Issues facing supercapacitor production

Supercapacitors were reliant on finite polymer binders and there is uncertainty on how ink mixing methodologies affect their performance

Currently the most prevalent binders used in supercapacitor production are polymers, soluble only in hazardous solvents such as *N*-methyl-2-pyrrollidone (NMP). This is often a concern for industry as the solvents can not only be polluting and a health hazard if released but requires noticeable amounts of energy and resources to produce, affecting the businesses economics. Alongside this, there was also the question of how these polymer binders affected the performance of the supercapacitor as well, with little information on how they differed to other binders, such as Carboxy-Methyl Cellulose (CMC) and Styrene–Butadiene Rubber (SBR). This invites a comparison between these two types of binder to examine if they affect the performance of the supercapacitor cells.

When producing the electrodes for supercapacitors, there are a few different methodologies used to mix the inks and coat the current collectors, with possibility of different mixing methods affecting the inks in different ways. These mixing methods could impact how the electrode structure develops during production, affecting the area the electrochemical double layer can act on. They could achieve this by potentially blocking off active surfaces or expanding the surface area through pores in the electrode surface, among several different scenarios. A similar question could also be raised about the thickness of the electrode and how the additional material and changes to the structure of the electrode impacts the performance of the cell. There does not appear to be much research on these factors, which would make them ideal to examine.

1.6.2 Possible innovation to address this issue

Examine performance differences between supercapacitors produced with different mixing methodologies and binders

Supercapacitors had been studied for while at the beginning of the study, so studies into how different elements within the production of them would be beneficial. Examining how different binders affect the capacity and performance of the cells would give some interesting data. There also appears to be little to no examinations of how the different mixing methodologies for the electrode inks may affect the performance of the cells, which could be an interesting area to examine. Examining both would give a better understanding of supercapacitors going forward and how to continue to improve their designs with current active materials.

1.7 Research aims of this project

The two literature reviews conducted for this degree provides several possible areas where innovation may be found within electric vehicle energy storage. The areas examined and their aims are detailed in table 1.1:

Table 1.1: Research areas and their corresponding submissions

Submission	Chapter detailing work	Aims and area
2	2	Examine supercapacitors and how differing binders, mixing methods, and wet thicknesses affect their performance.
4	3	Examine the environmental impacts between two similar battery packs, comparing lithium-ion chemistries and sodium-ion chemistries.
5	4	Develop tools to assist with life cycle assessment software in modifying models and production of data.

2. Supercapacitors

2.1 Identifying areas to progress with supercapacitors

Electrode binders are a key element of many modern energy storage solutions, as they hold the key materials of the electrodes together and adhere the electrodes to the current collector. However, many of the more widely used binders used are often most soluble hazardous solvents to be used in the electrode inks, with *N*-methyl-2-pyrrollidone (NMP) being one of the most widely used of these solvents (Chernysh et al., 2019). This has led to investigations into other binders that are water soluble, with distilled water being considered a suitable replacement for NMP, not only for it being non-hazardous to humans but also for its lower environmental impact from its production.

It has its own disadvantages in that regard though, such as graphite's hydrophilic nature often causing agglomeration in the water-based inks (O'Mahony et al., 2019). A mixture of two water soluble binders, carboxymethyl cellulose (CMC) and styrene–butadiene rubber (SBR), has shown promise for use in carbon-based supercapacitors, with it being decided to conduct a comparison between this mixture and polyvinylidene difluoride (PVDF), an NMP-soluble binder. Investigations within these areas are of interest to industry, as requested by the projects sponsor company, Johnson Matthey.

Within the lab scale production of supercapacitors conducted at the University of Warwick, two mixing methods are primarily used to produce the electrode inks used, high speed dispersion mixing and high torque kneader mixing. Examination of published literature suggested there was minimal information on how these mixing methods may affect supercapacitors, so it was decided to investigate this by examining how these mixing methods may affect the capacity of supercapacitors over time. If there was a significant difference between the two methodologies, it could present an interesting opportunity of innovation, such as comparisons with other mixing methods and development of new methodologies.

2.2 Carbon based supercapacitors

For this work, supercapacitors based on activated carbon inks were chosen to examine these issues. Active carbon supercapacitors, like many supercapacitors, rely on a mechanism known as the electrical double layer, which stores energy in a layer of charged ions across the surface area of the electrodes. Active carbon is also the most widely used supercapacitor active material, owing to its high surface area and relatively cheap cost compared with the alternatives (Weinstein and Dash, 2013).

2.3 Experimental work

2.3.1 Objectives and methodology

Within this work, the major objectives were to examine different aspects of the supercapacitor electrode's production and compare them with alternatives. These aspects included the comparison of two different binder mixes, two separate mixing methodologies and four different electrode wet thicknesses, which are detailed in section 2.3.2. This was to assess how changes to these different parts of the supercapacitor electrodes affected the performance of the cells produced from them, with measures of specific capacity and capacity retention being used to gauge this. This also included each of the sixteen variations the combination of different aspect needing to produce five data sets each from cells produced from each electrode design, to show through repeated tests that the results of this work are reliable. Along with this work, some Scanning Electron Microscopy (SEM) examinations of the electrodes was conducted to look for elements on the electrode surfaces that may affect the performance of the cells. This was also repeated with multiple samples of the electrodes.

2.3.2 Supercapacitor production

To produce the test supercapacitors, it was decided to use a button cell structure, as this would allow for a sufficient number of cells to be produced by a single batch of electrode ink, which would allow for a consistent set of electrodes to find appropriate results from. While studies have shown that coin cells lose capacity at a faster rate than pouch cells, they

are also relatively cheap and quick to produce in the quantities needed for this experiment (Bridgewater et al., 2021). The electrode ink was coated onto an aluminium foil current collector, due to its high conductivity and relatively low cost compared with copper, forming the electrode. A 1 mol solution of tetraethylammonium tetrafluoroborate (TEABF4) in acetonitrile forming the electrolyte, which is a common electrolyte used in supercapacitor testing (Azaïs et al., 2007)(Jin et al., 2014). The electrode inks are the major focus of the study, with the differing binders and solvents used in them, along with their differing mixing methodologies and wet coating thicknesses. Within the ink recipes, the activated carbon and carbon black remain the two consistent ingredients, with the activated carbon as the electrode's active material and the carbon black acting as a conductive agent to pass electrons to and from the electrolyte and current collector.

Binders and solvents

Two binder mixes were used in the test supercapacitor electrodes, with each one requiring a differing solvent. The first was a mixture of CMC and SBR, with a ratio of 2:3 of CMC:SBR, with deionised water being used as the ink solvent. This ratio was determined through multiple tests of the inks, with the binder mixes being changed to find an ink with the appropriate viscosity to be suitable for the coating methodology. The second group was made of pure PVDF, with NMP as the ink solvent. These differing groups of binders and solvents did require differing ink recipes, which are detailed in tables 2.1 and 2.2:

Table 2.1: CMC/SBR based electrode ink recipe

Recipe ingredient	Percentage mass in ink (%)
YP50F (Activated carbon)	25.50
C65 (Carbon black)	1.50
Medium viscosity CMC (2.5%) binder solution with de-ionised water	48.00
SBR binder	21.40
Additional de-ionised water	3.60

Table 2.2: PVDF based electrode ink recipe

Recipe ingredient	Percentage mass in ink (%)
YP50F (Activated carbon)	23.49
C65 (Carbon black)	1.35
PVDF 8% binder solution with NMP	27.00
Additional NMP	48.16

These recipes were based on previous research work conducted at the university, with recipes provided by work conducted with Alexander Roberts (Forghani and Roberts, 2021).

Mixing methodologies

With these two recipes, two mixing methodologies were devised for each binder group. The first utilised a high-speed dispersion mixer, which mixed the binder solution carbon black and additional solvent together while the activated carbon was added slowly, which took

around 10-15 minutes to achieve. After this the dispersion mixer had its speed increased to around 1500-1700 rpm, with the inks being mixed for 1 hour and 30 minutes. For the CMC/SBR based inks, an additional step is added, with the SBR binder being added at the end of the process and mixed into the inks for 5 minutes.

For the high torque kneader mixer, the binder solution, carbon black, activated carbon and a portion of the additional solvent were mixed at 100 rpm for 1 hour, with the mixing container cooled to 25 ^{o}C by the mixers cooling system for the duration of the mixing process. After this, the remaining additional solvent was added, with the blades of the mixer scraped to ensure an even mix of the inks before the mixing process resumed for 1 hour 30 minutes to incorporate the additional solvent. As with the high-speed dispersion mixer, for the CMC/SBR inks the SBR was added at the end of the process, being mixed for an additional 5 minutes.

As with the electrode ink recipes, these mixing methodologies were based off previous research work conducted at the University, with Alexander Roberts providing the initial methods, which were changed to achieve an appropriate viscosity (Forghani and Roberts, 2021). These methods were chosen as both methods are currently common methods for mixing inks for supercapacitors(Hu et al., 2018). The exact methodologies were derived from repeated experimentation to produce a homogenous mix, with assistance from methodologies provided by work conducted with Alexander Roberts (Forghani and Roberts, 2021).

Wet coating thicknesses

Alongside examining the binders and mixing methodologies of supercapacitors, the thicknesses of the electrodes were also looked at, with four different wet coating thicknesses (the thickness of the coated electrode while the ink is wet) being examined during this work. Thicknesses of 50 µm, 100 µm, 150 µm and 200 µm were examined, with the coating thicknesses being controlled using a doctor blade, which was used to spread the prepared inks onto a sheet of flattened and secured aluminium foil. This method was chosen as it is a common method of dispersing ink over a current collector in laboratories and(Boulanger et al., 2021). Other methods, such as spraying, are available but are not

widespread within industry at the time of this reports completion, with the doctor blade coating being considered the conventional method for supercapacitor electrode production (Garakani et al., 2021). The doctor blade set at the desired hight to control the wet thickness before spreading began, with figure 2.1 displaying a diagram of the doctor blade in action.

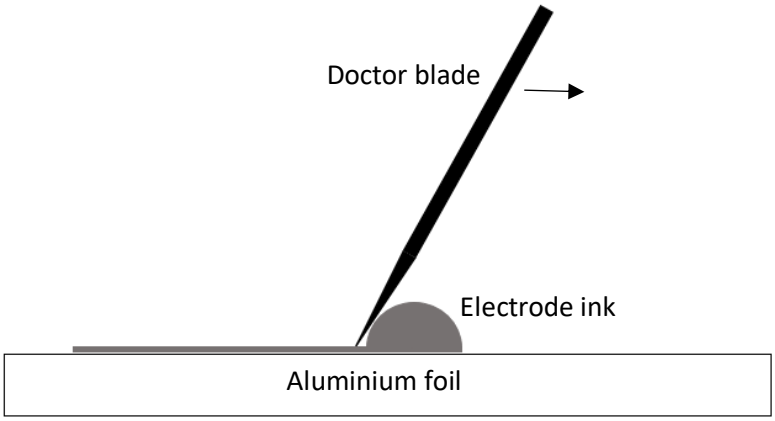

Figure 2.1 Doctor blade diagram for supercapacitor production (Lehtimaki, 2017)

Cell production and assembly

For the test supercapacitor cells, each of the electrode sheets were cut into 14 mm diameter disks, with two disks used per cell and the mass and dry electrode thicknesses being recorded for each cell. A slightly larger disk of a cellulose material was used as a separator, with two aluminium disks of 1 mm and 0.5 mm thickness and a spring being used to hold the cell materials in place and a basic button cell casing used to contain the cell materials. Button cells were used as they are widely regarded as a standard test in battery research (Stoller et al., 2011). A measurement of 100 µl of the 1 mol $TEABF_4$ electrolyte in acetonitrile was also added, with the electrolyte being added after the 1 mm aluminium disk and first electrode had been laid in the button cell casing. Figure 2.2 displays the inner structure of the completed cell:

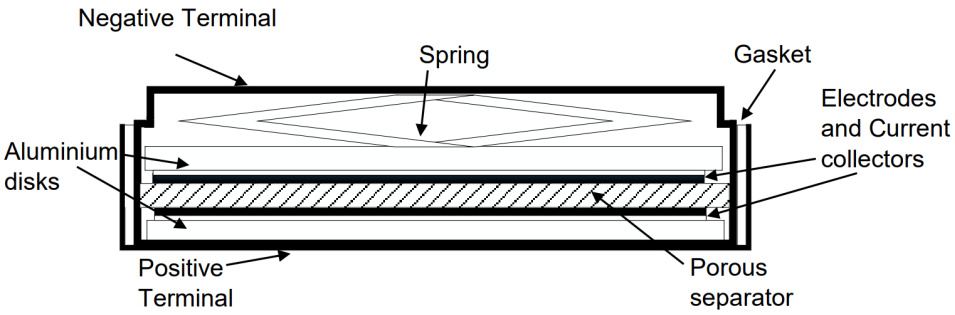

Figure 2.2: Button cell supercapacitor structure

For each variation of the electrodes, five cells were created for the next stage of the project, to show the repeatability of the cell capacities for each variable. This resulted in over 80 cells being produced and tested for this project.

2.3.3 Capacity cycling of supercapacitor cells

Once the cells were completed, they were placed in a cycling circuit and cycled at different current densities, with the cell being charged at a constant current until it reached 2.7 V before being discharged. This was repeated ten times for five different current densities, with values of 1 $A.g^{-1}$, 2.7 $A.g^{-1}$, 7 $A.g^{-1}$, 7.7 $A.g^{-1}$ and 10 $A.g^{-1}$ being used to determine the charging current of the cell, with this being measured from the mass of the electrodes in each cell. Figure 2.3 displays the cycles of a cell's voltage over time through the five current densities:

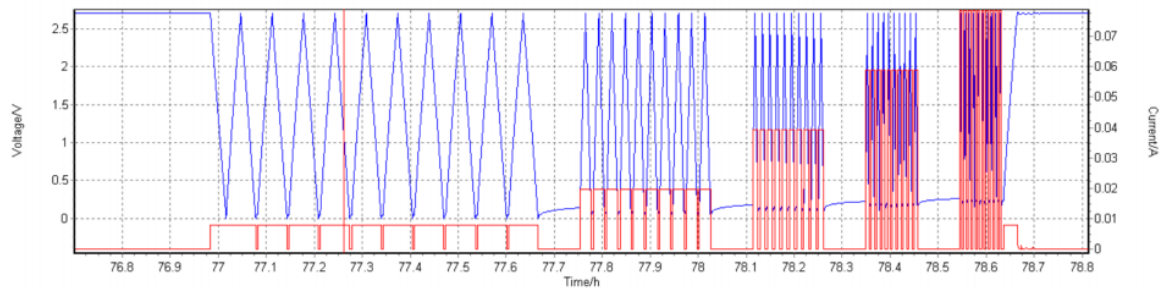

Figure 2.3: Graph of voltage and current during the cell cycling

After the repeated cycling, the cell was charged back to 2.7 V before being held at that value (known as floating) for 24 hrs before repeating the whole process. This would continue for 20 days, with the fourth day being considered day 0 to allow for the cells to be conditioned by the cycling. From the batches of 5 cells for each examined electrode type, one was selected to compare with its equivalents as a representative of its group.

2.3.4 Electron microscopic examination of electrode material

As part of the efforts to examine the electrodes and what may affect the supercapacitor performance, SEM microscopy was performed on some cuttings from a few the electrode sheets to examine their surfaces and any defects that may be present. This was conducted on the electrodes produced from the CMC/SBR based inks mixed with the high torque kneader mixer with 150 µm and 200 µm wet thicknesses, due to issues that cropped up with some of the cells produced from them. These issues ranged from abnormal readings when examining the capacity to high failure rates preventing trustworthy data being derived from them, which is detailed further in section 2.4.1. A 50 µm electrode with the same binders and mixing method was also examined to give a comparison with an electrode that did not suffer from these issues, acting as a baseline to assist in determining possible causes of the cell failures or abnormal readings. While there were plans to examine each of the electrodes, it was during this testing that the sponsor company withdrew support for the EngD, detailed further in section 2.7. As a result of this, a review of the work plan took place, and it was decided to target other work opportunities within life cycle assessment. This led to further work on SEM examination of the supercapacitor electrodes to be halted.

Possible reasons for the electrodes contributing towards the failure rates of the cells with thicker electrode range from possible ink contaminant to parts of the electrode detaching from the current collector. To examine this, a ZEISS Sigma Field Emission Scanning Electron Microscope (FE-SEM) was chosen to examine the electrodes, which were required to be prepared for use in the microscope. This included mounting the cut electrodes to be mounted on a metal platform, which was then secured within the microscope and a vacuum created in the sample chamber to allow the microscope to examine the electrode. The electrode surfaces were then examined at different magnification levels to locate defects

which may have contributed to the failures of the cells, such as contaminants or cracks in the electrode.

2.4 Results from supercapacitor creation and examination

2.4.1 Cycling data

Examining the data produced by the various cells did show a clear distinction between the binder types, with the CMC/SBR mixture offering a significantly larger specific capacity, in Fg^{-1}, than their PVDF counterparts in all the variations examined. The mixtures also showed significantly better retention of their specific capacity over the 17 days of cycling they endured after conditioning, often retaining 90-80% of their conditioned capacity while the majority of their PVDF equivalents plunged to between 60-40% within the same timeframe. However, this was with an organic solvent-based electrolyte and may not be applicable for other electrolyte types, such as water-based electrolytes. Figures 2.4 and 2.5 display the data collected for specific capacity and retention:

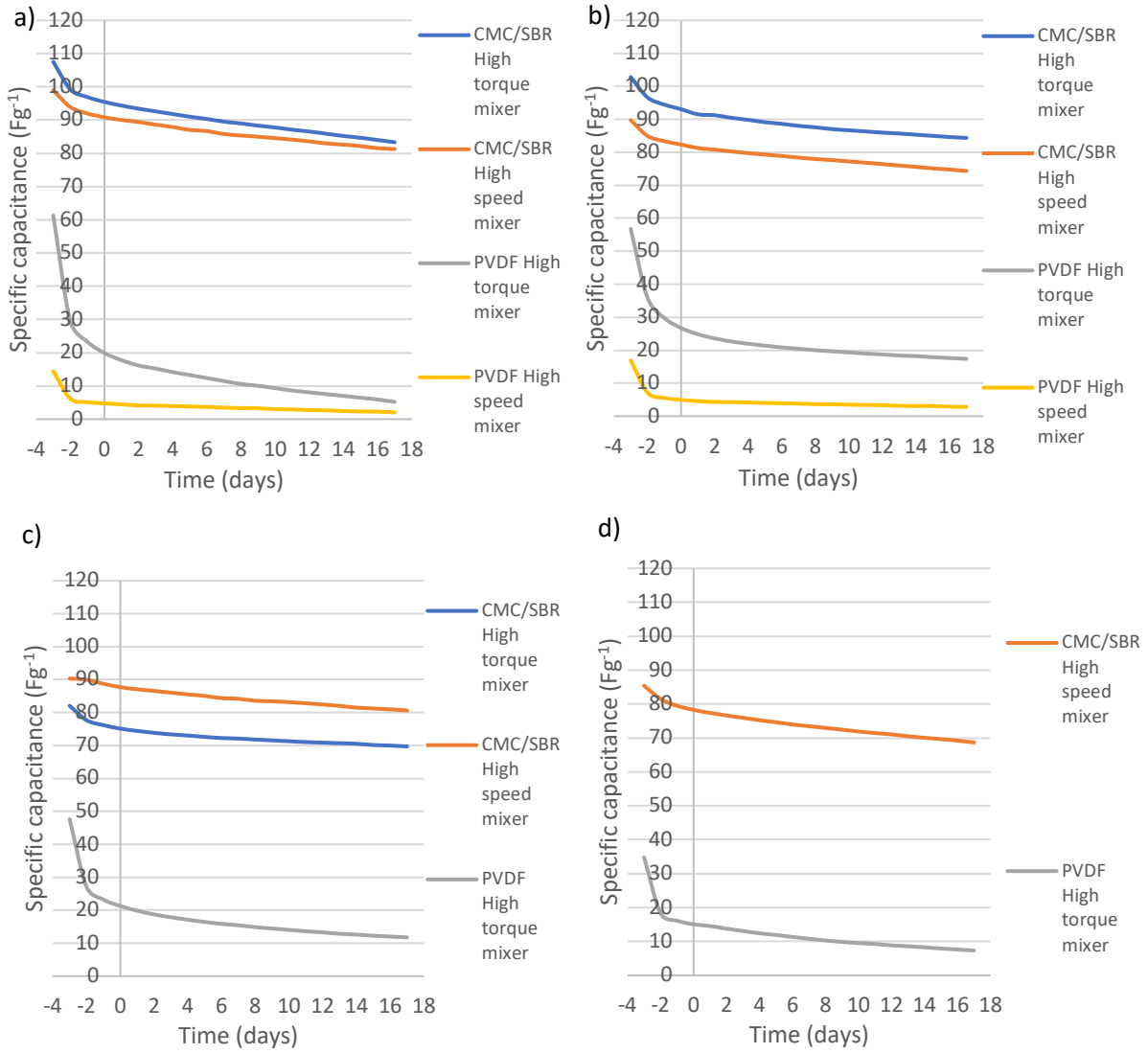

Figure 2.4: Graphs detailing the specific capacity over time for each electrode wet thickness, with a) 50 µm, b) 100 µm, c) 150 µm, and d) 200 µm electrode wet thicknesses

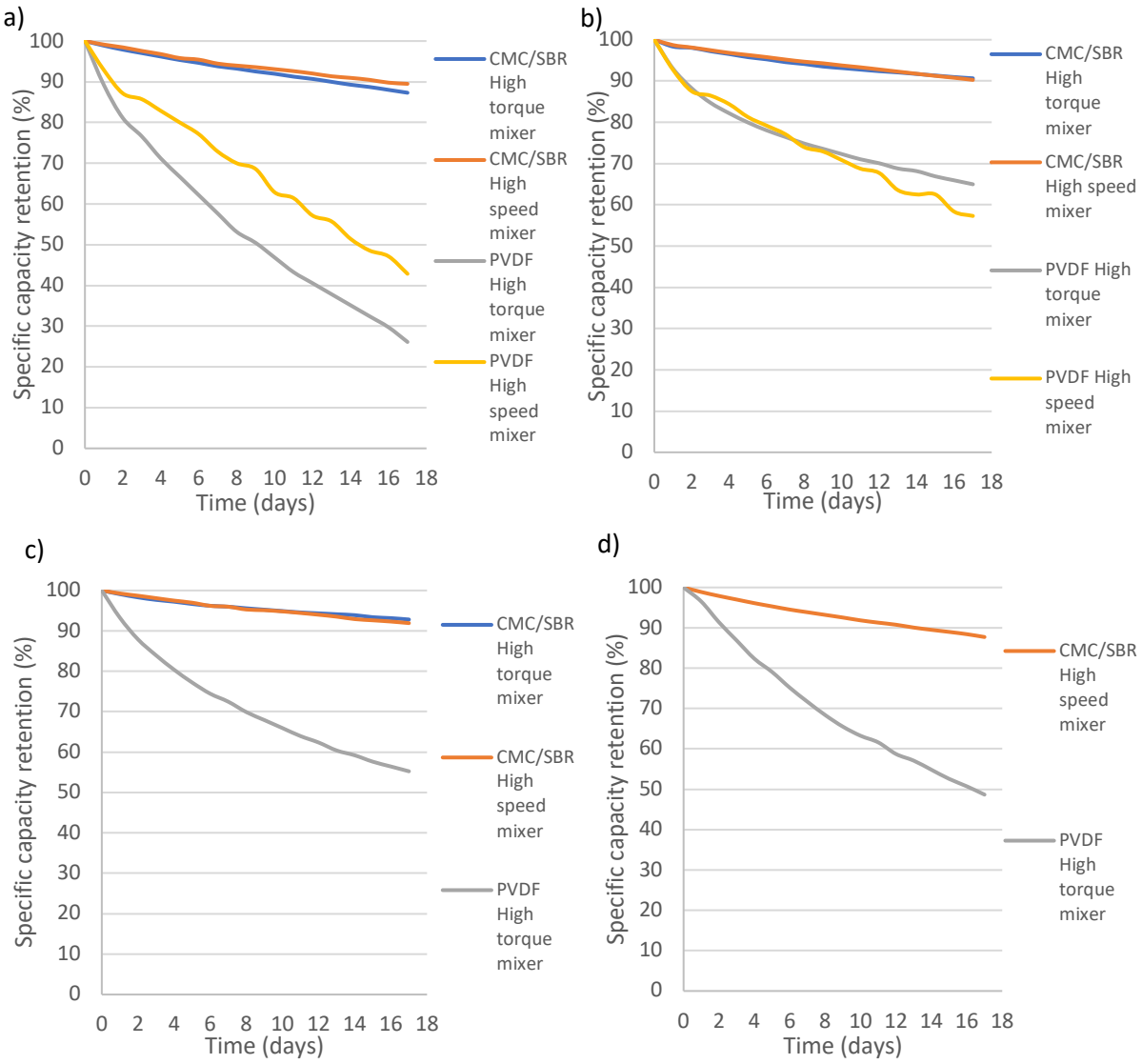

Figure 2.5: Graphs detailing the specific capacity retention over time for each electrode wet thickness, with a) 50 µm, b) 100 µm, c) 150 µm, and d) 200 µm electrode wet thicknesses

When comparing the two mixing methods, the differences between the binder mix and wet thicknesses seemed to have an impact. For the CMC/SBR recipes, the high torque kneader mixer providing higher specific capacity at the 50 µm and 100 µm electrode wet thicknesses than the high-speed dispersion mixer, although the high-speed offer slightly better or equivalent capacity retention for these thicknesses. For the PVDF binder electrodes, the situation is similar, with the high torque kneader mixer providing higher specific capacity than the high-speed dispersion mixer, although there is a much greater difference in lost capacitance, as seen in figure 2.5 a) and b). While this shows the benefits on performance that the high torque mixing method has, it also leads to questions on the feasibility of this

methodology. Would these benefits be financially or technically achievable at a scaled-up process of production, given that current high torque methodologies need to scrape the mixing blades at a point during the mixing process? Could this process be automated, and would such a piece of equipment be financially viable for large scale mixing of the inks?

For the other thicknesses some issues arose, as while for the CMC/SBR mixes at 150 µm seem to follow the same pattern as the previous wet thicknesses, the PVDF mix could only provide repeatable data for the high torque kneader mixer. This was due to the cells produced with the high-speed dispersion mixer PVDF ink all failing for a variety of reasons, with high current leakages and short circuits being some of the major factors. This could be caused by ink contaminants, the separator breaking allowing the electrodes to touch and cell overheating as some of the possible causes. These factors helped motivate examination of the electrodes under an SEM microscope, as displayed in section 2.4.2.

A similar set of issues were present for the high torque mixer, with high failure rates but enough data could be collected to provide a reliable result. The same issues occurred with the same ink type for the cells produced with 200 µm wet thickness electrodes. This was compounded by the CMC/SBR inks mixed in the high torque kneader mixer producing strange data for the cells produced with 200 µm wet thickness electrodes. Figure 2.6 displays the data derived from the five cells produced for this thickness, with figure 2.7 displaying data from a similar set of cells:

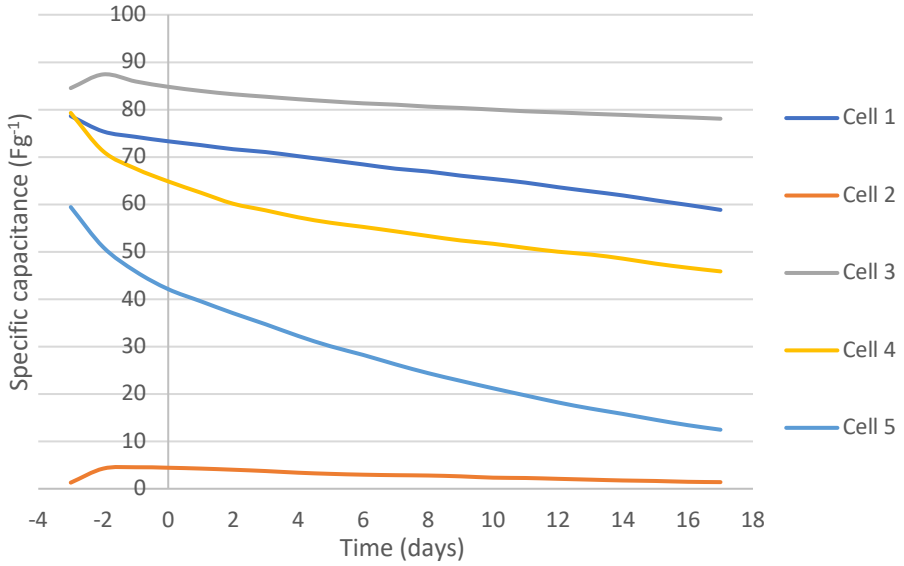

Figure 2.6: Graph of specific capacity over time – 200 µm CMC/SBR high torque kneader mixer cells -failure

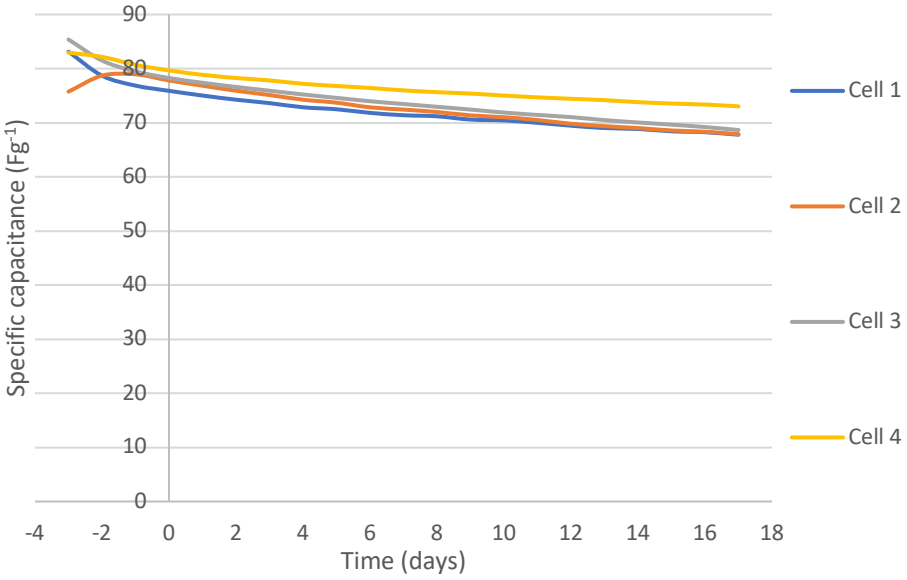

Figure 2.7: Graph of specific capacity over time – 200 µm CMC/SBR high speed dispersion mixer cells

As can be seen with the difference between figure 2.6 and 2.7, it is reasonable to see the results collected from the 200 µm CMC/SBR high torque kneader mixer cells as not being

suitable for use, as one set of data cannot be selected as representative of the batch. This could potentially be due detachment of parts the electrodes from the current collector, varying the surface area of the attached parts of the electrode. A fresh set of cells were produced, with a fresh set of electrodes, produced from a new batch of the ink, although these cells all failed for similar reasons as listed for the 150 µm high speed dispersion mixer PVDF ink-based cells. This does raise the question of why the cells failed at these thicknesses? To assist in understanding this, these cells, along with other CMC/SBR cells, had their electrodes placed under SEM's to be examined.

2.4.2 SEM examination

As there were several failures across the different cells, SEM examination was undertaken for the two electrode wet thicknesses that produced the most failures, those being 150 µm and 200 µm, along with an examination of a 50 µm electrode to compare against. All the electrodes looked at were produced from CMC/SBR inks mixed in the high torque kneader mixer, as while the 150 µm electrodes did produce enough successful cells for a representative value, it still had a high failure rate compared with other cells. Figure 2.8 display the surface of the 50 µm electrode at a 6.09 K zoom:

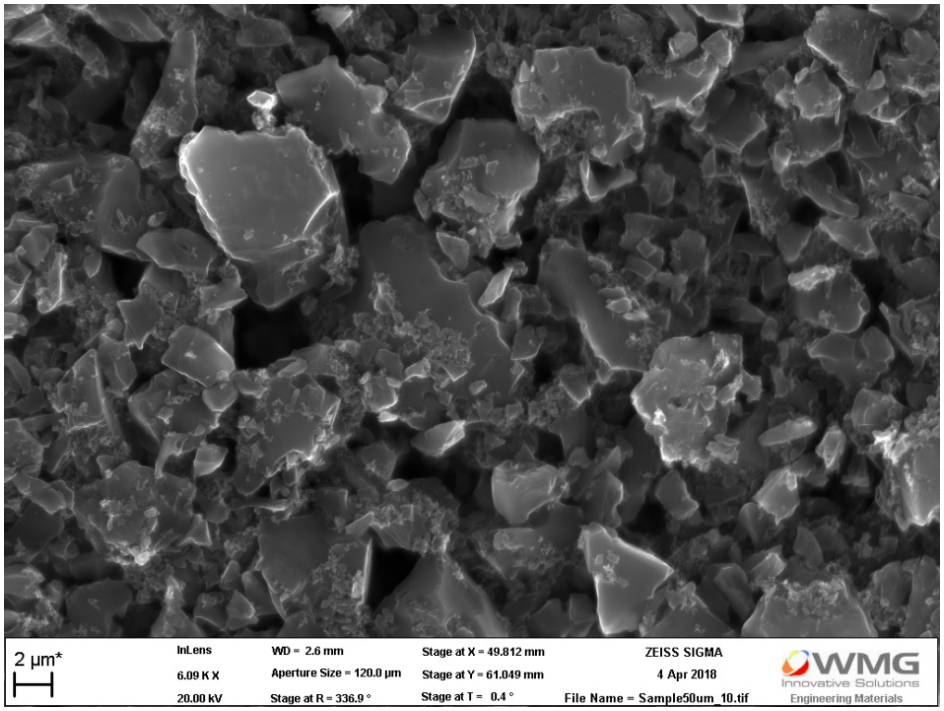

Figure 2.8: 50 µm electrode surface at 6.09 K zoom

In comparison, figure 2.9 displays the 200 µm electrode at a similar zoom:

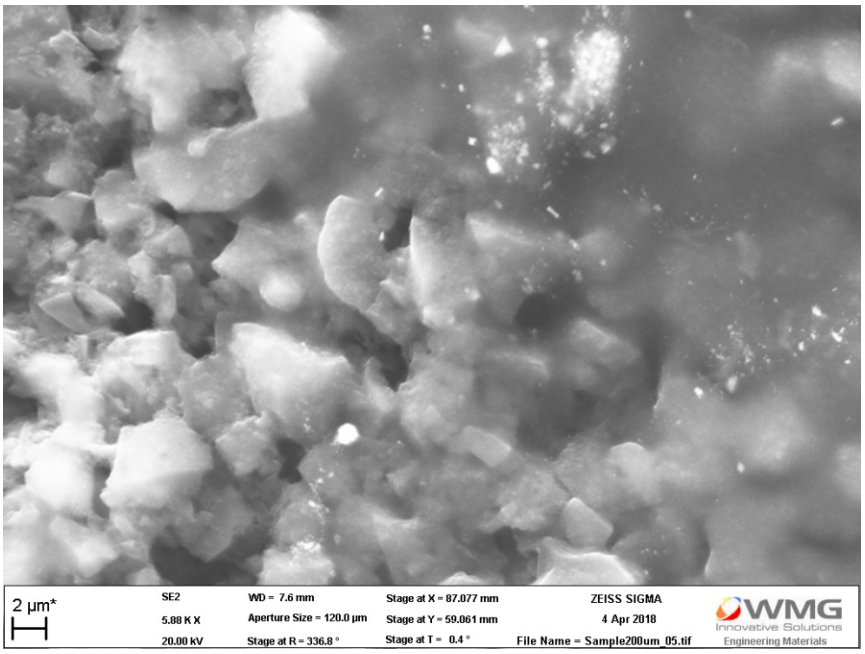

Figure 2.9: 200 µm electrode surface at 5.88 K zoom

As can be seen, figure 2.9 displays a large mass of a translucent substance covering a portion of the electrode surface, obstructing the active carbon for accessing the electrolyte in a cell. It was determined that this substance is likely residual binder, with CMC being the most probable substance, which could have contributed to the unusual distribution of cell specific capacities shown in figure 2.6.

Examining the 150 µm electrode showed similar makeups to the 50 µm electrode, although there was also evidence of contamination of the electrode inks, with figure 2.10 displaying what is believed to be a hair within the electrode ink:

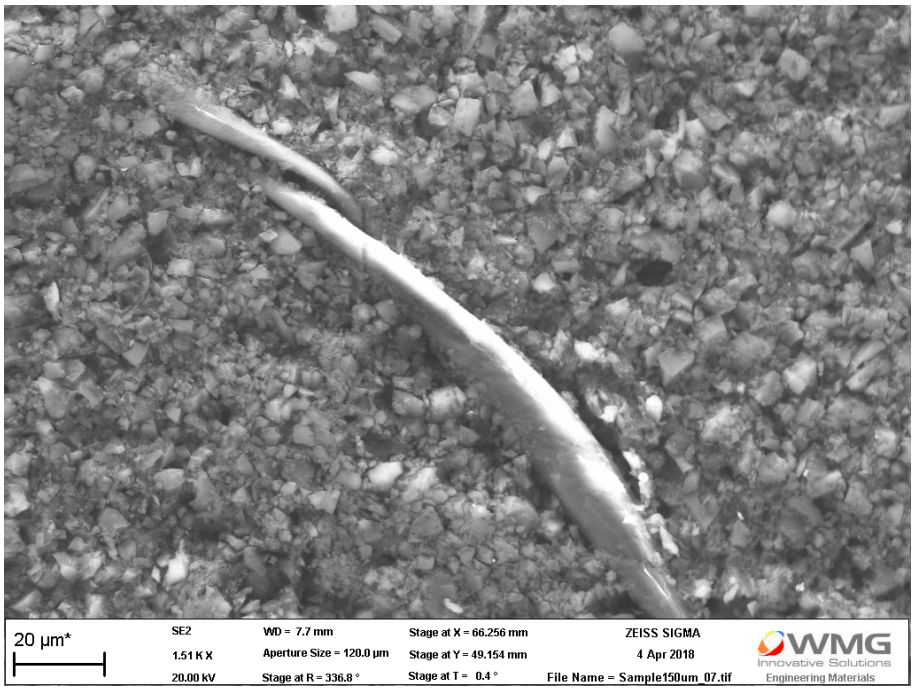

Figure 2.10: 150 µm electrode surface at 1.51 K zoom – hair contaminant

This, along with other contaminants, may explain why these electrodes were failing for some cells but not others. Other issues examined during the SEM study revealed several cracks within the 150 µm and 200 µm cells, which may have been due adhesion failures and could be symptomatic of the electrodes partially detaching from the current collectors.

2.5 Potential innovation

The data collected shows that the CMC/SBR binder mix offers significantly larger specific capacities for the cells, which indicates that there are benefits to utilising these materials as binders in supercapacitors. There is the question of whether this would be applicable with a water-based electrolyte, as there is also interest in moving away from organic solvents being used in electrolytes.

Examining the different mixing methods there is a noticeable improvement of the high torque kneader mixed capacity values for the PVDF cells, with the difference less significant for the CMC/SBR cells. However, this conclusion is only applicable for the 50 µm and 100 µm cells, with the high-speed dispersion mixer offering better capacity for the CMC/SBR cells for the 150 µm cells. This brings into question whether the mixing method is responsible for this change, or if other factors are involved in the difference. There is also the question of whether the additional difficulties that the high torque kneader mixer methodology brings, such as the need to scrape the mixing blades during the production process, are economically viable if the methodology is to progress past the lab scale.

Comparing the wet thicknesses there does not appear to be significant benefits to the increased wet thicknesses, with the 50 µm offering the highest specific capacity for the CMC/SBR based electrodes and 100 µm offering the highest for the PVDF based electrodes. The thicker electrode coatings don't provide a proportional increase in capacity compared with their thinner counterparts, in part due to that the increased material doesn't increase the surface area the electrochemical double layer can work on to the same degree. While the increased wet thicknesses do improve the capacity retention between the 50-150 µm wet thicknesses, this raises the question of whether this doubling or tripling of the ink materials used in the electrodes is worth the relatively small increase in capacity retention.

2.6 Summary - Supercapacitors

The work conducted here showed several interesting directions the work on supercapacitor could go in, with options for different binder mixes, electrode thicknesses and production methodologies. From this work, a few possible research questions arise:

1) Do CMC/SBR based binders offer similar capacities for water-based electrolytes, compared with their organic solvent-based counterparts?
2) If they don't provide a similar or higher capacities, are there changes to the ink recipes that could rectify this?
3) Is there an environmental or economic cost benefit to an increased electrode thickness?
4) Is the mixing methodology solely responsible for the differences in specific capacity or are there other factors involved?

2.7 Refocus of the EngD

While these could have led to innovations and improvements derived from this work, at the end of this stage of the degree there was uncertainty on the direction going forward, especially as papers covering similar subjects were being published around the same time. One example of this was a paper comparing CMC with PVDF along with other binders being published in 2018 (Bresser et al., 2018). Along with this, there was also concerns on whether, while innovative within the exact area, these conclusions would also apply to other supercapacitor active materials. While active carbon is currently the most widely used active material, others are rapidly being developed that hold the potential for significantly improvements over active carbon supercapacitors, with graphene being one such material (Wu, Feng and Cheng, 2014). Would these changes have the same affect with a different active material?

While this work had brought forward some interesting points with the current generations of supercapacitors, the changes in active material may lead this work to be a dead end of research. After discussions with Johnson Matthey and the industrial supervisor, it was decided against continuing to examine this area for the degree, with the company seeing the industrial development outpacing what an EngD degree could achieve, and subsequently withdrawing from the degree. To continue the degree, a new sponsor company was searched for, with consultancy company Ricardo PLC agreeing to step into the role. After discussions with academic supervisors and Ricardo PLC, it was decided to shift the focus of the degree to a different area within electric vehicle energy storage, to benefit

from the background knowledge of the previous project. With the new sponsor company of Ricardo PLC, it was decided to focus the remaining degree on battery units and their environmental impacts.

3. Battery pack Life Cycle Assessment

3.1 Battery pack innovation

Batteries have been an important part of electrical devices and road vehicles for decades. The recent surge in electric vehicles within the last decade has sparked interest in new battery pack technologies, both to improve the pack's performance but also to keep up with the expected demand.

Examining the environmental impacts of batteries, life cycle assessments offer an excellent methodology for examining the emissions produced during their lifetime. Within life cycle assessment software, a wide range of databases are available with a variety of different processes that can be incorporated into a model to give data on its impacts. However, many key materials for battery production are absent from these databases or may not give the detail of the processes that a user may want. This is only compounded by the rapid pace of development in battery technologies, with both battery chemistries and production methods changing from year to year, which can lead to information quickly becoming outdated. This can lead to issues when sourcing information for LCA models from literature, as published papers are likely to be behind the times with how modern batteries are produced. This can also be applicable for other data sets, such as energy generation which is rapidly changing in many nations as their economies develop, along with their energy industries gravitating to renewable energy sources from political and economic pressures.

Within the studies of life cycle assessment, a direct comparison of equivalent battery packs between two significantly different battery chemistries as lithium-ion and sodium-ion appears not to have been conducted, with most LCA studies comparing similar battery chemistries. Within battery pack research, there has been interest in sodium-ion battery chemistries, due to it offering solutions to some of lithium-ion batteries issues, with material availability being one of them, as sodium is much more readily available than lithium. Therefore, there are benefits to comparing the environmental impact of such battery packs with lithium-ion battery packs, along with where in the production process emissions are produced, along with why one chemistry emits more than the other. This was an area of interest to Ricardo PLC, who co-operated with the university for this work and the tool development project, as described in section 4.

3.2 Selecting the software, designing the battery packs and the production processes

3.2.1. Life cycle assessment software and methodology

With the decision to produce life cycle assessment models for these battery packs, the question of which software should be used to build these models had to be addressed. All the software and production methods are based off ISO 14040, with many automating some of the processes used in producing life cycle analysis. While Microsoft Excel was briefly considered, as it has been used in industry for LCA work, it was decided to produce the models with a dedicated LCA software, which offered a range of benefits for producing the model, including the use of available data from dedicated databases. As to which software would be used, four dedicated software packages were compared with each other to determine which would be best for this project and any future projects going forward. The software examined included GaBi, GREET, openLCA and SimaPro, with comparisons being made on their user friendliness, databases available, cost and adaptability.

This comparison drew some interesting conclusions, with SimaPro being eliminated from consideration due to concerns of availability, as SimaPro had a far higher cost than the other options for the project. Although GaBi had a similar price as SimaPro, it was already available to the project through the University of Warwick which gave it an advantage over SimaPro. GREET was also eliminated, as while it did offer some interesting options for LCA production, it was primarily designed for work with well to wheel fuel which made it less suitable for working with battery production compared with the other tools. This left GaBi and openLCA, both of which offered a range of interesting options for producing and examining the models, with various advantages and disadvantages when directly compared. However, openLCA's open-source and modifiable nature was a factor that ultimately led it to be selected for the project as modifying or adding to the tool offered a range of options for further innovation within the degree. Table 3.1 displays a decision matrix that assisted in determining the best software for use with this work. No weighting was used the decisions in the matrix:

Table 3.1: Decision matrix for LCA software

Software	Cost	Process availability	Ease of use	Adaptability	Report functions	Presentation	Overall
GaBi	5	5	5	4	4	4	27
openLCA	5	4	5	5	5	5	29
GREET	5	3	4	3	4	5	24
SimaPro	1	1	3	4	4	N/A	14

With the software chosen for the models, the question then arose to which methodology within the multitude available within LCA methods was best for these models, all of which follow ISO 14040 as the basis for LCA practice. While initial production of the model focused on the IMPACT 2002+ methodology, further examination of what was needed from the models, along with discussions with academic supervisors, led to a new methodology to be chosen. IMPACT 2002+ presented its impact values as endpoint categories and after examining the objectives of the models, it was decided that midpoint categories were needed to provide the data desired from the models, as midpoint categories offer a more precise examination of the battery pack's impacts. To this end, the ReCiPe v1.13 methodology was considered, as it offered a range of different categories with clear units, including Global warming potential (GWP) in kg CO_2 eq. Other methods offered similar benefits, although ReCiPe v1.13 was considered to have the clearer units which could be understood by a wide audience. One example of this was the Metal Depletion unit, which was measured in kg Fe eq for ReCiPe v1.13 but as kg Sb eq in other LCA methodologies, such as ILCD 1.0.8 2016's midpoint version. Other LCA methodologies were examined but most were lacking in the versions available on openLCA, with versions of TRACI and CML2001 lacking some of the possible units ReCiPe offered. A comparison was made between IMPACT 2002+ and ReCiPe to determine which methodology was most appropriate for the models, with the comparison being displayed in table 3.2:

Table 3.2: Decision matrix for selection of LCA methodology

Methodology	Impact unit precision	Range of impacts examined	Impacts being understandable to the public	Total
IMPACT 2002+	2	2	1	5
ReCiPe **V1.13** E	5	4	5	14

As can be seen in table 3.2, ReCiPe V1.13 offered a better range of impact categories and had more precise and understandable units for those without LCA knowledge through its use of midpoint categories. This made it ideal for use with these models. From the ReCiPe V1.13, it was decided to examine the global warming potential (GWP) and terrestrial acidification as the key impacts being examined for the battery packs. They were selected due to GWP's importance in understanding a processes impact on climate change and terrestrial acidification's links to acid rain and other phenomena damaging to the environment. Several other impacts were also examined, including fossil fuel depletion and metal depletion, to give an overview of the battery packs use of non-renewable resources. Human toxicity and marine ecotoxicity were also examined, as these had been examined in other literature studies on similar battery packs.

3.2.2. LCA methodology

To produce the models within openLCA, the first stage was to set the boundaries of LCA to determine what processes would be covered. It was decided to cover the processes from cradle to gate with the electric vehicle battery packs, starting at the extraction of raw materials through to the final assembly of the pack, read to be installed into a vehicle. Figure 3.1 displays a generalised overview of these boundaries:

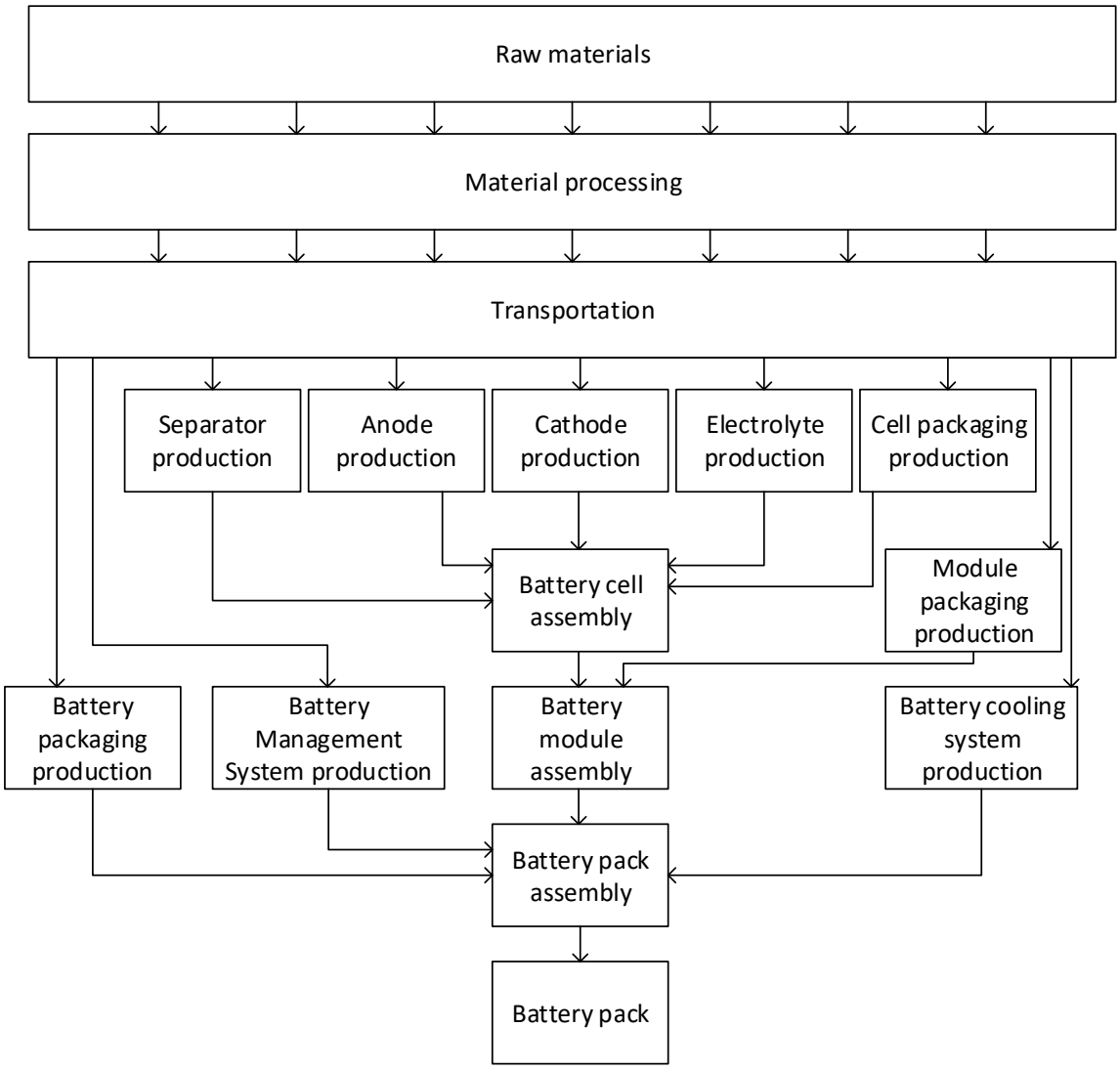

Figure 3.1: Overview of battery pack production

With the boundaries for the analysis set, the next stage was to determine the battery packs specifications and the different processes and materials needed in their manufacture. This led to a detailed literature search, which gave a wealth of different datasets on the manufacture of similar battery packs and the raw material used to produce them, which were used alongside process data provided in openLCA's databases. The datasets varied primarily as they covered different battery chemistries or more general processes to produce key materials, such as aluminium. The data was sourced primarily from peer-review papers and papers from respected institutions, such as the European environment agency, to ensure there was a high confidence in the accuracy of the data, although data was also sourced from publicly available sources from companies, such as Nissan. The data found was

focused on the inputs and outputs of raw material and energy, as many of they used different LCA methodologies, which would have different weighting within their environmental impact categories compared with ReCiPe V1.13. These were used within openLCA to construct the models for each battery chemistry, with changes being made to the models when appropriate, such as updated electricity data for the different processes. Details on the sources from literature of key data can be found in appendix A at the end of this report.

3.2.3. Battery pack design

For this comparison, an electric vehicle battery pack was chosen to be the base for both chemistries, with the pack design being based on the design used in the Nissan Leaf, which utilises a pouch cell configuration. Other cells, such as prismatic and cylindrical, are also used in electric vehicle battery packs, but are not as prevalent as pouch cells and would have several differences in their environmental impact, owing to the different materials and quantities used in their casing. A capacity of 60 kWh was chosen to give desirable range, with the model being designed to allow for examination of the whole pack's impacts, as well as the emissions per kWh of capacity for the pack. The two battery chemistries chosen to compare with one another were a lithium nickel manganese cobalt Oxide active material, with a 5:3:2 ratio of nickel manganese and cobalt (532 LiNMC), and a O3 type sodium metal oxide active material. These materials were chosen as there was an interest in both these materials and examining them to compare with other similar materials, including 111 LiNMC. Within the battery market, a 622 ratio is currently the standard within LiNMC batteries, although it is rapidly being usurped by an 811 ratio (Miao et al., 2019). Neither have production data easily available however, while the 532 ratio does, which made it an easy choice for this project. A decision was also made to keep as many of the components of the battery packs the same between the two chemistries to better compare how the chemistries impacted the emissions of battery pack production.

The 60 kWh battery packs were based off 40 kWh battery packs used by the Nissan Leaf in 2018 (Marklines, 2018). Within this, it is assumed to operate at 350 V, with the cells providing the 60 kWh capacity arranged into modules of eight cells each. The exact configuration of

modules depending on the battery chemistry to reach the required capacity, as each one provided a different capacity for the same 261 x 215 x 7.9 mm dimension cells within them. For this model, the lithium-ion pack used 26 modules while the sodium-ion pack used 30 to reach the 60 kWh capacity. Both pack are also modelled as using an aluminium radiator and glycol coolants for the cooling system, along with a packaging system comprising of aluminium, steel and polymers (L.A.W. Ellingsen et al., 2014).

3.2.4. Battery pack structure

The battery pack was structured to contain four major components, the battery modules (including cells), the battery management system (BMS), the battery cooling system and the structural packaging. The modules' structure consists of eight battery cells, along with a packaging and management system comprising of aluminium sheets, copper wires, polyethylene, and electrical circuit boards. This was derived from a similar design used by Nissan, as well as shown in other literature (L.A.W. Ellingsen et al., 2014). This provided a battery pack specific capacity of 0.223 kWh kg^{-1} for the 532 NMC lithium-ion pack and 0.133 kWh kg^{-1} for the O3 type sodium-ion pack. As previous life cycle assessments of similar battery packs indicated that the battery cells were the largest contributor to environmental issues, they were made the focus of these models, with less detail being granted to the other components of the battery pack. Figure 3.2 displays the structure of the battery pack, with an image from public domain, while figure 3.3 displays the pack assembly process:

Figure 3.2: Battery pack cross section (Kane, 2019)

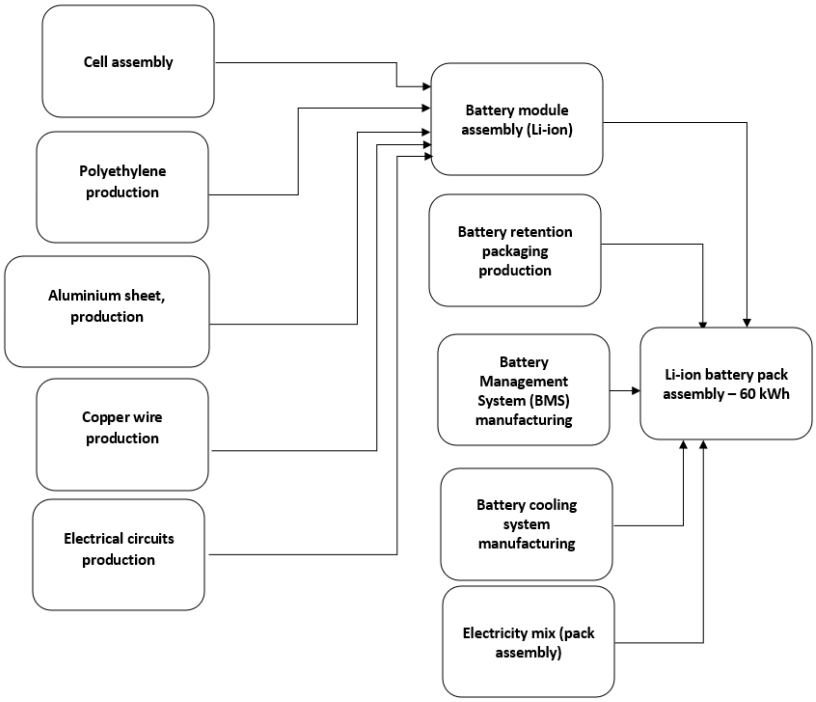

Figure 3.3: Battery pack and module production process

3.2.5. Battery cell assembly

The battery cell has five major components and is assembled in a multi-stage process which detailed different parts of the production of the cell. The process is assumed to start with the initial assembly of the battery anode, cathode, separator, and casing, with the cell using 24 pairs of anodes and cathodes to produce each cell. This was derived from the design of Nissan LEAF cells used as the base of the pouch cell in this model. After this, the cell is filled with the electrolyte and sealed. The cell is then pre-charged before passing to the module assembly stage. Alongside the processes listed, the cells also were assumed to be produced in a dry room, which was necessary given the cell electrodes sensitivity to moisture in the air. Figure 3.4 displays the structure of the cell from public domain, while figures 3.5 and 3.6 display the assembly processes of the battery cells:

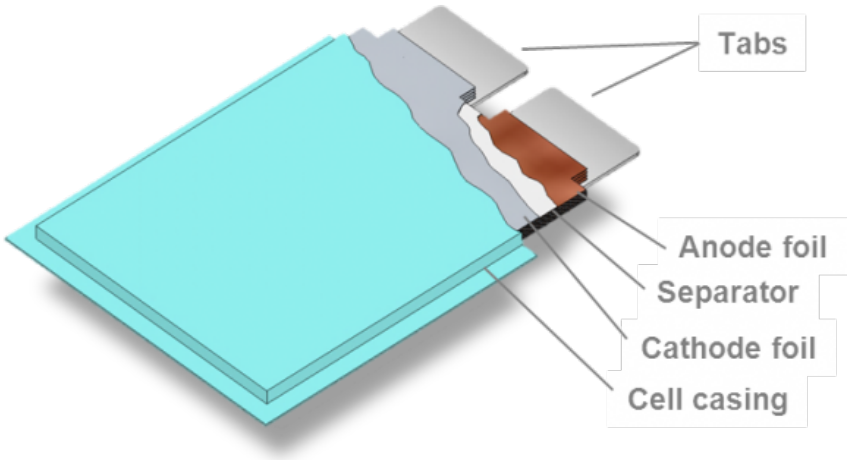

Figure 3.4: Pouch cell structure (EWI, 2021)

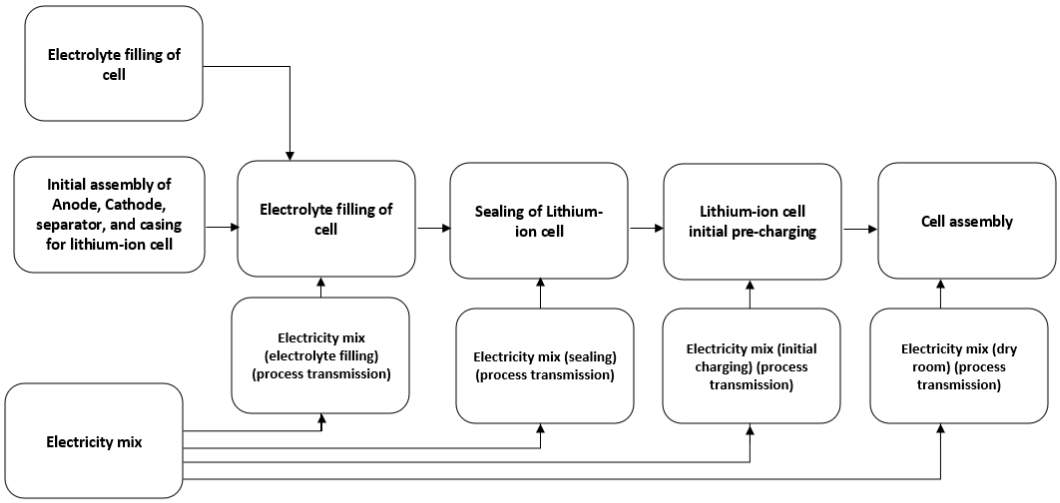

Figure 3.5: Assembly process of battery cells for LCA model (part 1)

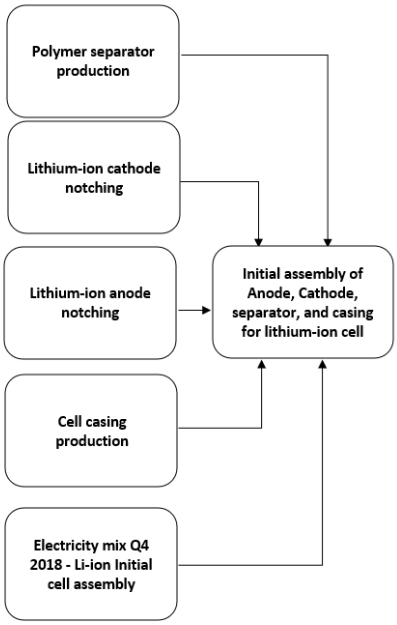

Figure 3.6: Assembly process of battery cells for LCA model (part 2)

3.2.6. Battery separator and casing production

The separator used in the cell to keep the anode and cathode apart was decided to be a polymer separator, commonly used within industry, with two different polymers, polyethylene, and polypropylene, being used to produce the separator. The cell casing

would be produced as a layered material of aluminium foil and polymers, with nylon 6 and polypropylene being used to manufacture the casing for use.

3.2.7. Battery electrolyte

The electrolyte requires two vital components, those being the solvent used, along with the metal salts needed to provide the ions necessary for the battery to function. The solvent is different for each battery pack, with ethylene carbonate being chosen for the lithium-ion cells and propylene carbonate being chosen for the sodium-ion cells. Similar electrolyte salts were chosen for the two models, to help minimise the differences between the packs, with lithium hexafluorophosphate being used for the lithium-ion cells and sodium hexafluorophosphate being used for the sodium-ion cells. Both salts are created from a process that uses phosphorous pentachloride and a fluoride of the applicable metal, which in turn needed to be produced from their base chemicals, phosphate (P_4), chlorine (Cl_2), fluorine (F_2), lithium (Li) and sodium (Na).

3.2.8. Battery anode and cathode production

The battery cell anodes and cathodes are manufactured in similar ways, as both require multiple stages of processing to produce the shaped electrodes used in the cells. The first stage of both was to mix their active materials, carbon black, binder, and solvents into an electrode ink, which was then spread on a metal current collector. For the sodium-ion battery pack, both the anode and cathode use aluminium foil as the current collectors, while the lithium-ion battery pack use aluminium foil for its cathode and copper foil for its anode. Both are then dried, with the cathodes of both packs also requiring processes to dispose of the solvent vapour as they both used NMP as the base of their cathode inks. The dried electrodes are then calandared to give them an even surface before being cut in a process known as notching to the sizes needed for the cell assembly process. Figure 3.7 displays the production process of both the anode and cathodes:

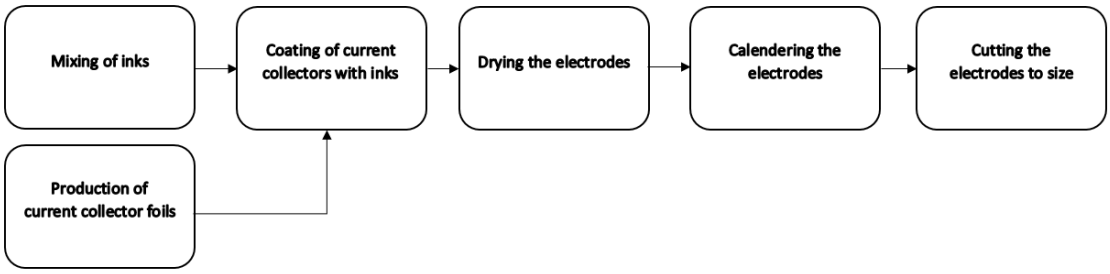

Figure 3.7: production process of the anodes and cathodes in the lithium-ion and sodium-ion battery cells

3.2.9. Battery materials production

Aluminium and copper production

The aluminium and copper production for the battery pack followed the Hall–Héroult process for aluminium and the Outokumpu process for copper. The aluminium was assumed to be produced from mined bauxite ore, the most common ore for aluminium(Schwarz, 2004). This needed to be initially processed into aluminium oxide, a process involving the bauxite being mixed with sodium carbonate and sodium hydroxide, before being heated to removed inpurities, which are then remov(The Aluminium Association, 2013). The aluminium oxide is the dried and converted into molten aluminium via electrolysis, which uses a considerable amount of electricity, along with the production of carbon anode used in the electrolysis process (The Aluminium Association, 2013) then cast into ingots, before being rolled into battery grade foil, with care taken to keep the aluminium free of contamination during the rolling process(The Aluminium Association, 2013) (European Aluminium Association, 2013).

Meanwhile the copper used the Outokumpu process after floatation of the mined chalcocite ore to purify the ore, before it is roasted and melted in a flash furnace, before being reduced to produce the molten copper and cast to produce the final copper ingots (Thinkstep, 2020). These are also rolled into battery grade foil for use in the battery current collectors, along with different processes where needed in the battery pack, such as copper wiring (European Aluminium Association, 2013). Figures 3.8 and 3.9 display these processes:

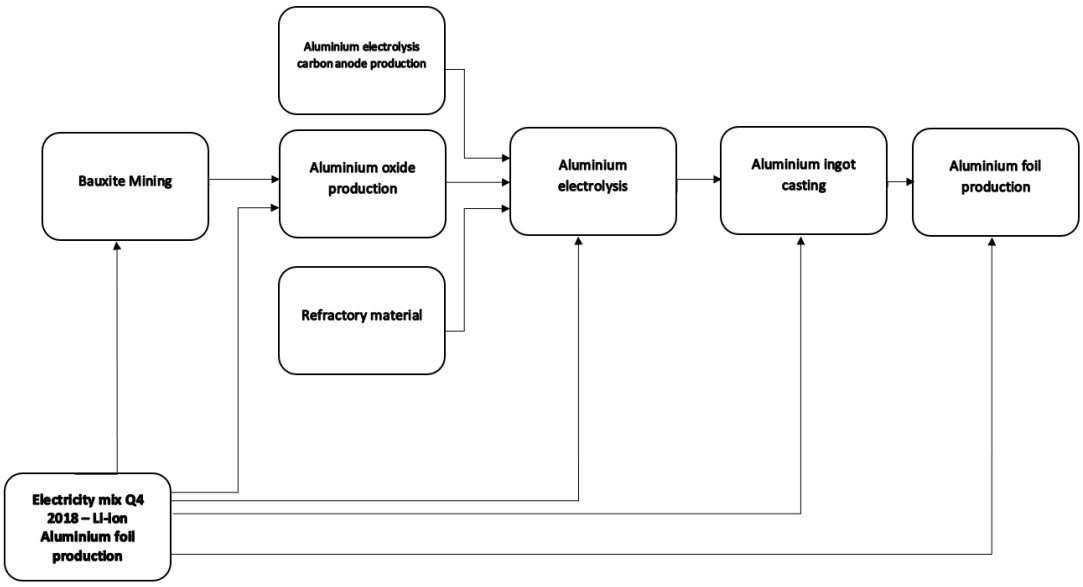

Figure 3.8: Process flow diagram of aluminium production

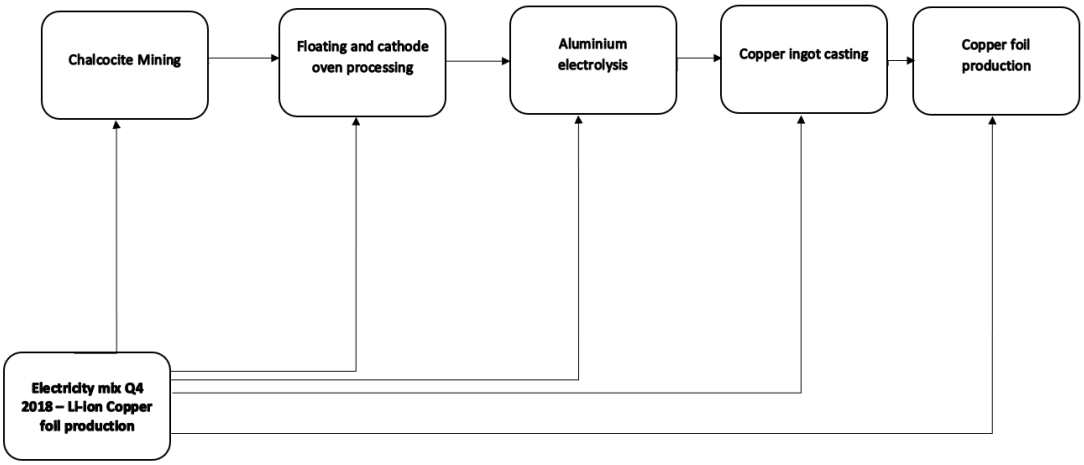

Figure 3.9: Process flow diagram of copper production

Anode materials

The key components of the anode inks used in the anodes for both battery packs were graphite, carbon black and de-ionised water, with each pack using different binders in line with literature sources. The lithium-ion battery pack anodes used a mix of CMC and SBR in

its ink as a binder, like the supercapacitor electrodes mentioned in chapter 2 of this report, while the sodium-ion pack anodes used poly-acrylic acid (PAA) as its binder.

The graphite can be manufactured synthetically as well as mined, with this model utilising a synthetic method using coke and hard pitch, while the carbon black is assumed to use a similar method with acetylene as a feed stock (Dai et al., 2018). Both undergo a process of baking at 1000^{o}C before being heated to 3000^{o}C to graphitise them into their respective products. The de-ionised water is produced through reverse osmosis of groundwater, to remove the impurities present. The CMC was derived from cellulose extracted from sugarcane, with a synthesis process being used with the cellulose, sodium hydroxide, mono- and iso-propanol, all being mixed in a stirred tank before phase separation, neutralisation, washing with ethanol, and filtration before drying the result (Alizadeh Asl, Mousavi and Labbafi, 2017). Meanwhile the SBR was derived from the free-radical polymerisation of butadiene with styrene at around 30-60 ^{o}C (Polymer Properties Database, 2015). Finally, the PAA was produced from free-radical polymerisation of acrylic acid, which also used chemical such as sodium pyrosulphate and potassium persulphate as chemical indicators, before the final polymer is purified for use (Dai et al., 2018). The final composition of the anode ink can be seen in table 3.3:

Table 3.3: material masses used in production of wet (MTI Corporation, 2013) (Yuan et al., 2017a)

INPUT	**VALUES**
Graphite	0.2894 kg
Carbon Black	0.0031 kg
CMC	0.0069 kg
SBR	0.0069 kg
De-ionised water	0.3473 kg
Aluminium	0.3464 kg

Cathode materials

The cathode inks followed the same basic structure of the anode inks, with an active material, carbon black, a binder and solvent to produce the ink. Both the lithium-ion and sodium-ion inks used PVDF as the binder and NMP as the solvent, with the major differences being the active material and the exact composition of the inks. As described in earlier sections, the lithium-ion cathode uses 532 LiNMC as its active material, while the sodium-ion cathode uses an O3 type sodium metal oxide, with iron, manganese, titanium, and nickel being the major transition metals used to produce it. The active material production is described in more detail below in tables 3.3 and 3.4, with the carbon black production is already described in the section on anode materials.

To produce the PVDF used, a similar free-radical polymerisation process as the one used to production PAA, is used to polymerise di-fluoroethylene in a suspension between 10-150 ^{o}C and at pressures of around 1-30 MPa (Dai et al., 2018). For the NMP production, butyrolactone was reacted methylamine at 250-400 ^{o}C and 6-12 MPa in an exothermic reaction, with the resultant liquid then being distilled into NMP (Lammens et al., 2011). The overview of the lithium-ion cathode ink production can be seen in table 3.4 and figure 3.10:

Table 3.4: material masses used in production of wet cathodes (Liu et al., 2014) (Yuan et al., 2017a)

Input	Values
Cathode active material	0.3237 kg
Carbon Black	0.0254 kg
PVDF	0.0146 kg
NMP	0.2091 kg
Copper	0.4272 kg

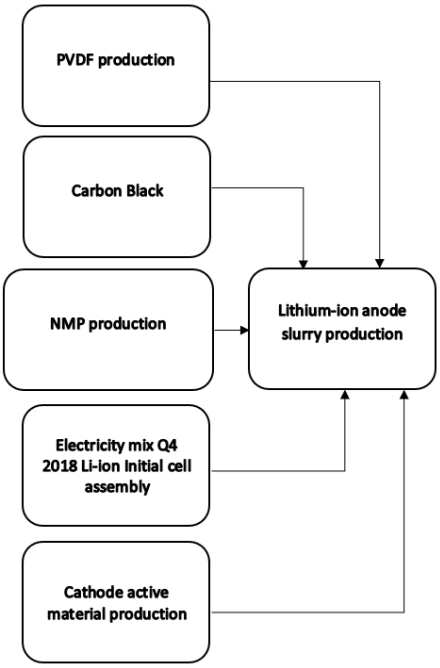

Figure 3.10: Cathode ink production for lithium-ion battery pack

Cathode active materials

The cathode active materials of the battery packs were produced in similar manners, with key metal and chemical compounds being examined in depth following them from excavation as ores through to the final processing into the active materials. The lithium-ion LiNMC used lithium carbonate and several metal sulphates to be produced, while the sodium-ion O3 type sodium metal oxide was produced from sodium carbonate and several metal oxides. While the LiNMC data could be drawn from an industrial scale process (Ahmed et al., 2017), no data at such a scale could be found for the O3 type sodium metal oxides, most likely due to it being a relatively new development. To this end, the quantity and methodology of producing the O3 type active material was derived from a lab-scale process, as this was proven to produce the desired product and was derived from a peer reviewed source (Yue et al., 2015). Table 3.5 displays the input materials used in the lithium-ion cathode active material, while table 3.6 displays the inputs for the sodium-ion cathode active material:

Table 3.5: 532 LiNMC cathode active material production material inputs

Input	Values
Ammonium hydroxide 30% solution	0.698 kg
Cobalt Sulphate	0.370 kg
Lithium Carbonate	0.399 kg
Manganese Sulphate	0.541 kg
Nickel Sulphate	0.923 kg
Oxygen, in air	0.083 kg
process water	15.285 kg
Sodium Carbonate	1.265 kg

Table 3.6: O3 type sodium metal oxide cathode active material production material inputs

Input	Values
Iron (III) Oxide	0.154 kg
Manganese (IV) dioxide	0.137 kg
Nickel (II) oxide	0.145 kg
Sodium Carbonate	0.409 kg
Titanium Dioxide	0.154 kg

Each of the martials described here were examined back to their entrance into industrial processing, the cradle of the battery packs life cycle. For the metal oxides, carbonate, and sulphates, this began at the extraction of their ores, and brine in the case of sodium, at mines around the world.

The sodium carbonate began as a brine, which were extracted and purified into a sodium chloride brine before undergoing the Solvay process, which uses ammonium and limestone to convert the sodium chloride into sodium carbonate via carbonisation and calcination

(Steinhauser, 2008). For this model, while lithium can also be extracted from brines, the lithium was chosen to be sourced from Australia, which primarily extracts lithium from ores (Talens Peiró, Villalba Méndez and Ayres, 2013a). This was due to Australia being one of the largest producers of lithium in the world (Talens Peiró, Villalba Méndez and Ayres, 2013b). The lithium ore chosen was spodumene, which was roasted, soaked in sulphuric acid, and roasted again to produce lithium sulphate in a slurry, which was then neutralised and filtered (Talens Peiró, Villalba Méndez and Ayres, 2013a). The resultant filtrate then has impurities precipitated out with lime and sodium carbonate, before re-adjusting the pH with sulphuric acid, evaporating the fluids left and adding sodium carbonate to precipitate out the lithium carbonate, which is then extracted with a centrifuge (Talens Peiró, Villalba Méndez and Ayres, 2013a). Lithium extracted from brines follows a similar set of processes to the sodium carbonate production but is not available in Australia. Figure 3.11 displays the process flow diagram for the sodium carbonate production, while figure 3.12 displays the lithium carbonate process flow diagram:

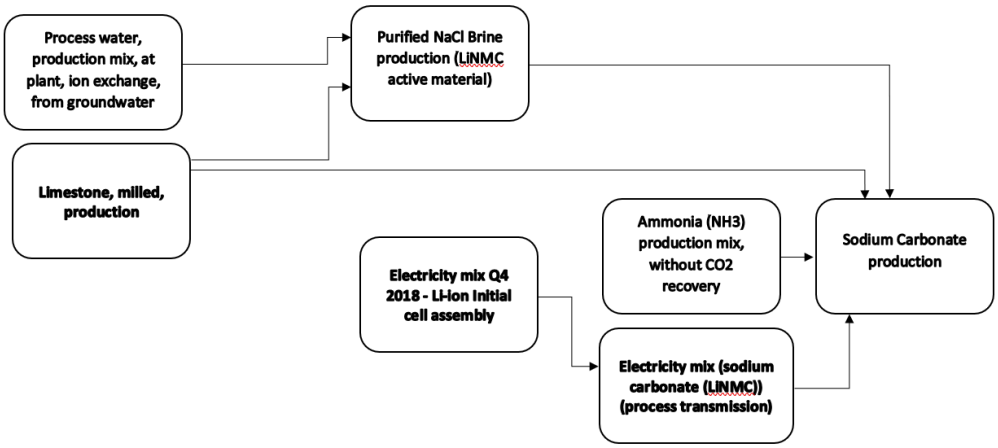

Figure 3. 11: Sodium carbonate production process

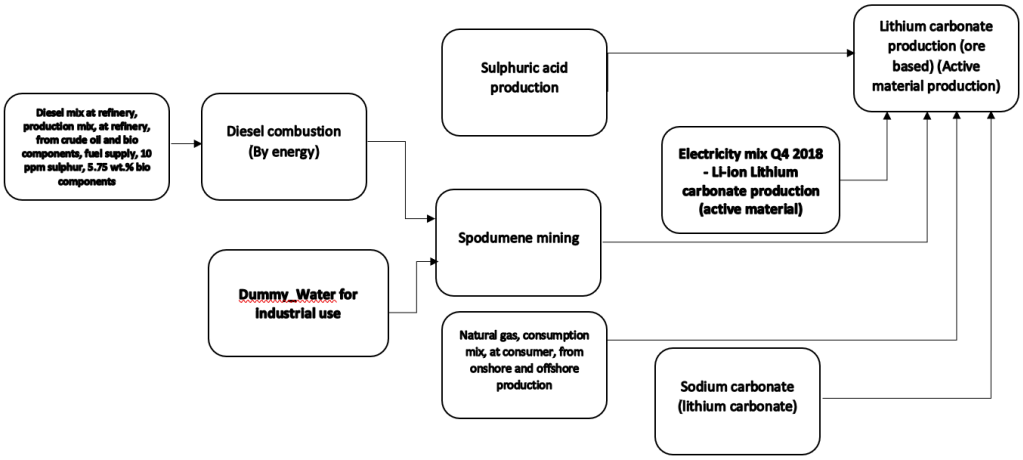

Figure 3.12: Lithium carbonate production process

The nickel and manganese sulphates were produced in similar manners, with the initial stages being the production of the pure metals. The nickel was extracted from laterite, with Australia being a key supplier of nickel ore, with the ore undergoing beneficiation before the nickel is leached out of the ore in a sulphuric acid solution (Khoo et al., 2017). The acidic solution is then neutralised, the solvents removed and the nickel undergoes hydrogen reduction to refine it into a pure metal (Khoo et al., 2017). Sulphuric acid is then used to manufacture the nickel sulphate (Thinkstep, 2020). The nickel production process diagram can be seen in figure 3.13:

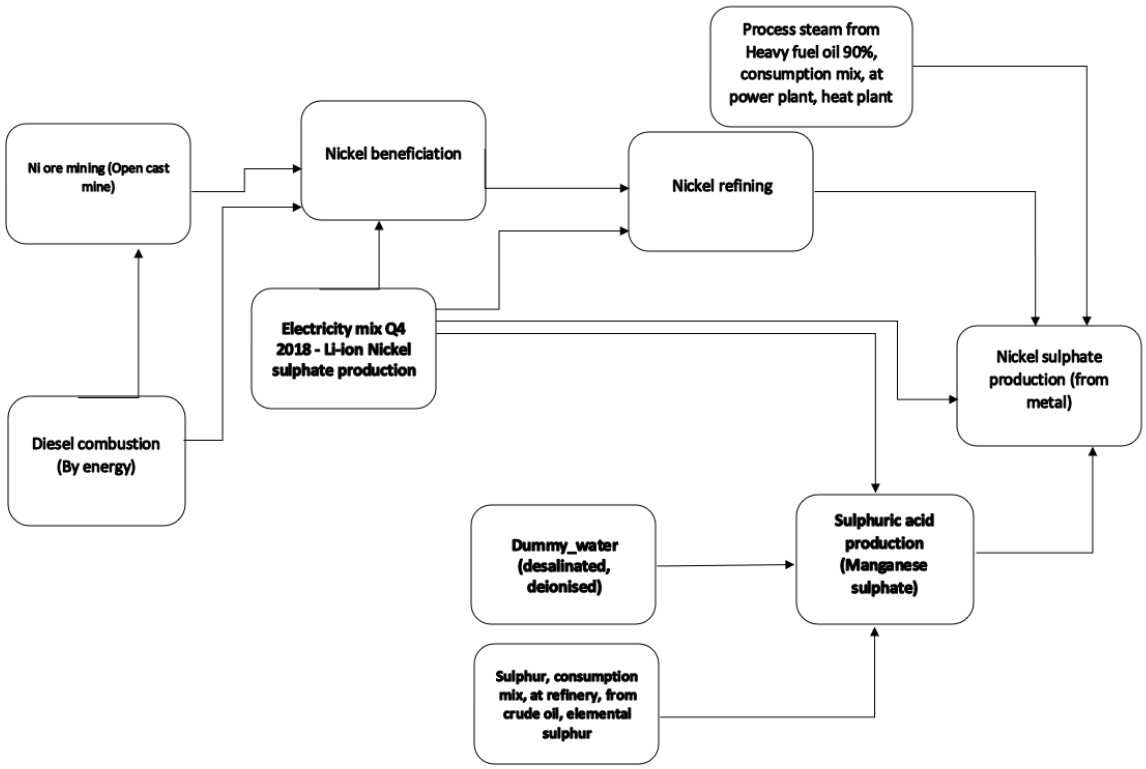

Figure 3.13: Nickel sulphate production process

The manganese was produced from pyrolusite, which was also undergoes beneficiation after extraction (Khoo et al., 2017). The manganese is then leached out of the ore with acids ore bases before being purified and recovered in an Electro-refining process (Baba et al., 2014). As with the nickel, the manganese is converted into manganese sulphate through a reaction with sulphuric acid (Thinkstep, 2020). This is seen in figure 3.14:

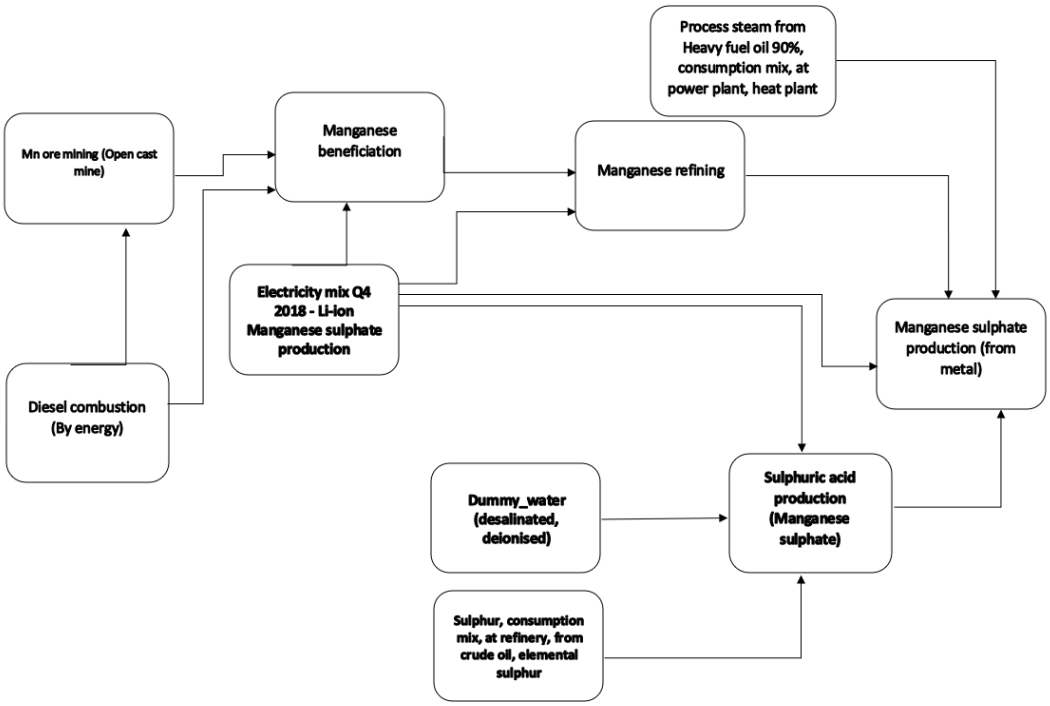

Figure 3.14: Manganese sulphate production process

The cobalt sulphate was produced through a different process, with the processes being divided between the processing of cobalt ore into cobalt hydroxide, which is in turn converted into cobalt sulphate (Q Dai et al., 2019). The production of cobalt hydroxide occurs in the Democratic Republic of the Congo (DRC), while further processing occurs elsewhere, with China being the largest purchaser of the DRC's cobalt materials (Q Dai et al., 2019). After mining, the ore is milled and undergoes floatation, with a number of the sulphate-based ores also requiring further processing, including roasting or pressure oxidation, with the whole cobalt sulphate production detailed by (Q Dai et al., 2019). The cobalt concentrate is then leached with sulphuric acid and sulphur dioxide, which converts the Co^{3+} ions into Co^{2+} ions, with the resultant mix being purified and precipitated into cobalt hydroxide with magnesium oxide. The cobalt hydroxide is then transported to China, where the final cobalt sulphate is produced with sulphuric acid and sodium metabisulphite, which is present to convert any remaining Co^{3+} ions, with the cobalt sulphate then being purified and dried into crystals suitable for use in batteries (Q Dai et al., 2019). This process is shown in figure 3.15:

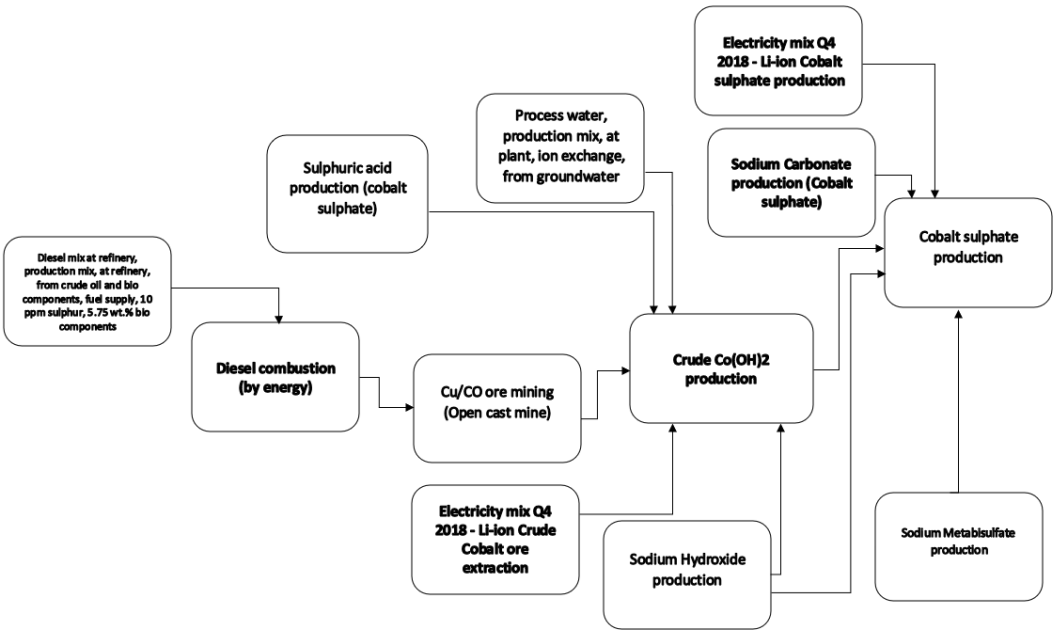

Figure 3.15: Cobalt sulphate production process

For the sodium-ion material production, the same process was used for the production of sodium carbonate, along with similar processes being used to produce pure nickel as described in the nickel sulphate production. Nickel (II) oxide is produced from nickel metal by first melting the metal in a furnace and atomising the liquid metal into irregular droplets and a powder, with the powder being collected and separated into different particle sizes (Koehler, 2015). The appropriately sized particles were then heated in an oxygenated atmosphere at 400 ^{o}C to produce the nickel oxide (Lewis, 1997).

Manganese oxide on the other hand is produced directly from ore, with the processes of beneficiation, leaching and purification being identical (Abdykirova et al., 2016). The difference is that the electrorefining is replaced with an electrolysis process, which produces manganese dioxide (Abdykirova et al., 2016). Iron (III) oxide can be manufactured from iron ore, which first requires processing into iron (II) sulphate (O'Neil et al., 2006). The sulphate can also be derived as a by-produce of pickling steel during its production (Kanari et al., 2018). The titanium dioxide is produced in a similar manner, with ores being processed into titanium sulphate by leaching ores with sulphuric acid, before the sulphate is hydrolysed and calcinated into titanium dioxide (Middlemas, Fang and Fan, 2015).

3.3 Data sources

Many of the materials used in the production had processes detailing their environmental impact present in the databases made available for the software. OpenLCA offers several databases for free, with this project utilising the NEEDS complete, ELCD 3.2 and Ecoinvent 3.5 LCIA methods databases, along with data collected from the GaBi database provided by the University of Warwick. These databases were produced by established companies and organisations that have used LCA methodologies extensively, with the NEEDS and Ecoinvent databases being developed by ESU Services and the ELCD being developed by the European Commission (ESU Services, 2021) (OpenLCA, 2021).

Not all the required data for the model was provided by these databases, as expected, this this initiated a literature search to find appropriate data for the key processes not covered by the databases. One process was the production of the electrical circuit boards, which were vital for the manufacture of the BMS and battery module components of the pack. The paper that provided this process listed the materials needed and the energy demand for their production, which was the data required for the model (Majeau-Bettez, Hawkins and Strømman, 2011). While this was also applicable for other materials, including the production of NMP, other materials, most notably the cathode active materials for the cells, required multiple different papers to address different stages of their production from cradle to gate, which are detailed in Appendix A. Details on locations of material extraction and processing, and the year the data is sourced from are detailed in section 3.5.

The additional processes were also beneficial, as it allowed the model to examine their production in more detail and provide a better view on where their emissions were originating from. Both active materials were based off a solid-state production process for 111 LiNMC, with the base materials being prepared for the process, then being milled together, and passed through a furnace at 800-950^{o}C, with the temperatures changing for each process where appropriate. Each active material used different parts of this process, with the 532 LiNMC using all the elements of the process described in the paper, while the O3 type sodium oxide uses only a few stages, in line with other literature detailing production of sodium-ion active materials of the same type (Yao et al., 2017) (Ahmed et al., 2017).

Alongside requiring data on the production of the base materials for the material, data needed to be sought for the assembly of the battery cells and pack. This data was provided by two papers, one by Yuan et al. (2017b) detailing the manufacturing material and energy demands for each stage of the cell assembly process, although it had to be assumed that all the energy demands were electrical in nature, unless other energy sources, such as heat or gas, were listed. For the battery pack, data was derived from a paper by L.A.W Ellingsen et al, (2014), which detailed different key elements of the battery pack production being produced in an industrial scale plant.

The quantities of each material for one cell were not sufficient for the size cell being used in the pack, with the cells from a Nissan Leaf being used as the design base. This was rectified with appropriate scaling of the required materials, cells, and energy quantities to fit with the design, including for the battery pack, with the sole exception being the BMS, which was assumed to be the same size for most battery packs, with any differences being negligible.

3.4 Model construction

With the data found, the models could begin construction. For several of the components, such as the production of the battery packaging and cell casing, the model examined their assembly materials and energy demands as a single process. In openLCA, this was constructed as a single file within the larger model with inputs and outputs, which had to be manually decided based on the data given, with checks needed to be made to ensure the mass and energy balances of the process were correct. Other processes then fed into these assembly process with the input flows of the process, the materials and energy used as the inputs of the process, being used to connect the production processes of the input material and energy mix.

While the assembly processes for the BMS, battery cooling system, and packaging system were expressed as single processes within the openLCA model, a different approach was used for the cells, an area of more interest for the models. The production process of the cells was constructed with a long list of different individual processes, which allowed for the different stages of production, listed in section 3.2, to be examined in the final model for their contributions to the battery pack production emissions. The following figures display

the processes within the model that make up the larger assembly process, with figure 3.16 displaying the production of the anodes and cathodes, while figure 3.17 displays the assembly, electrolyte filling and pre-charging processes:

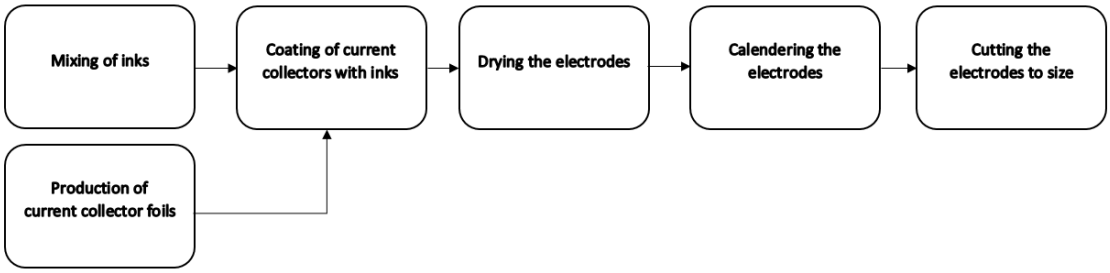

Figure 3.16: Electrode manufacturing process for openLCA model

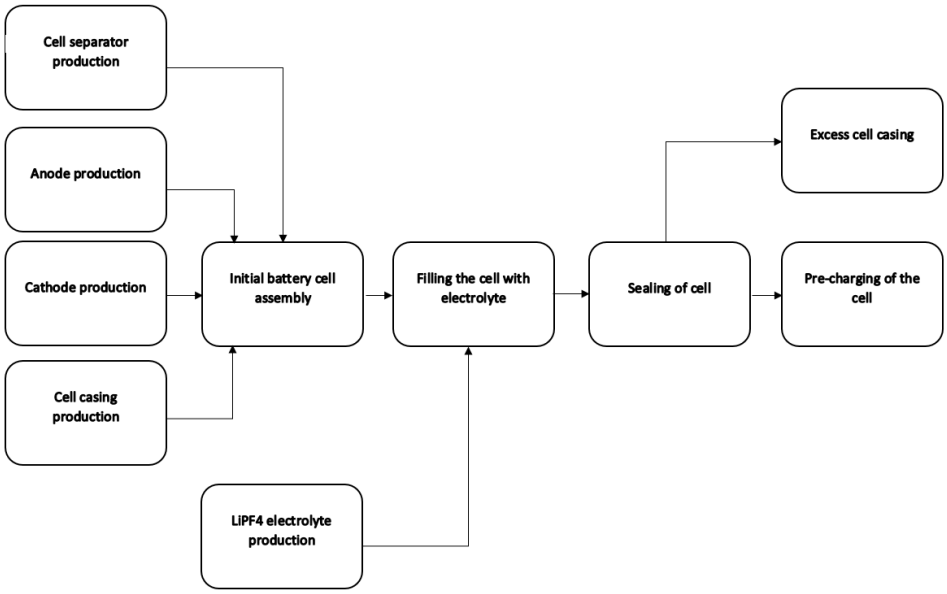

Figure 3.17: Assembly process of battery cell

Along with the processes shown in figure 3.17, an additional process was added after the pre-charging of the cell to display the energy demands needed for the production of the cells within a dry room. While there could be arguments to distribute the additional energy usage between the other processes, presenting it as a single process would give a better optic on how the use of a dry room affects the emissions of the battery pack. For the base materials used in the battery cell, each one required its own process or set of processes to

accurately model to model the emissions. Some of the materials that used multiple processes did so to allow for a more in-depth examination of the different stages of their production, while others required them due to the need to use different sources of data for the various stages of their production. The cathode active materials production and the current collector foils production were of particular interest, given their importance in the battery pack and the multiple and varied processes needed to produce them.

Along with producing new processes within openLCA to fill gaps in the model, some processes were created to keep data up to date. While initially electricity grid data from the databases listed for openLCA were used, research quickly revealed that the data used was out of date, with data being derived from values from 2002-2010, with electricity grids globally changing considerably since that period (International Energy Agency (IEA), 2021). These new processes took a different approach to those used by openLCA, as while the openLCA processes listed direct material inputs and emissions, these newer processes drew electrical energy from processes of electricity generation, such as electricity generated from gas. This allowed for an easily modifiable process, as it relied on national percentages of energy generation methods within their grid. It also allowed for more readily available and up to date data to be used, with national governments and international organisations listing their electricity data in this manner, with the International Energy Agency (IEA) and UK government providing such information. This was then combined with data from openLCA's databases on the impacts of each energy generation method to construct a process for the energy mix of a nation, which was assumed to be uniform for each country. Table 3.7 displays an example of this, with the electricity mix for the UK:

Table 3.7: UK energy generation methods proportions within the electricity grid (Q1 2019) (UK Government, 2019) (International Energy Agency (IEA), 2021)

Source	Share of energy produced (%)
Coal	2.13
Oil	0.35
Gas	40.85
Nuclear	17.39
Hydro	1.84
Wind and Solar	23.92
Bioenergy	11.55
Other fuels	1.97

This offers an easy way to add new electricity mixes, as the process file that contains this data can easily be copied within openLCA and changed when needed to account for the different energy mixes found around the world. This allowed for the different electricity data values needed for the model to be created quickly and with an easy means to update them when new data arose.

3.5 Model iteration and improvement

While the initial version of the models covered the full length of the production process, there were some difficulties getting the desired data, such as the breakdown of aluminium production, which would be useful given its prominence in both packs. While the openLCA databases offered data to produce aluminium, its production was only displayed as a single process, lacking the breakdown of the process the model desired. This led to other sources of the data being found, ranging from other LCA databases to literature, and integrated into the model, with aluminium being one of the most comprehensive. The literature data for aluminium broke the production of aluminium down into multiple different processes, from the extraction and processing of aluminium oxide through to the rolling of the aluminium into foil used for the current collectors, along with the battery and cell packaging. This helped improve the model, as it allowed for a more in-depth examination of the aluminium

production of the battery pack and how different parts of its manufacture contribute to its impacts.

Changes were also made to the electricity mix processes as well, with the initial design linking production methods to electricity mixes for each country the materials were produced in, with one electricity mix process for each nation. This was due to the high electricity demand of different stages of the battery production process and a desire to examine the different impacts of each stage, with other energy sources, such as natural gas for heating, were relatively small in comparison to the electricity demand. This was changed to group processes by the raw material that would be produced with them and giving them unique electricity mix processes, which further assisted in the granularity of the model and allowing for different parts of the production process to be examined. This would also make the model easier to modify in the future, should a new electricity mix be needed for a process, whether from a change in a nation's energy generation methods in the future or if the process is moved to a new nation. Figure 3.18 displays the difference between the two designs within the model:

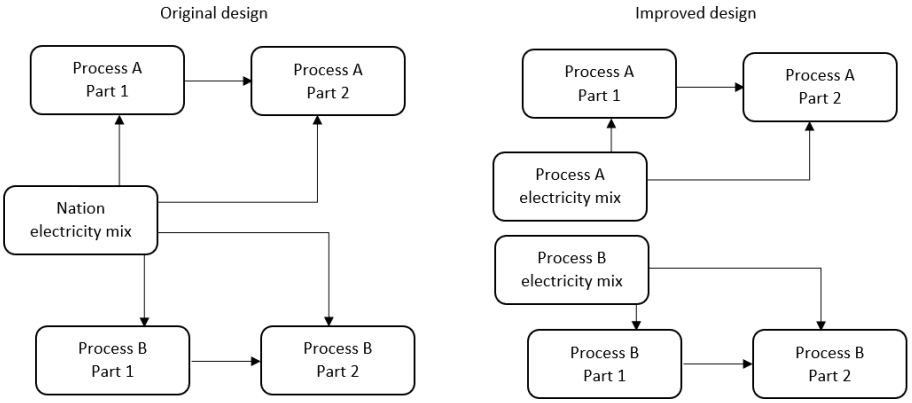

Figure 3.18: Original and improved model design for electricity mixes

Along with the changes to the electricity and aluminium, other changes were made. While distances covered for each key material were added to the initial model, they only covered distances between nations, whereas it was decided that more precise locations were needed for the model. This examined the distances travelled by each material through cargo ship and lorry transportation methods. This resulted in multiple mine locations needing to be found, the distances between them and the UK manufacturing centre calculated, and

how much of that distance was coved by different transport solutions. The UK centre was decided to be based in Coventry, as there is a UKBIC manufacturing centre already present, along with a large amount of interest in establishing a manufacturing facility in the same region (UK Battery Industrialisation Centre (UKBIC), 2021). It was assumed for this model that all battery assembly processes would take place at this facility, starting with the production of the cathode active material and ending with the final battery pack. This means that the data would be beneficial for a potential future development in Coventry and the processes conduced within it. It was assumed that the shortest distances were used in this model, from processing location to the nearest port being covered by cargo lorry transportation, with cargo ships used to transport the materials between nations. Except for cobalt sulphate, it was assumed that materials were extracted and processed within the same location. Table 3.8 displays the different locations various materials were sourced from, listing the location and the nation it is in:

Table 3.8: Locations of raw materials used in battery model (excluding energy demands) 2019

Material	Location
Acetylene	Immingham, UK
Carbon black	Tonbridge, UK
Synthetic graphite	Humber, UK
Organic solvents	Teesside, UK
Polymers	Dumfries, UK
Steel	Port Talbot, UK
Lithium	Greenbushes, Australia
Manganese compounds	Groote Eylandt, Australia
Nickel compounds	Greenbushes, Australia
Titanium compounds	Tongling, China
Iron compounds	Cooljarloo, Australia
Copper	Chuquicamata, Chile
Aluminium	Weifang, China
Cobalt compounds	Guangzhou, China
Sodium compounds	Tianjin, China
Cobalt ore	Katanga, Democratic Republic of the Congo (DRC)

These locations were chosen as they represent extraction and processing facilities of these material across the global, with the electricity mixes for each material being changed to match with the mixes used in their respective country. Each nations energy mix was assumed to be uniform across the different locations the materials were sourced from within that nation, due to a lack of verifiable data on energy mixes in specific locations (International Energy Agency (IEA), 2021). Preference was given to UK based suppliers for certain materials, such as polymer and steel production, as the UK has production facilities for these materials so it would make sense for a UK based battery assembly plant to use materials from these facilities. Other locations used were based on the largest producers of these materials by nation, such as Australia for lithium production, with appropriate facility locations found within these nations (US Geological Survey, 2022). The exception for this was

nickel, as Indonesia was the largest producer at the time but the government had instituted a ban on the export of nickel, leaving Australia the largest producer after them (NS Energy, 2021)(Listiyorini, 2022). These locations were used for both the lithium-ion and sodium-ion models, as they were assumed to be manufactured in the same location.

3.6 Model results

3.6.1 Battery pack results comparison

From the finalised models, a range of different data sets were produced with the ReCiPe v1.13 methodology, with several different impact categories being of interest. Figure 3.19 displays the global warming potential and human toxicity between the two battery packs, both shown as a percentage of the lithium-ion packs impact:

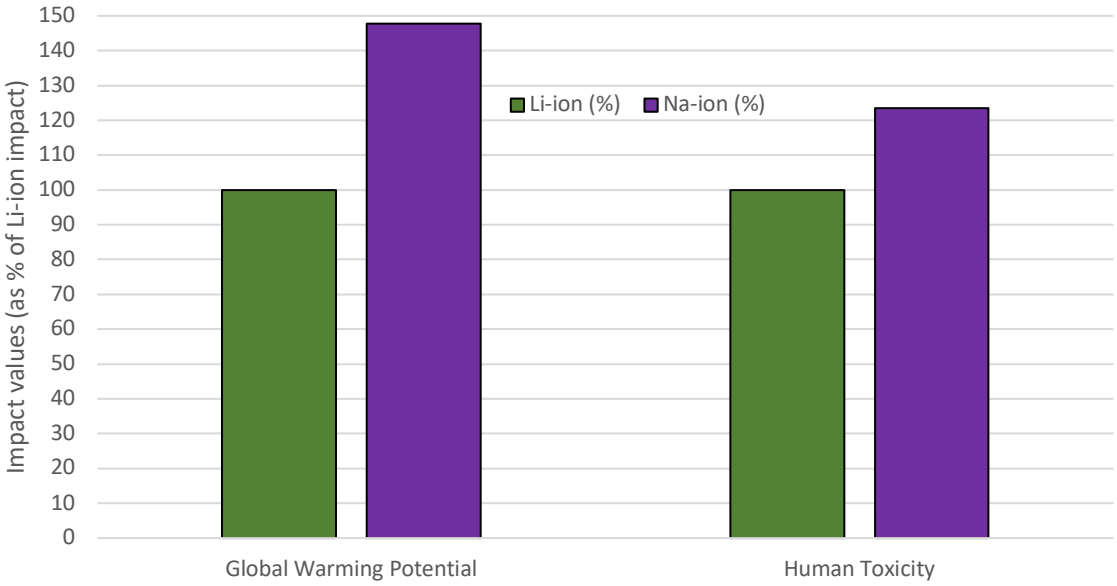

Figure 3.19: Global warming potential (GWP) and human toxicity comparisons between battery packs

As can be seen, the sodium-ion battery pack produces almost 50% more GWP compared with the lithium-ion, while also producing around 25% more human toxicity impact. This can primarily be tied to the requirement for more cells to meet the 60 kWh capacity the battery packs needed, as cells made with O3 type sodium metal oxides more often have lower capacity per unit mass compared with the 532 LiNMC cells (Qiang Dai et al., 2019). This inherently leads to not only higher material and energy demand to manufacture the cells but also additional material for the other components of the battery pack, such as the packaging and cooling system. This can be seen when examining the overall masses of the

modelled battery packs, with the sodium-ion battery pack having a 22.7% increase in modelled mass, sitting at 509.32 kg, compared with the lithium-ion pack at 415.25 kg. This shows similarities to the increase in human toxicity although does not fully explain the increase in GWP. Further examination revealed that most of the increase in mass was due to the increase in materials that have a high GWP in their production, such as steel, aluminium, copper, and rare earth elements used in the production of the cathode active materials. This would explain the disproportionate increase in GWP shown in the sodium-ion pack compared to the lithium-ion pack. Similar patterns can also be seen in other impact categories, as seen in figure 3.20, 3.21, and 3.22, further reinforcing this hypothesis:

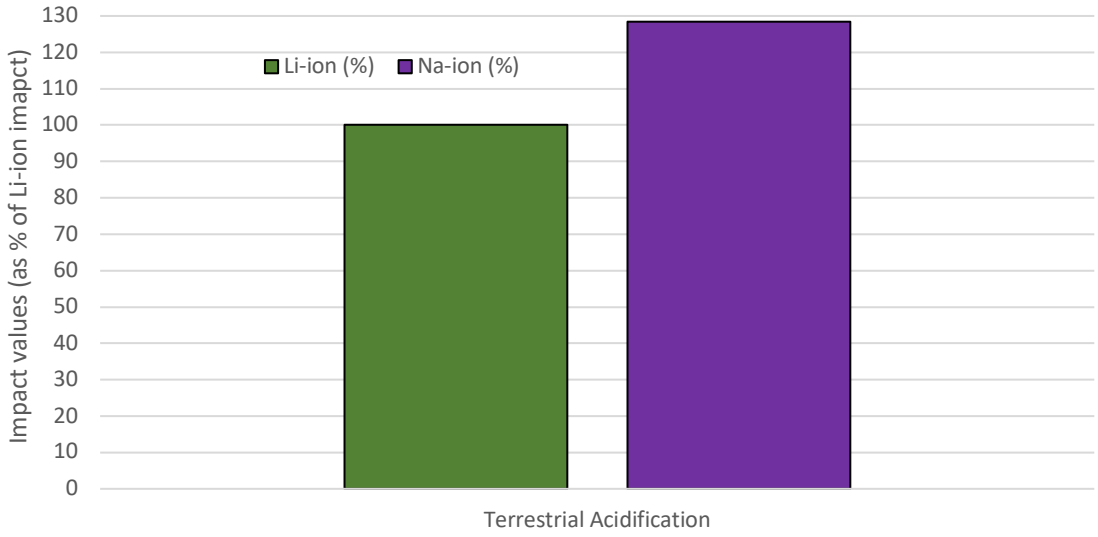

Figure 3.20: Terrestrial acidification comparison between battery packs

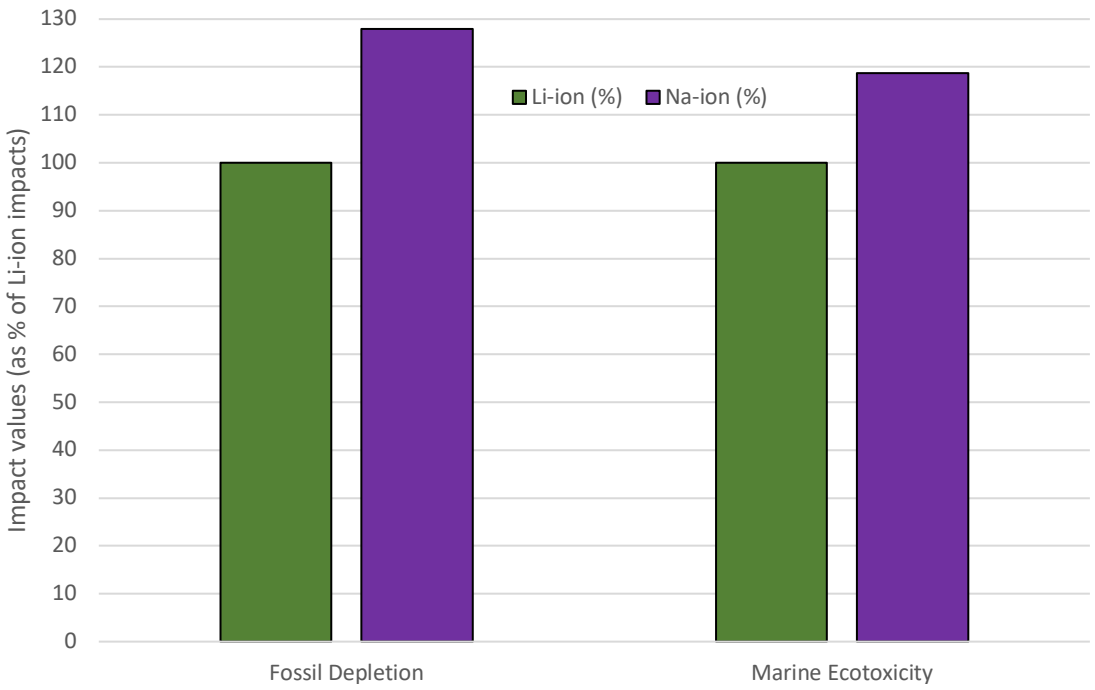

Figure 3.21: Fossil depletion and marine ecotoxicity comparisons between battery packs

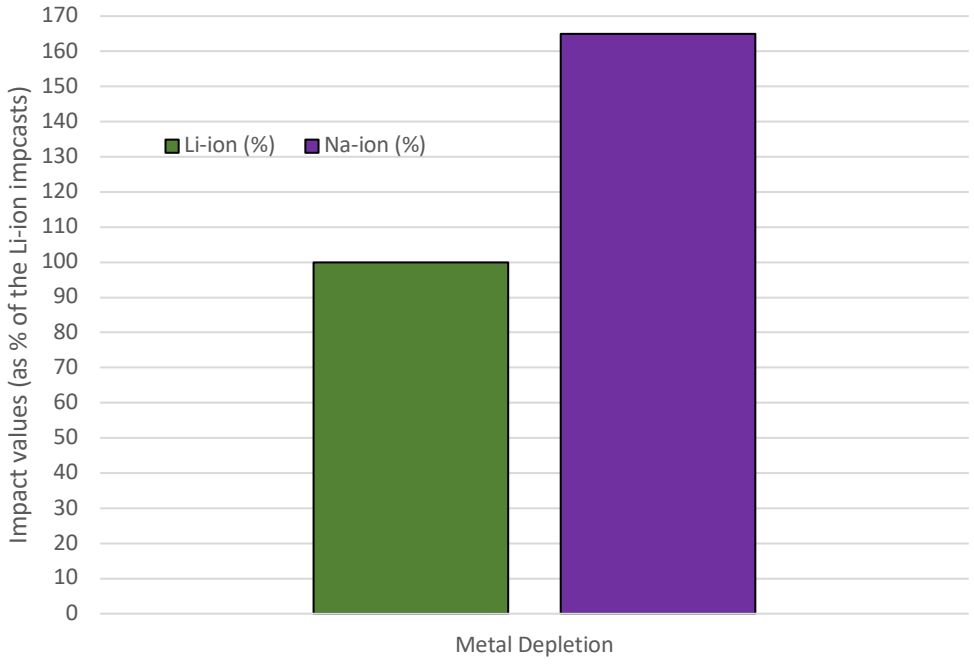

Figure 3.22: Metal depletion comparison between battery packs

The graphs shown above have similar figures to that of human toxicity, with metal depletion being an obvious exception with around a 65% increase between the sodium-ion and lithium-ion battery packs. This is most likely related to the increased number of cells the sodium-ion pack required, which requires a larger quantity of materials and a larger cooling system the battery pack would need to effectively cool these cells. This this is further supported by a similar increase in GWP seen in figure 3.19, which is attributed to the increase in metals, particularly steel and aluminium, both by the increased overall mass and the increase in the number of sodium-ion cells required .

Alongside the data produced by the openLCA models, data was also recovered from literature for both lithium-ion and sodium-ion battery packs to compare with the produced data. The literature data was chosen to be as close to the battery chemistries of the modelled battery pack as possible with the data available at the time. While some of the data was derived from different methodology, they were considered appropriate for comparison as their methodologies were similar. One example being the data from Accardo et al (2021) utilising CML as its LCA methodology, which was the basis for the ReCiPe midpoint values used in this paper (Goedkoop et al., 2013). Table 3.9 displays this comparison, with the literature data examining a 111 LiNMC battery pack, and a Manganese, Magnesium, Titanium, and Nickel based layered oxide sodium-ion battery pack:

Table 3.9: Comparison of model and literature LCA data for battery packs

Impact factor	Li-ion pack	Na-ion pack	Li-ion pack literature (ACCARDO ET AL., 2021)	Na-ion pack literature (PETERS ET AL., 2016)
Active material	532 LiNMC	O3 type metal oxide	111 LiNMC	Layered metal oxide
Specific capacity (kWh kg^{-1})	0.224	0.138	0.197	0.128
Global warming potential (kg CO_2 eq kWh^{-1})	74.319	109.78	135.62	140.330
Terrestrial Acidification (kg SO_2 eq kWh^{-1})	0.214	0.274	3.78	1.51
Human Toxicity (kg 1,4-DCB eq kWh^{-1})	35.094	43.325	N/A	168.15
Fossil Depletion (kg oil eq kWh^{-1})	35.711	45.699	N/A	37.35

The differences between the results of the literature data and the data collected from the models can be attributed to the different active material and the different specific capacities they offer. Lower specific capacity would require more materials to achieve the same capacity, which explains the higher values as both literature sources have lower specific capacities to the packs examined in these models. There is also the question of how the different active material compositions affect the impacts of the battery packs, with the 111 LiNMC active material requiring more cobalt compared with the 532 LiNMC. This increases the impact of the production of the active material, as the extraction of cobalt has a high set of impacts per kg compared with manganese extraction (Accardo et al., 2021). Similarly, the layered sodium-ion active material in the literature study excludes the iron component

found in the modelled sodium-ion battery pack, with a magnesium component taking its place (Peters et al., 2016). This probably contributed to the increased impacts of the literature study, as the iron oxide was assumed to be derived directly from Bauxite ore with minimal energy demand, being derived from data of a similar process used to produce manganese oxide (Norgate and Haque, 2010). In comparison, common methods of magnesium hydroxide, listed as the magnesium source in the literature study, are derived from magnesium salts, such as magnesium sulphate, which require higher energy demands for multiple processes (Peters et al., 2016) (Jarosinski et al., 2020)

3.6.2 Active material results comparison

Examining the active materials of two battery chemistries displayed some surprising results, with the sodium-ion active material producing only 24.3% of the lithium-ion active material's emissions, with the sodium-ion terrestrial acidification values being as low as 14% of the lithium-ion values. This is seen in figures 3.23 and 3.24:

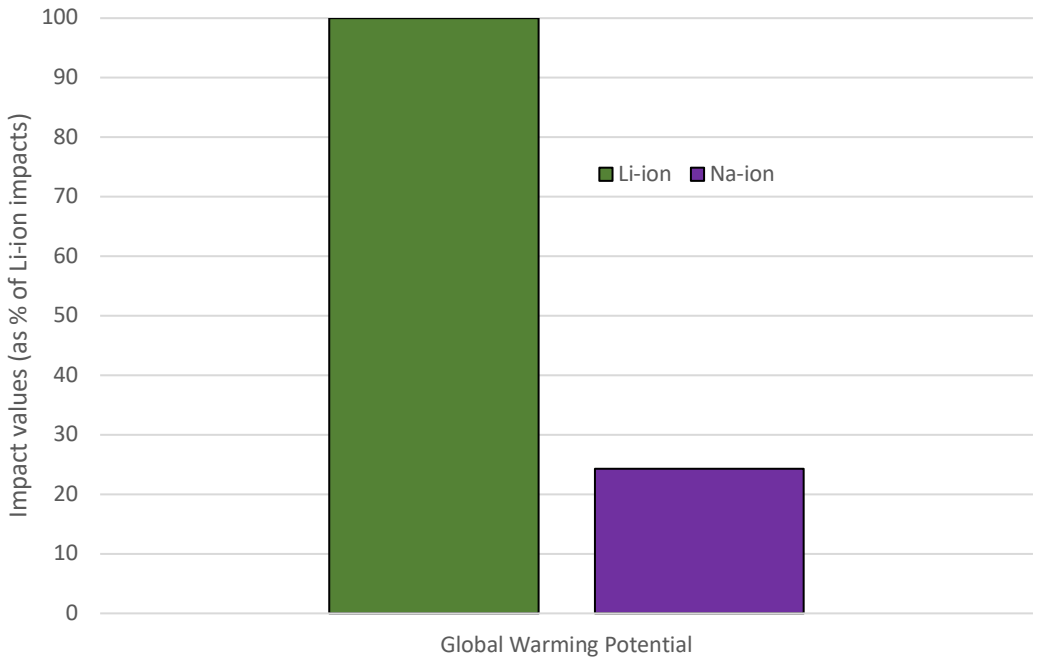

Figure 3.23: GWP comparison between battery active materials for the whole battery pack

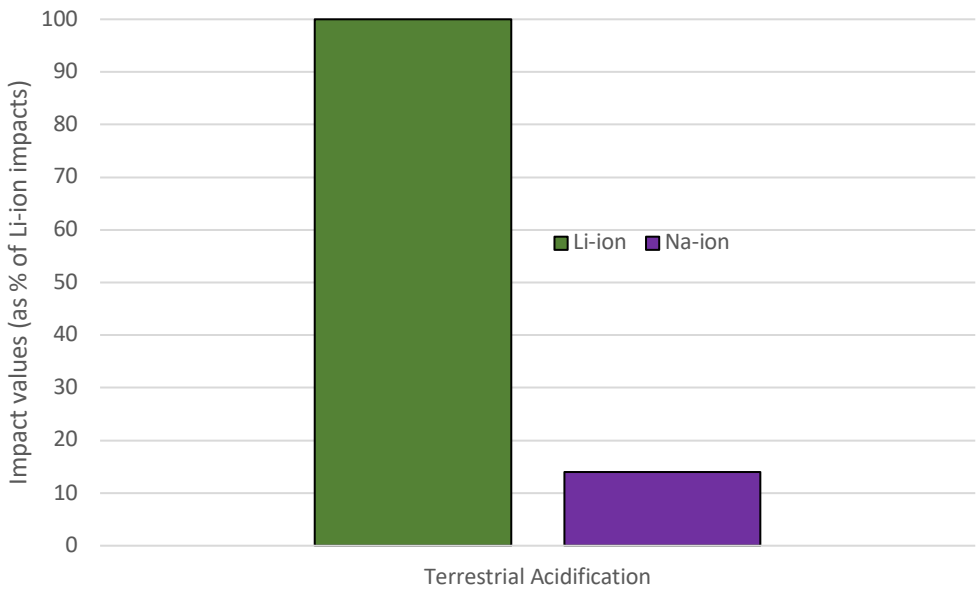

Figure 3.24: Terrestrial acidification comparison between battery active materials for the whole battery pack

The difference has connections to the higher quantity of active material present in the lithium-ion cathodes compared with the sodium-ion cathodes, although the most likely justification is the differences in the processes used in each. While both use data from a 111 LiNMC production process, the 532 LiNMC active material follows it much more closely, while the O3 type sodium oxide production only uses elemental and is derived from a lab-scale production process detailed in literature. Inherently, processes change between lab-scale and industrial-scale, as processes that can be produced in a small batch may not scale up to a continuous or semi-batch large scale process, whether this is an issue with the process's chemistry or economic viability. The lab scale process did follow many of the similar stages present in the industrial scale lithium-ion active material, with data for energy demand per kg also derived from this lab scale process. The absence of cobalt and the inclusion of other metals which have lower impacts, namely titanium and iron, is likely also be a factor in the lower impact values of the sodium-ion active material.

3.6.3 Aluminium material used impact comparison

As can be seen in figure 3.25, the aluminium GWP emissions for the sodium-ion battery pack was significantly higher than the lithium-ion, with the assumption that all the materials were

virgin, with almost a 260% increase over the lithium-ion emissions. With the increased dependency on aluminium within the sodium-ion battery pack, both from the requirement for more cells and the cells use of aluminium for both current collectors, this graph shows some of the impacts this brings. As can be seen, the electrolysis's high emissions relative to the other stages also shows the problems with the continued use of virgin materials, although these emissions for the electrolysis process does include the production of consumed anode and cathode elements of the electrolysis. This demonstrates the benefits a more granular model offers, an aspect that was also shown in the comparison of the active materials. While applying a different aluminium production process, such as one employing a more efficient electrolysis process, may affect the different internal division of the emissions and potentially reduce the overall emissions.

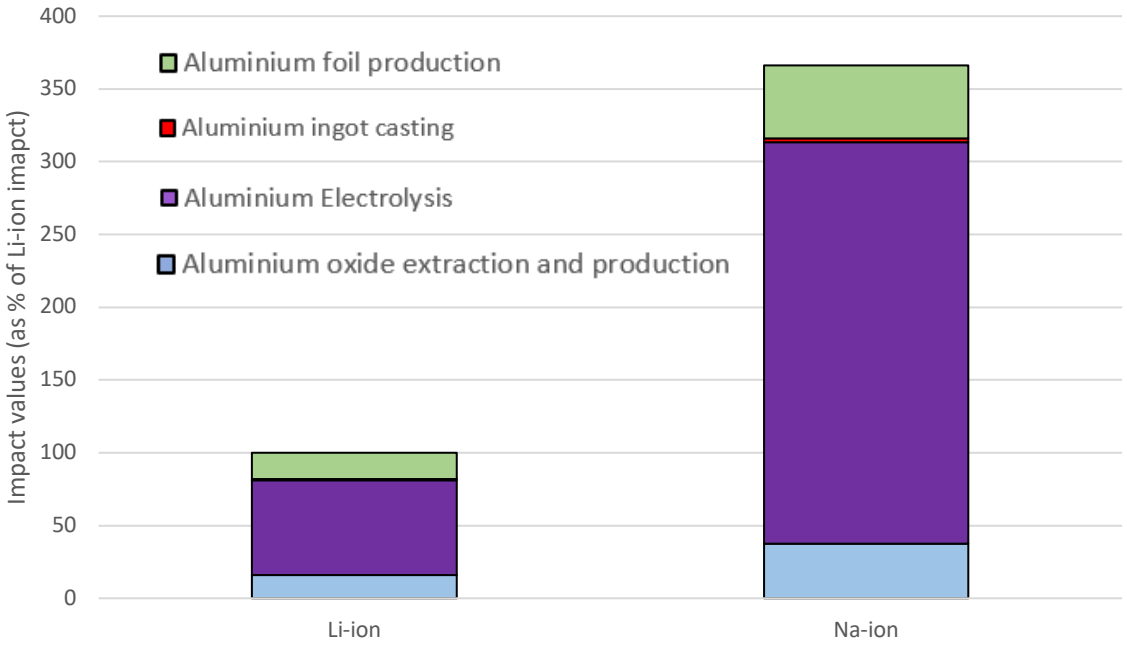

Figure 3.25: Breakdown of global warming potential impacts of aluminium production by stages between lithium-ion and sodium-ion battery packs

3.7 Innovation within the battery pack models

The models do show that with current technologies, the O3 type sodium-ion battery pack is currently far more impactful than the LiNMC battery packs it was compared with, with the reduced capacity of its equivalent cells being one of the major contributors. Therefore, improvements to the battery chemistry of the sodium-ion pack would absolutely be beneficial, with an increase in specific capacity reducing the number of cells needed to reach the pack's desired capacity. Improvements to the production processes, such as developing improved recycling methodologies to allow for recycled aluminium and copper to be used within the cell would most likely give reduced emissions, although this is dependent on the process itself.

The biggest issue with the use of the models is the data available, whether the databases need expanding as new processes arose or the data on offer struggles to remain up to data or limited the user's ability to examine the processes in the detail they needed. The new chains of processes that needed to be constructed for the models, whether it be the electricity generation or aluminium production, were beneficial and were designed to be easy to update should changes be made in the future, as well as improving the granularity of the models. The electricity grid mixes were specifically created to allow for different proportions of generation methods to be combined, with different nations having different proportions of renewable and finite energy generation methods. This allows for the energy mixes to be updated with new data when available and for changes to be made to the model when appropriate, such as moving the battery pack production location to a new nation with a different energy mix. This occurred during the development period of the models, with the original data for the UK electricity mix being from 2018, which was updated to the 2019 data when it was made available. This also showed the value of granularity within the model, as it allowed for a breakdown of the different energy demands of the battery pack production process and how they contributed to the overall impact of final product.

3.8 Summary – battery pack LCA models

The LCA models produced provided substantial amounts of useful data on both battery packs and their environmental impact. The major issue with the sodium-ion battery pack is its specific capacity being so low compared with the lithium-ion pack. This not only raises the material needed, and therefore its environmental impact, but the increased mass would also affect the performance of a vehicle equipped with a sodium-ion pack compared with a lithium-ion pack of the same capacity. The production of the models has also brought about innovation within how the models are constructed, with the desire for improved detail on different aspects of the model fuelling the need to break down single processes into multiple ones within the models.

While arguments could be made that the data is already derived from other LCA models, which examine the multiple processes used in creating a product, there is definite benefits in showing how each stage in the production of key components affects the emissions of a final product. Showing why a material or component produces an impact value by breaking down the different stages of its production provides a wealth of information to a user, which can be used to reduce the impact that part of their product has.

This could also motivate different industries to take interest in how their suppliers produce the materials that go into their product and provide them with the information on why certain materials produce the emissions assigned to them. Would an automotive company, motivated to cut their own emissions, be willing to pressurise their suppliers to improve their emissions, with data informing them where they could improve? New regulations require manufactures to understand their supply chains to a more accurate degree than ever before, so work like this should assist the automotive industry to locate these impacts within their entire supply chain. By giving a full overview of the manufacturing process from cradle to gate, this work should give companies most of the information they need in a single place to allow them to optimise their and their suppliers' processes. This may include reducing their consumption of specific materials if they produce significant higher impacts compared with compatible alternatives. This may include fully eliminating their use, such as pushes to remove cobalt as a key battery material or the use of recycled aluminium in battery production (Ryu et al., 2021). These efforts do however also need consideration of other impacts they may have outside of reduced environmental impacts, such as difficulties

in recovering aluminium from the current collectors of the cell, with most ending up in slag(Beheshti, Tabeshian and Aune, 2017).

Life cycle assessment currently only focus on environmental impacts, leaving a gap for examining social impacts which some practitioners have begun to examine (Jørgensen, Dreyer and Wangel, 2012). Given concerns over the ethical conditions within many key material production processes for the automotive industry, this could be an interesting area to examine (Amnesty International, 2016).

From the production and use of these models, two major commercial issues do also present themselves for further investigation:

1) Can the process of modifying the models be simplified?
2) Are there better options for processing the data produced by the models?

4. Development of tools for improving user experiences and cost-effective practice with LCA software

Deriving from the research questions proposed in the summary of section 3, the production of tools to interact with the models produced was considered the best path to take to offer answers to the proposed questions.

4.1 Initial design goals

Producing new tools to assist in the production and use of life cycle assessment models for use in industry would be innovative. Within industry, life cycle assessment software is not commonly used, with many relying on database software, like Microsoft Excel, to conduct life cycle assessments. This is most likely due to the limited number of companies that conduct LCA studies, along with the complicated nature of life cycle assessment software, which requires extensive training to use effectively and can be time consuming. In contrast, Microsoft Excel is not designed for LCA use and can require additional work that is automated in the LCA dedicated software but has the advantage of it already being a widely used piece of software, which cuts out the time needed to train users. However, the software is not designed for LCA work and requires data to be manually input and calculation performed by the user's design, effectively requiring the users to build the framework for their LCA model while the model is constructed. They also risk embedding errors within their worksheets, whether that is from incorrect data values or minor errors in formulae construction, which can have large systematic consequences for these models.

Therefore, tools that simplify the process of using the software and working with the data it produces would be greatly beneficial for industry. These tools would allow for changes to be made to the models and locate desired data quickly, building a more user-friendly experience which could also be used by someone inexperience with the software. This should help enable designers and engineers to modify LCA models and find appropriate data without the expertise expected of a LCA specialist.

After examining the lithium-ion model produced earlier, two modification tools were decided upon. The first would allow for the modification of the locations of different

materials and components used in the production process, by changing the distances covered and energy mixes used in their production. This was seen as a key sensitivity, as high energy demand from different processes contributed notably to the impacts of the battery pack production, with changes to location potentially impacting the overall impacts. The second would modify the battery chemistry of the cell active material, which should allow for easy comparisons of different chemistries. Given how different battery chemistries alter the quantity of different materials required to make a single cell, along with different charge densities changing how many cells were needed to reach the desired capacity, this was also considered a key sensitivity within the model. A third tool concept was also chosen to be taken forward, which would sort through the data produced by the LCA model and provide the user with the data they need in a more accessible form.

4.2 Python programming language and additional tools for tool creation

Part of the reason for choosing openLCA during the production of the battery pack models was due to the modifiable nature the software had, allowing it to be modified by external code, which is perfect for this project. The tool is based on the programming language Java, although it does list Python as another language that can be used with it. Given Python's easy readability and ease of prototyping, it was chosen over Java, with different open-source modules also enhancing Python's capabilities within the project.

Alongside the baseline python code, a module known as openpyxl was used to allow the Python tools to interact with Microsoft Excel workbooks. While Python does offer database options within the included modules, they require a significant amount of additional code around them to function in a user-friendly manner. Excel offers an easy means to store data within an understandable framework, which can also be expanded or altered when needed. Given one of the major objectives of the tools is user-friendliness, Excel was the obvious choice for storing the data needed for each tool, especially when the functions within openpyxl offer a wide range of options for interactions between Python code and Excel.

After some initial testing, it was discovered that, while openLCA advertises compatibility with Python code, the program only responds to Jython code, another programming language that acts as a bridge between Python and Java programs.

4.3 Production of the tools

4.3.1 Location modification tool

The supply chains for battery production are still developing as new sources of key materials are discovered, while others fall out of favour, or are lost, to mine depletion, political deals, or a variety of other issues that occur in national and international trade. Therefore, there would be interest in a tool that allows for easy assessment of how different locations of material sources affect the impacts of battery production, with the emissions of their transport and the electricity mix used to manufacture being considered.

The first tool produced for this project was one seeking to fill this niche, through the modification of the transport distances and electricity mixes of the openLCA model. After some design conceptualisation, the production process could be broken down into four sections, with the first one being the modification of the battery models to accommodate the tool.

openLCA tool modification

This involved the production of separate parameters within the individual processes that the tool would modify, which is available within openLCA's process structure. The parameters are stored in a table interface with columns for different data relevant to each of the parameters. For this tool, each parameter was given a unique name, with the initial values they correspond to being put in their value column. Figure 4.1 displays the initial set of parameters used for one of the electricity mix processes, with data sourced from the UK government and the IEA (UK Government, 2019) (International Energy Agency (IEA), 2021):

Input parameters

Name	Value	Uncertainty	Description
biomass_refb1	0.01398911689630184	none	In units of energy TWh
coal_refb1	0.6760282639966528	none	In units of energy TWh
gas_refb1	0.02759646305158562	none	In units of energy TWh
hydro_refb1	0.1793329245839257	none	In units of energy TWh
nuclear_refb1	0.03738881473523528	none	In units of energy TWh
oil_refb1	0.001487443917531491	none	In units of energy TWh
other_fuels_refb1	0.0	none	In units of energy TWh
wind_solar_refb1	0.06417697281876726	none	In units of energy TWh

Figure 4.1: List of input parameters for electricity mix

With these parameters set, the next step was to add dependent variables, which are used for calculating new values from the input parameters. For the distance values, this was to convert the distance values from km to kgkm, the value used in the transport processes used in the model. In the electricity mixes, this was to ensure the final parameters used in the model were direct fractions, totalling 1.0. Figure 4.2 displays this example:

Dependent parameters

Name	Formula	Value
biomass	biomass_refb1 /newtotal	0.01398911689630184
coal	coal_refb1 /newtotal	0.6760282639966528
gas	gas_refb1 /newtotal	0.02759646305158562
hydro	hydro_refb1 /newtotal	0.1793329245839257
newtotal	wind_solar_refb1 +biomass_refb1 +oil_refb1 +gas_refb...	1.0
nuclear	nuclear_refb1 /newtotal	0.03738881473523528
oil	oil_refb1 /newtotal	0.001487443917531491
other_fuels	other_fuels_refb1 /newtotal	0.0
wind_solar	wind_solar_refb1 /newtotal	0.06417697281876726

Figure 4.2: Dependent parameters for electricity mix calculating fraction split of electricity mix

As can be seen in figure 4.2, the dependent parameters use equations with both input and dependent parameters to calculate the new values. While not needed in all situations,

which is shown in figure 4.2, recalculating the electricity mix values was added to account for possible discrepancies in electrical mix data in literature. The dependent parameters were then used to convey the values calculated into the input flows within the process.

Excel database construction

With the changes made to the openLCA model complete, the next stage was to produce an excel workbook to hold the input and output data needed for each run of the tool.

To achieve this, the first stage was to determine the range of data that should be covered. The concept of the tool was to list two locations to travel between, an initial location and destination, with the initial location being used to determine the electricity mix. Therefore, the first stage was to devise a list of locations, with the destinations being chosen as potential locations of battery manufacturing plants. This led to the UK, Germany and China being chosen for these destinations, as all three countries have battery plants located within them or had plans to build plants within their borders, along with China being the processing location of cobalt compounds within the battery model. A range of other nations were then chosen for the initial locations, including places such as Australia, France, the USA, and Indonesia. With the locations chosen, data on the distances between them and their electricity mixes needed to be found or calculated. A number of online tools, most notably Google Maps and sea-distance.org, were used to determine the distances materials would cover whilst being transported to their intended destination, with it being assumed all transport was by cargo ship or road-based transport (Google, 2020) (Sea-distances, 2020). As with the electricity mixes used in the models in section 3, reports and information from governments and international organisations were critical in determining the electricity mixes for each nation (International Energy Agency (IEA), 2021).

As the data was collected, it was fed into a excel workbook, with two worksheets being used to separate out the data for the electricity mixes and the distances covered. Tables 4.1 and 4.2 displays the layout of these two sheets with examples:

Table 4.1: Distance database setup

Material locations	Destination	Distance (km) (by sea)	Distance (km) (by land)
Australia	UK	17,409	-
Austria	UK	41	1,531
Democratic Republic of the Congo (DRC)	China	16,327	-
New Caledonia (French)	China	7,762	-
UK	China	18,071	-

Table 4.2: Electricity mix database setup

Location	Generation method	Mix (% as fraction)
UK	Gas	0.4085
UK	Oil	0.0035
UK	Coal	0.0213
UK	Wind/solar	0.2392
UK	Nuclear	0.1739
UK	Biomass	0.1155
UK	Other Fuels	0.0197
UK	Hydro	0.0184

Once the data logged, a final worksheet was devised for the excel database to record the processes that were to be changed, along with the initial locations and destinations the tool set them to. This was chosen to have an easy way to find written record of what the changes to the model represented. Each process was given its name, with two columns next to them left blank for the tool to fill in. The remaining columns were used to store the input parameter names for each process, with figure 4.3 displaying the final table, with some of the input parameter columns cropped out for readability:

Process name	Production location	Transport desination	Sea dis	Road dis	Biomass ref	Coal ref	Gas ref	Hydro ref
Cobalt ore extraction	Katanga, DRC	Guangzhou, China	seadisc2	roaddisc2	biomass_refc2	coal_refc2	gas_refc2	hydro_refc2
Cobalt sulphate prodution	Guangzhou, China	Coventry, UK	seadisc	roaddisc	biomass_refc	coal_refc	gas_refc	hydro_refc
Manganese sulphate production	Groote Eylandt, Austr	Coventry, UK	seadisd1	roaddisd1	biomass_refd1	coal_refd1	gas_refd1	hydro_refd1
Lithium carbonate production	Greenbushes, Australi	Coventry, UK	seadisc5	roaddisc5	biomass_refc5	coal_refc5	gas_refc5	hydro_refc5
Aluminium foil production	Belfast, UK	Coventry, UK	seadisb1	roaddisb1	biomass_refb1	coal_refb1	gas_refb1	hydro_refb1
Copper foil production	Chuquicamata, Chile	Coventry, UK	seadisc1	roaddisc1	biomass_refc1	coal_refc1	gas_refc1	hydro_refc1
Graphite production	Humber, UK	Coventry, UK	seadisb3	roaddisb3	biomass_refb3	coal_refb3	gas_refb3	hydro_refb3
Carbon black production	Tonbridge, UK	Coventry, UK	seadisb4	roaddisb4	biomass_refb4	coal_refb4	gas_refb4	hydro_refb4
Acetylene production	Immingham, UK	Coventry, UK	seadisb	roaddisb	biomass_refb	coal_refb	gas_refb	hydro_refb
NMP production	Kiddiminster, UK	Coventry, UK	seadisd2	roaddisd2	biomass_refd2	coal_refd2	gas_refd2	hydro_refd2
Lithium hexafluorophosphate production	Basingstoke, UK	Coventry, UK	seadisd	roaddisd	biomass_refd	coal_refd	gas_refd	hydro_refd
Anode additives	Milton, UK	Coventry, UK	seadisb2	roaddisb2	biomass_refb2	coal_refb2	gas_refb2	hydro_refb2
Cell packaging	Dumfries, UK	Coventry, UK	seadisb5	roaddisb5	biomass_refb5	coal_refb5	gas_refb5	hydro_refb5
Electrical circuits	Cambridge, UK	Coventry, UK	seadisc3	roaddisc3	biomass_refc3	coal_refc3	gas_refc3	hydro_refc3
Battery cell and pack assembly	Coventry, UK	Coventry, UK	seadisc4	roaddisc4	biomass_refc4	coal_refc4	gas_refc4	hydro_refc4
Nickel sulphate production	Groote Eylandt, Austr	Coventry, UK	seadisd3	roaddisd3	biomass_refd3	coal_refd3	gas_refd3	hydro_refd3
Polymer production	Dumfries, UK	Coventry, UK	seadisd4	roaddisd4	biomass_refd4	coal_refd4	gas_refd4	hydro_refd4
Seperator production	Dumfries, UK	Coventry, UK	seadisd5	roaddisd5	biomass_refd5	coal_refd5	gas_refd5	hydro_refd5
Steel production	Port Talbot, UK	Coventry, UK	seadiss	roaddiss	biomass_refs	coal_refs	gas_refs	hydro_refs
PVDF production	Kiddiminster, UK	Coventry, UK	seadiss2	roaddiss2	biomass_refs1	coal_refs1	gas_refs1	hydro_refs1
Lithium carbonate production (active material)	Greenbushes, Australi	Coventry, UK	seadiss1	roaddiss1	biomass_refs2	coal_refs2	gas_refs2	hydro_refs2

Figure 4.3: Control worksheet table for distance tool

Python code for tool

Once the database had been constructed, the tool's code could be produced. The first stage was to call up all the code modules that would be needed within the code, which used the python 'import' function to call up essential modules, with tkinter, number, os, and subprocess being among those needed. The path function was also imported, as this was used to import the openpyxl code from a separate file in the computer, which had been recommended when downloading python modules that were not part of the original toolset. The path function used a path to the required files, formatted at "C:/Users/user/openpyxl_file/Lib", to produce a means for the "import" function to import the openpyxl module.

With the modules imported into the code, the first step in production the tool was figuring out the structure of the interface the tool would use. It was decided to use a popup window with four elements, three dropdown menus to select the material location, destination and processes and a button to run the modification code. The dropdown menus originally used the "optionmenu" function from the tkinter module, but this was quickly replaced with the "combobox" function, as it offers a clean look and has functions for a scrollbar on the menu, which would be useful for the large number of locations being covered by the tool. To populate the three dropdown menus, the openpyxl module provided functions that could collect data from a specified range of cells within the excel workbook, with the required columns from the distance worksheet and control worksheet being collected. While a

directly specified range of cell could have been used, it was decided to import the entire column to allow for easy expansion of the locations available to the tool by simply adding their data to the excel worksheet. To achieve this, the data collected was limited to the desired column for each dropdown menu and additional code was used to prevent the collection of empty cells and to remove the column title. This data was compiled into a list, which the dropdown menus draw from to populate themselves. Figure 4.4 displays the final tkinter interface for this tool:

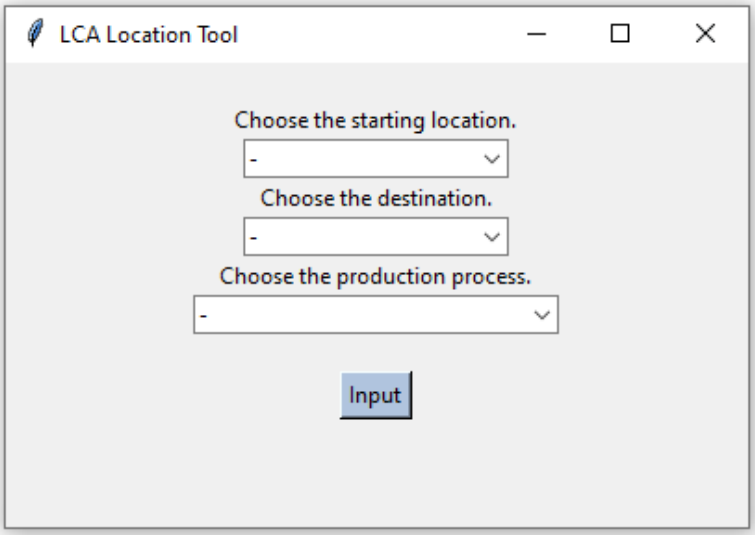

Figure 4.4: Location tool interface

From this interface, the next step in the code was to use the data requested by the dropdown menus and modifying the openLCA model to match the data. This used a multitude of lists within the Python code, which were established with names but are initially empty. Openpyxl's read data function was used again, with the values selected in each of the dropdown menus being used to find the appropriate data, with the database set up so that only one set of values is correct. For the distance list, the code searched in the material location and destination columns for a row which contained the location names selected in the dropdown menus, which was then used to select and extract the distance data set from the spreadsheet. This was placed in the first list, with a similar process being

used for the electricity data, although this pulled from multiple rows listing the different proportions within the electricity mix for the material location, with these values being listed in order in the second list.

For the process names, a more complex set of code was needed, as it had to record the new values for the material location and destination within the control sheet. So, after determining the row with the desired process names listed in its appropriate column, the code used a write function from openpyxl to overwrite the values in the material location and destination columns for that row in the control worksheet. The code then saved the excel file with another openpyxl function to keep the changes made. After this, the parameter names listed in the columns after this were extracted and placed into another list within the Python code.

With the needed data extracted, the next stage was to modify the LCA parameter values in openLCA. As this would require Jython code to execute, and that Python based programs cannot read values from code that is also running, the data collected was written to a dedicated python file by the code. This required a named but blank .py file to be created within the Jython folders, with the python code and excel workbook also being placed there as well to allow for the Jython interpreter to be accessible for the Jython code. The Python code then was set up to merge the distance list and the electricity value list into a single list, with the distance values at the start, which aligned with the order of the parameter names in their list. These lists were then written to the storage .py file, which was then saved and closed to preserve the data recorded. Figure 4.5 displays the layout of the storage file:

```
list1 = [19835, 668, 1, 0.02759646305158562, 0.001487443917531491, 0.6760282639966528,
dd = ["Coventry, UK", "seadisb", "roaddisb", "biomass_refb1", "coal_refb1", "gas_refb1"
```

Figure 4.5: Storage python file

After this, a couple of line of code were set up with the “subprocess” function to run the Jython code automatically after the data had been saved to the blank file. Along with this, an additional line of code was added, to check that the Jython code completed its tasks as intended before progressing. Finally, the code was set with a “root.mainloop” function so

that the interface remained open after the code completed its tasks, so that another change could be made as needed without having to restart the program.

Jython code

The Jython code required some different work compared with the Python code, due to Jython being based on Python 2.0 rather than Python 3.0 used earlier. This also required the files containing the Jython code to be labelled differently, as the .py file type would attempt to run the Jython code with the Python interpreter, which wouldn't work. To solve this issue, a .jy file type had to be created and set up to run the file through the Jython interpreter present, with this then being set as the file type for the file containing the Jython code.

Within the python code, the first stage was to extract the data lists from the storage file, which was achieved by importing the list names in a similar manner to importing the modules, with the "import" function. With the data imported, the two lists were used to feed into a set of processes that changed the values of the named parameters in openLCA, drawing the parameter names from the list dd and the values from list1. Figure 4.6 displays the code used to modify the parameters as needed:

```
paramrd = dao.getForName(dd[1])[0]

paramrd.value = (list1[0])

dao.update(paramrd)
```

Figure 4.6: Jython code for changing openLCA parameters

4.3.2 Battery chemistry tool

For the next tool, it was decided to implement a tool to modify the battery chemistry within the model to provide comparisons between equivalent battery packs. To achieve this, it was decided to modify the existing location modification tool to change different parameters. It

was decided to just examine the different ranges of LiNMC chemistries, which consisted of different ratios of the key metals within the final production, with 1:1:1, 5:3:2 and 8:1:1 ratios of nickel: manganese: cobalt being used within the tool. It was assumed that energy demands for the production of each active materials would be the same, as the data for each chemistry is derived from data relating to the production 111 NMC (Ahmed et al., 2017). Similarly, each cell was assumed to remain the same size to minimize the necessary variables the tool would need to modify, although each cell would have a different capacity for each chemistry. Therefore, most of the changes between battery chemistries will likely be due to the impacts of the raw material extraction and refinement, along with changes to the charge density of each chemistry. This is supported by the cathode active material in the original model having the largest contribution to the packs global warming potential and metal depletion (MD) at the point of battery assembly, contributing 37% of the GWP and 23% of the MD. The first stage of producing this tool was the same as the location modification tool, with the implantation of parameters to represent the major inputs to produce the battery active material, as can be seen in figure 4.7. This was to allow for the modification of the proportions of these materials within the input of the active material production process.

Input parameters

Name	Value	Uncertainty	Description
CoSm	0.369634965	none	kg of CoSO4 used in process
limass	0.399449006	none	kg of LiCO3 used in process
MnSm	0.540638866	none	kg of MnSO4 used in process
NaCmass	1.26517791	none	kg of NaCO3 used in process
NH4OHm	0.697960321	none	kg of NH4OH used in process
NiSm	0.922957656	none	kg of NiSO4 used in process
O2m	0.082667201	none	kg of O2 used in process

Figure 4.7: Input parameters for battery active material production

With this implemented, an excel workbook was created to store the data needed by the tool. With further experience in producing excel database from the previous tool and the lower complexity of the tool being production, only a single table was needed to store all the data needed, which can be seen in figure 4.8:

Chemistry	Chemical	Quantity (kg/kg Li-NMC)	Variable name	Notes
111 NMC	LiCO3	0.4	limass	Data provided from process report (Ahmed, S, Nelson, P A, Gallagher, K G, Susarla, N, Dees, D W, 2017,Cost and energy demand of producing nickel manganese cobalt cathode material for lithium ion batteries, Journal of Power Sources, 342, pp 733-740)
111 NMC	NiSO4	0.616153846	NiSm	
111 NMC	MnSO4	0.601538462	MnSm	
111 NMC	CoSO4	0.616923077	CoSm	
111 NMC	NaCO3	1.26517791	NaCmass	
111 NMC	NH4OH	0.7	NH4OHm	
111 NMC	O2	0.08275861	O2m	
532 NMC	LiCO3	0.399449006	limass	Data derived from similiar data in process report (Ahmed, S, Nelson, P A, Gallagher, K G, Susarla, N, Dees, D W, 2017,Cost and energy demand of producing nickel manganese cobalt cathode material for lithium ion batteries, Journal of Power Sources, 342, pp 733-740)
532 NMC	NiSO4	0.922957656	NiSm	
532 NMC	MnSO4	0.540638866	MnSm	
532 NMC	CoSO4	0.369634965	CoSm	
532 NMC	NaCO3	1.26517791	NaCmass	
532 NMC	NH4OH	0.697960321	NH4OHm	
532 NMC	O2	0.082667201	O2m	
811 NMC	LiCO3	0.396174854	limass	Data derived from similiar data in process report (Ahmed, S, Nelson, P A, Gallagher, K G, Susarla, N, Dees, D W, 2017,Cost and energy demand of producing nickel manganese cobalt cathode material for lithium ion batteries, Journal of Power Sources, 342, pp 733-740)
811 NMC	NiSO4	1.464627959	NiSm	
811 NMC	MnSO4	0.178735809	MnSm	
811 NMC	CoSO4	0.183307057	CoSm	
811 NMC	NaCO3	1.254807662	NaCmass	
811 NMC	NH4OH	0.693305994	NH4OHm	
811 NMC	O2	0.081967206	O2m	

Current Battery Chemistry
532 NMC

Figure 4.8: Database of LiNMC chemistry input compositions

All the values shown in figure 4.8 were calculated from the same source as the models 532 ratio, with the 111 LiNMC composition being the data used from the paper (Ahmed et al., 2017). As can be seen in the top right-hand corner of figure 4.8, a record of battery chemistry was also implemented in a similar manner to the location records in section 4.3.1.

With the database constructed, the Python and Jython code used in the location modification tool was duplicated and modified to use the new data format. This included changes to the user interface as only one dropdown menu was required, which resulted in the interface shown in figure 4.9:

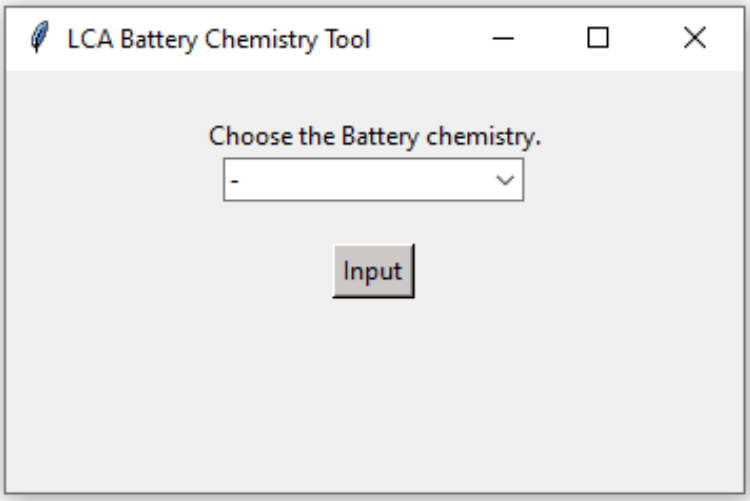

Figure 4.9: Battery chemistry tool interface

Battery pack chemistry iteration - cell number changes

Initial testing of the battery chemistry tool produced good results but was hampered by too many assumptions. To correct this, the tool was expanded to include battery module number, with the code expanded to include further iterations of the code shown in figure 4.6 to adjust for the larger number of parameters used. To expand the data sets used, new values needed to be calculated for how many 8 cell modules would be needed to reach 60 kWh capacity for the battery pack for each battery chemistry. This was calculated with data detailing the battery cell capacities for each chemistry and calculating how many cells were needed for to reach the desired capacity, with the number divide by 8 and rounded up to find the nearest whole number. Table 4.3 displays the data produced from these calculations:

Table 4.3: Battery chemistry module number data

LiNMC chemistry	Energy density (kWh per cell)	Module number required
111 LiNMC	0.2768	28
532 LiNMC	0.2911	26
811 LiNMC	0.4549	17

Along with this, new data was needed for the battery pack cooling systems and structural packaging for the new chemistries being examined, with the masses of each being scaled in relation to the number of modules needed for each battery chemistry, as seen in table 4.4:

Table 4.4: Battery chemistry packaging and cooling system masses

LiNMC chemistry	Battery retention packaging mass (kg)	Battery cooling system mass (kg)
111 LiNMC	54.0516	7.2882
532 LiNMC	50.1907	6.7671
811 LiNMC	32.8170	4.4250

With this data, the database could be updated, along with the addition of new parameters within the openLCA model. Figures 4.10 and 4.11 display these new additions:

Chemistry	Chemical	Quantity (kg/kg Li-NMC)	Variable name	Notes
111 NMC	LiCO3	0.4	limass	Data provided from process report (Ahmed, S, Nelson, P A, Gallagher, K G, Susarla, N, Dees, D W, 2017,Cost and energy demand of producing nickel manganese cobalt cathode material for lithium ion batteries, Journal of Power Sources, 342, pp 733-740)
111 NMC	NiSO4	0.616153846	NiSm	
111 NMC	MnSO4	0.601538462	MnSm	
111 NMC	CoSO4	0.616923077	CoSm	
111 NMC	NaCO3	1.26517791	NaCmass	
111 NMC	NH4OH	0.7	NH4OHm	
111 NMC	O2	0.08275861	O2m	
111 NMC	Module no	28	modulenumb	
111 NMC	Battery packaging mass	54.05160348	pack_mat_mass	
111 NMC	Battery cooling system mass	7.2881915	pack_cool_mass	
532 NMC	LiCO3	0.399449006	limass	Data derived from similiar data in process report (Ahmed, S, Nelson, P A, Gallagher, K G, Susarla, N, Dees, D W, 2017,Cost and energy demand of producing nickel manganese cobalt cathode material for lithium ion batteries, Journal of Power Sources, 342, pp 733-740)
532 NMC	NiSO4	0.922957656	NiSm	
532 NMC	MnSO4	0.540638866	MnSm	
532 NMC	CoSO4	0.369634965	CoSm	
532 NMC	NaCO3	1.26517791	NaCmass	
532 NMC	NH4OH	0.697960321	NH4OHm	
532 NMC	O2	0.082667201	O2m	
532 NMC	Module no	26	modulenumb	
532 NMC	Battery packaging mass	50.19077466	pack_mat_mass	
532 NMC	Battery cooling system mass	6.7676064	pack_cool_mass	
811 NMC	LiCO3	0.396174854	limass	Data derived from similiar data in process report (Ahmed, S, Nelson, P A, Gallagher, K G, Susarla, N, Dees, D W, 2017,Cost and energy demand of producing nickel manganese cobalt cathode material for lithium ion batteries, Journal of Power Sources, 342, pp 733-740)
811 NMC	NiSO4	1.464627959	NiSm	
811 NMC	MnSO4	0.178735809	MnSm	
811 NMC	CoSO4	0.183307057	CoSm	
811 NMC	NaCO3	1.254807662	NaCmass	
811 NMC	NH4OH	0.693305994	NH4OHm	
811 NMC	O2	0.081967206	O2m	
811 NMC	Module no	17	modulenumb	
811 NMC	Battery packaging mass	32.81704497	pack_mat_mass	
811 NMC	Battery cooling system mass	4.42497342	pack_cool_mass	

Current Battery Chemistry
532 NMC

Figure 4.10: Final battery chemistry excel database layout

Input parameters

Name	Value	Uncertainty
modulenumb	26.0	none
pack_cool_mass	6.767064	none
pack_mat_mass	50.19077466	none

Figure 4.11: Module number, battery cooling system mass and battery retention packaging mass parameters

4.3.3 Data presentation tool

Along with simplifying the ability to modify the model, another area of interest was the ability to process the data produced by the model more effectively. To assist in this, it was decided to focus on processing the data from the model exported as an Excel document. This was done as openLCA exports its data in a repeatable and consistent framework, which would allow for the tool to be applicable to other data sets produced by openLCA with minimal changes to the Python code. It also eliminated the need to use Jython for this tool,

which ideally would speed up the tool as it eliminates the need to run a separate file as part of its process, something unavoidable in the other tools. As an additional user convenience option, it was also decided to place all the processed data in a generated excel workbook that would be saved separately to the tool.

The first stage was to examine the exported data and build a control excel database to act as the base of the tool. With a desire for user friendliness and the probability that multiple sets of data would be required by a user at any one time, the tkinter interface options used in the previous tools were deemed unsuitable for this. As the model had close to 300 processes present, which were displayed individually in the data, it would be unwieldy to attempt to locate the processes desired in tkinters dropdown menus. This prompted the change to using the excel document as a user interface, with mechanics for dedicated and easy to use search function being already tested within excel.

Search Function

For this search function, the first stage was to set up a repeatable process to number the process names within individual cells and to change this numbering in response to an input, in this case a typed process name or part of its name in a designated cell. In addition to this, it was decided to also organise the processes into different categories to help users find the data they need, with the category names being added next to the process names. Figure 4.12 displays the two formulae used in excel to enable the search function, with figure 4.13 displaying the result and its use:

```
=IFERROR((SEARCH($G$2,C4)*SEARCH($J$2,D4))+ROW()/100000,"")

=IFERROR(RANK(B4,$B$4:$B$415, 1),"")
```

Figure 4.12: Formulae used in excel search function

a)

Rank	Search assist	Processes	Categories
1	1.00004	Li-ion battery pack production - 60 kWh	Battery pack assembley
2	1.00005	Acetylene production	Anode materials production
3	1.00006	Aluminium electrolysis	Aluminium production
4	1.00007	Aluminium Ingot casting	Aluminium production
5	1.00008	Aluminium oxide production	Aluminium production
6	1.00009	Aluminium sheet, production mix, at pla	Aluminium production
7	1.00010	Alumnium foil production	Aluminium production
8	1.00011	Ammonia (NH3) production mix, withou	Chemical production
9	1.00012	ammonia,gas, at regional storehouse, p	Chemical production
10	1.00013	Ammonium hydroxide solution product	Active material production
11	1.00014	Anode additives (CMC/SBR mix)	Battery cell assembley
12	1.00015	Battery cooling system manufacturing	Battery pack assembley
13	1.00016	Battery grade graphite production	Battery cell assembley
14	1.00017	Battery Management System (BMS) ma	Battery pack assembley
15	1.00018	Battery module assembly (Li-ion)	Battery pack assembley
16	1.00019	Battery retention packaging production	Battery pack assembley
17	1.00020	Bauxite Mining	Aluminium production
18	1.00021	Benzene, production mix, at plant, techr	Chemical production
19	1.00022	Bioethanol from wheat, at plant, single	Chemical production
20	1.00023	Calendering of lithium-ion anode	Battery cell assembley
21	1.00024	Calendering of lithium-ion cathode	Battery cell assembley
22	1.00025	Carbon anode production (Al productio	Battery cell assembley, Aluminiu
23	1.00026	Carbon Black (anode supply)	Anode materials production
24	1.00027	Carbon Black (cathode supply)	Cathode material production
25	1.00028	Carbon Black production	Anode materials production
26	1.00029	CarboxyMethylCellulose (CMC) product	Anode materials production

b)

Rank	Search assist	Processes	Categories
		Li-ion battery pack production - 60 kWh	Battery pack assembley
		Acetylene production	Anode materials production
		Aluminium electrolysis	Aluminium production
		Aluminium Ingot casting	Aluminium production
		Aluminium oxide production	Aluminium production
		Aluminium sheet, production mix, at pla	Aluminium production
		Alumnium foil production	Aluminium production
		Ammonia (NH3) production mix, withou	Chemical production
		ammonia,gas, at regional storehouse, p	Chemical production
		Ammonium hydroxide solution product	Active material production
		Anode additives (CMC/SBR mix)	Battery cell assembley
		Battery cooling system manufacturing	Battery pack assembley
		Battery grade graphite production	Battery cell assembley
		Battery Management System (BMS) ma	Battery pack assembley
		Battery module assembly (Li-ion)	Battery pack assembley
		Battery retention packaging production	Battery pack assembley
		Bauxite Mining	Aluminium production
		Benzene, production mix, at plant, techr	Chemical production
		Bioethanol from wheat, at plant, single	Chemical production
15	16.00023	Calendering of lithium-ion anode	Battery cell assembley
16	16.00024	Calendering of lithium-ion cathode	Battery cell assembley
		Carbon anode production (Al productio	Battery cell assembley, Aluminiu
		Carbon Black (anode supply)	Anode materials production
		Carbon Black (cathode supply)	Cathode material production
		Carbon Black production	Anode materials production
		CarboxyMethylCellulose (CMC) product	Anode materials production

Figure 4.13: Search function, with a) displaying the neutral version, while b) uses a search term to find processes containing it

The categories were listed in a separate worksheet within the workbook, with figure 4.14 displaying the result:

Categories from search assistance
Active material production
Aluminium production
Anode materials production
Battery cell assembley
Battery management system production
Battery pack assembley
Cathode material production
Cell casing production
Chemical production
Cobalt sulphate production
Copper production
Electrical circuit production
Electricity generation
Electrolyte production
Fuel processes
Manganese sulphate production
Miscellaneous proceses
Nickel sulphate production
Separator production
Transport distances

Figure 4.14: Category list for data presentation tool

These categories were chosen as they break up the model into easy to understand sections that relate to key aspects of the manufacturing process and the current supply chain of materials within it. The complexity of the metal sulphates production necessitated their own categories, given the range of individual processes listed in the model that influence and contribute to the overall impacts of their production. Other categories were separated to allow for easier searches for those unfamiliar to the model, such as grouping the multitude of transport processes and electricity generation methods together as seen above.

With the categories listed, a final search setup was established on another worksheet to keep the look clean and easy to understand. A separate search input cell and category cell were designated to feed into the main search function, while the formula in figure 4.15 were used to display the search results cleanly by rank and hiding the ones not relevant to the search, as seen in figure 4.14:

```
=IFERROR(VLOOKUP(I8,'Process references for Li pack'!$A$4:$D$415,3,FALSE),"")
```

Figure 4.15: Formula to order results by rank

Catergories	
Search for process	

Rank	Process
0	
1	Li-ion battery pack production - 60 kWh
2	Acetylene production
3	Aluminium electrolysis
4	Aluminium Ingot casting
5	Aluminium oxide production
6	Aluminium sheet, production mix, at plant, primary
7	Alumnium foil production
8	Ammonia (NH3) production mix, without CO2 recov
9	ammonia,gas, at regional storehouse, production
10	Ammonium hydroxide solution production
11	Anode additives (CMC/SBR mix)
12	Battery cooling system manufacturing

Figure 4.16: Search function in control worksheet

Control tables

As this tool does not use the tkinter user interfaces, the excel control sheet was adapted to control the inputs of the tool. Two control tables were set up to provide different information from the tool, one to list the processes being examined and the second to list addition factors that would be vital for processing the data. An additional smaller table was added at the top of the control worksheet to name the workbook the tool would produce, as later testing of the tool revealed that openpyxl overwrote the previously produced excel workbooks unless they were named differently.

For the smaller table, it was decided this would detail the impact type being examined, the type of graph the exported excel workbook would produce and the type of data the tool would process from the exported data. The exported data was split between a variety of different formats, with the two of interest for this tool both examining environmental impacts. One type looks just at the emissions of a single process, while the other accounted for all the emissions in and upstream of the process.

For the graphs, four options were decided upon, with the tool offering the production of bar graphs, pie charts, an option to produce both, and line graphs, all of which could be produced from the options offered by the Python toolsets. The environmental impacts were directly taken from the ReCiPe v1.13 LCA methodology, with values such as GWP and terrestrial acidification being among the ones examined. As the Python tools require precise labelling while searching for values, it was decided to store the values and options selected in tables within the workbook, with them being placed alongside the categories used in the search function as seen in figure 4.16. These were then used as a baseline to add in dropdown menus within the table, with a dropdown menu also being utilised within the search function to select the categories.

The larger table detailed the processes the tool would look to compile data on, which required a means to record them. As with the smaller table, dropdown menus were used to allow users to select processes from the search function, with the selection coming from the search function shown in figure 4.16. The dropdown menu also remains on the selected process, even if the processes position changes within the search functions list. An additional part of the table was added to the top to label the graphs produced and to table the worksheet the data would be placed in within the generated workbook, with the full layout of the three tables shown in figure 4.17:

Document title	processingtest		
Graph 1 title		Graph 1 impact type	climate change
testgraphs		Graph type	pie chart
Flow		Examination type	Process upstream impacts
Cathode active material production			
PVDF production			
Carbon Black production			
NMP production			

Figure 4.17: Layout of data presentation tool control sheet

The larger table and data type table were then replicated four more times below to allow for multiple sets of data to the examined within one run of the tool, as well as to reduce the number of workbooks a user would need to examine a set of processes.

Python code

With the excel control workbook setup, the Python tool could then be produced. After importing the necessary modules, including numbers, os, and openpyxl, the first stage of the tool was to open the workbook and extract all the necessary information from the control excel worksheet. This was achieved through openpyxl's load_workbook and sheet_ranges functions, with the document title first being extracted, along with the processes, graph title and other information as seen in figure 4.17. The processes and other information were placed in two lists, while the document title was merged with a function representing ".xlsx", which is needed to save the titles name correctly within openpyxl.

Once the required data was extracted, the code then used it to search through the exported data. The information detailing the examination type was used to select the worksheet

within the exported excel workbook, with the impact type used to select the row within the exported data the processes impact data would be found in. After this, each process name gathered was used to find the appropriate column, which combined with the row number gave the cell the desired data resided in, with said data then being extracted. This was then placed in an individual list with the name of the process it corresponds to, with the process repeating for each process name gathered. This set of lists were then placed within another list, with figure 4.18 displaying how the new list would appear:

List_final = ((process, value), (process, value), (process, value), ……., (process, value))

Figure 4.18: List for gathered data in data presentation tool

With the data collected, the code then used openpyxl's functions to create a new excel workbook and add a new worksheet in it, with the graph name gathered from the control excel sheet used to name it. In this new worksheet, the data collected was inserted into cells to form a table in the first two columns. Two titles were then inserted above the table, one just labelled "Processes" and the other being the environmental impact the data represented, which had its units added to the end using the same process as the workbook title mentioned earlier on.

With the data present in the worksheet, the program then constructed a graph to display the data. The graph type was selected from the name gathered from the control excel worksheet, with IF functions used to determine which graph would be produced. The functions to produce the graph were imported from openpyxl, with the inserted data being used as the base for the graph, with the program also setting a size and position within the worksheet. After completing all this, the program saved the excel file under the desired name produced earlier.

Once this initial version of the tool was produced, it was tested to ensure all the functions worked as intended. Once this was established, the program was converted to fit into a while loop, which would repeat the program for every set of data the user set up in the control excel database. This did require some changes to the program compared with the

initial version, including re-locating certain functions either to be within or outside the loop function, but the final version operated for each set of processes in the same manner as described above. The final output of this tool would produce a single excel workbook with a different worksheet for each set of processes.

4.4 Iterations and improvements to the tools

4.4.1 Error and completion message boxes

While not initially implemented, to assist in ensuring the code operated effectively, a variety of message boxes were programmed into the Python tools, both to confirm successful uses of the tools and to assist users in trouble shooting issues. This was achieved with the "messagebox" function in tkinter which could be programmed to display a variety of messages as required by the designer. This was also to assist in debugging the program as it was developed.

4.4.2 Progress bars for tools

During the various iterations of the tools, there was some concern on how users could be informed on whether the process was progressing as expected, which led to the decision to include a visual progress bar for each tool. This was achieved by functions present within the tkinter module, which allowed for a window to be opened, to display a progress bar, for the progress bar to advance as the program ran and for the box to close once required. Figure 4.19 displays the final produce of this design:

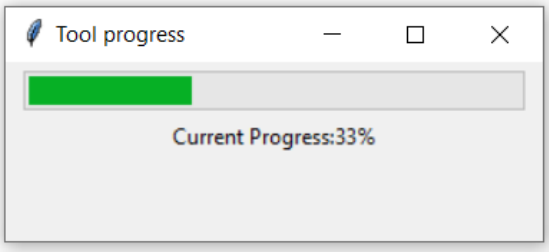

Figure 4.19: Progress bar window

While this program was easily implemented for the data presentation tool, with the functions to progress the bar being activated with each loop of the tool, the same code did not work for either the location modification tool or the battery chemistry tool. After a thorough investigation, it was discovered that the tkinter module did not allow for multiple windows to be open from the same Python file. This was fixed for these two tools by placing the progress bar code in a separate file and running this file with the subprocess function.

4.4.3 Streamlining the code

While the tools generally ran efficiently, there were areas that testing and debugging revealed were slowing their processes down, primarily from unnecessary lines within the code. These lines were removed to improve the performance of the code, with some other improvements including the replacement of original functions with improved variants, along with the removal of multiple print functions, which had only been present for debugging.

4.4.4 The toolbox user interface

While each of the tools worked effectively on their own, discussions with Ricardo PLC recommended that all the tools should be organised and easily reachable from a central repository. This led to the development of the toolbox, which used tkinters user interface functions to produce an easy-to-follow central program to access each of the tools. Each of the tools was assigned to a button within the window, which was labelled accordingly, with another set of buttons opening the excel control files corresponding to each tool. With this achieved, the toolbox also had several quality-of-life improvement made, including colour co-ordination of the tool buttons to match their excel access buttons, as well as the addition of a title and a WMG logo. Figure 4.20 displays the final result:

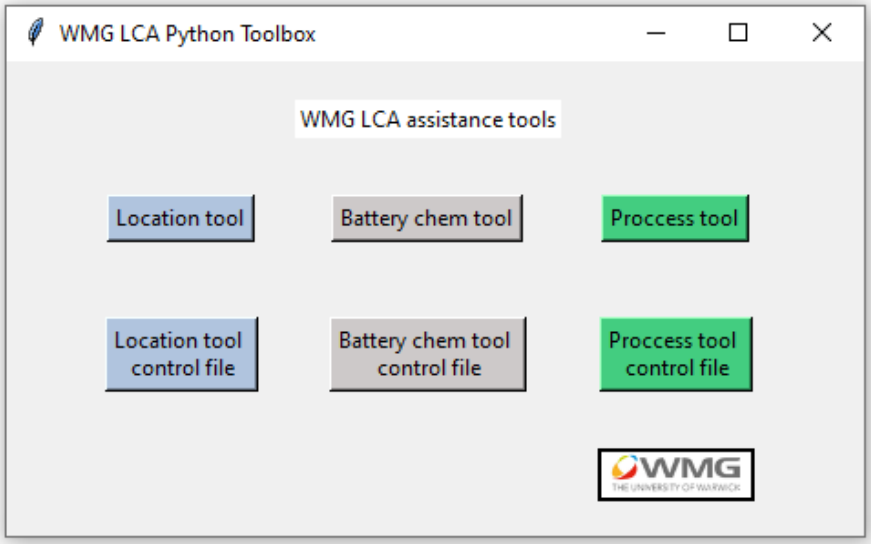

Figure 4.20: Toolbox user interface

4.5 Validation of tools functions

To confirm that the tool operated as intended, several scenarios were conducted to examine how each of them operated with the openLCA model and data. This was to ensure that the tools operated as intended and to examine what impact on the use of the model and its data the tools had. The Li-ion model from section 3 was used in all these tests.

4.5.1 Location modification tool

For this tool, a test was performed to change the production location of a major emission contributor to examine what impact this would have by comparing the emissions data from the two locations. This used the most up to date electricity mix data available at the time, with the process assumed to occur during 2019 (International Energy Agency (IEA), 2021). The aluminium current collectors were the component chosen, with Weifang, China being the original location for their production. The data for this arrangement was recorded, before using the location modification tool to change the production location to Balatonfüred, Hungary and recording the new data set. Figures 4.21 and 4.22 display the results of this

comparison, examined over the entire pack due to concerns of visibility of the differences at a per kWh level:

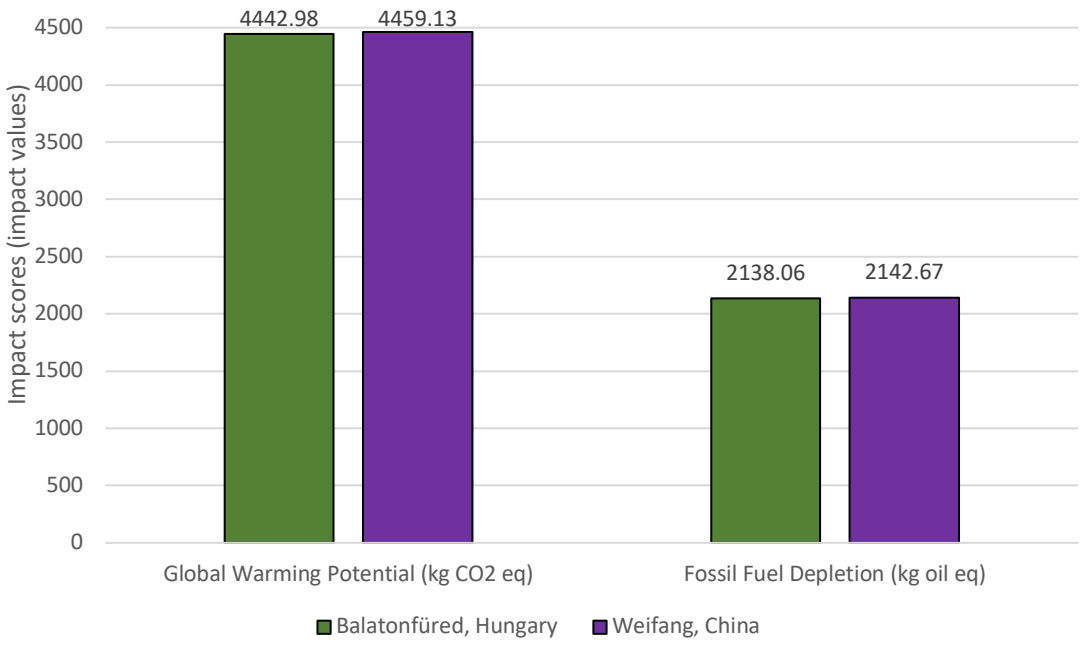

Figure 4.21: Graph of overall impacts for one battery pack comparing production locations for aluminium current collectors, global warming potential and fossil fuel depletion

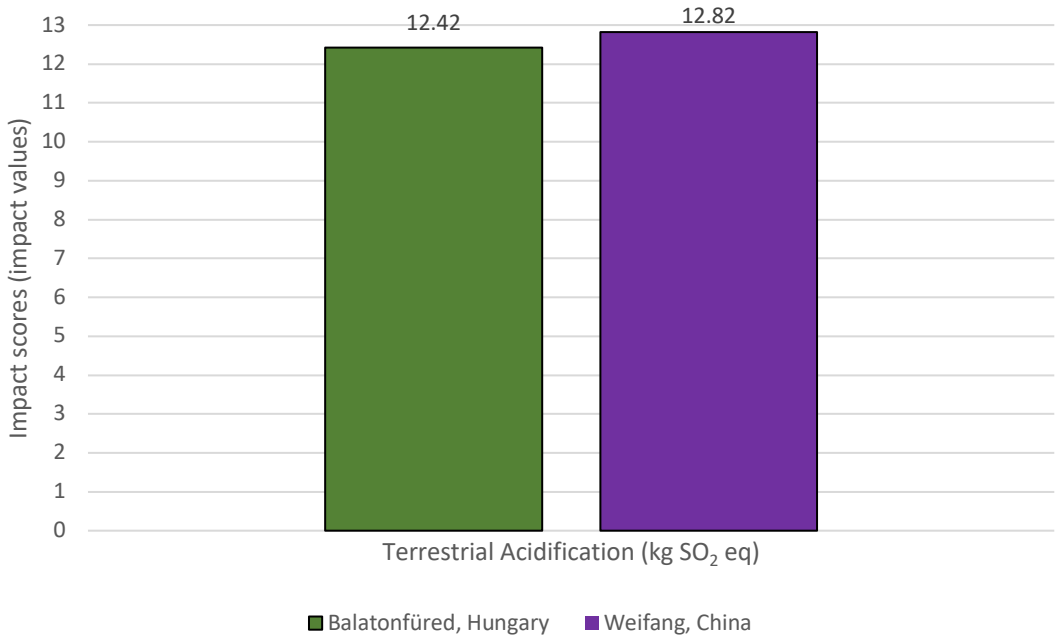

Figure 4.22: Graph of overall impacts for one battery pack comparing production locations for aluminium current collectors, terrestrial acidification

The graphs show a slight difference in the impacts produced, although this is a very small difference compared with the overall impacts of the model, with each impact category having less than a 5% difference in impacts. This does show that the location of the process does influence the impacts, both in the transport distances and energy mixes needed for the process. The differences in distance covered by different transport methodologies changed the contributions the transport of the aluminium made to the overall impact. The different electricity generation methods, such as combustion of coal or wind generation, also have substantial difference in their impacts per kWh of electricity produced. This in turn affects how the different electricity mixes of each nation contribute to the overall emissions due to the proportion of electricity produced by each production method.

As another test of this tool, it was decided to re-locate the battery assembly plant within the model, with the original model's assembly plant located in Coventry, UK. For this test, a plant in the Saarland, Germany was chosen and as with the previous test it was modelled using data from 2019 (UK Government, 2019) (International Energy Agency (IEA), 2021). Using the tool to change these values was relatively easy, although slowdown occurred as the changes

continued due to the age of the computer being used and possibly optimisation issues with the tools code. Figures 4.23 and 4.24 display the results of this change:

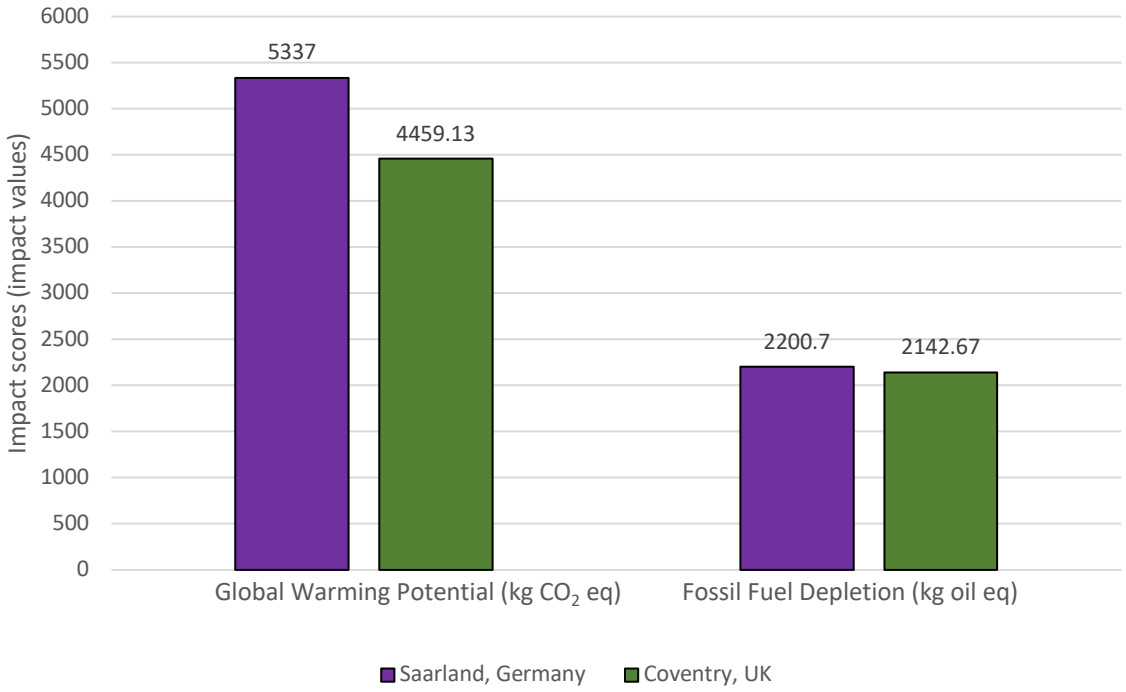

Figure 4.23: Graph of overall emissions for one battery pack between different li-ion battery assembly plants, global warming potential and fossil fuel depletion

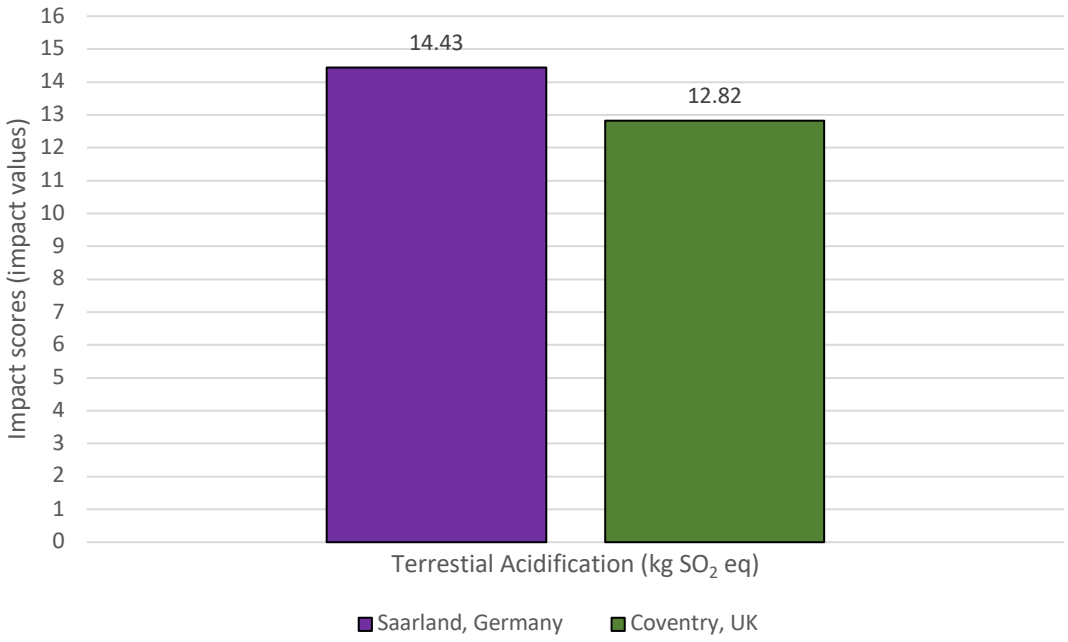

Figure 4.24: Graph of overall emissions for one battery pack between different li-ion battery assembly plants, terrestrial acidification

This change produced a much more apparent difference in the data examined, with it assumed that all energy demands, such as use of dry rooms, remained the same between the plants, with the Saarland plant producing larger emissions compared with the Coventry plant. Some of this can be contributed to the UK suppliers for certain key materials, such as carbon black, needing to cover further distances to the Saarland compared with Coventry. The biggest contributor however was the difference between the UK and German electricity mixes, as Germany has a higher dependence on coal compared with the UK for electricity generation.

4.5.2 Battery chemistry tool

To examine this tool, as with the material location tool, a comparison was devised between the three LiNMC battery chemistries the tool could produce with the model at hand. After running the tool through each battery chemistry and recording the required data, figures 4.25, 4.26 and 4.27 display the results of this comparison, displayed as impacts per kWh to align with similar data provided for other battery LCA work in literature:

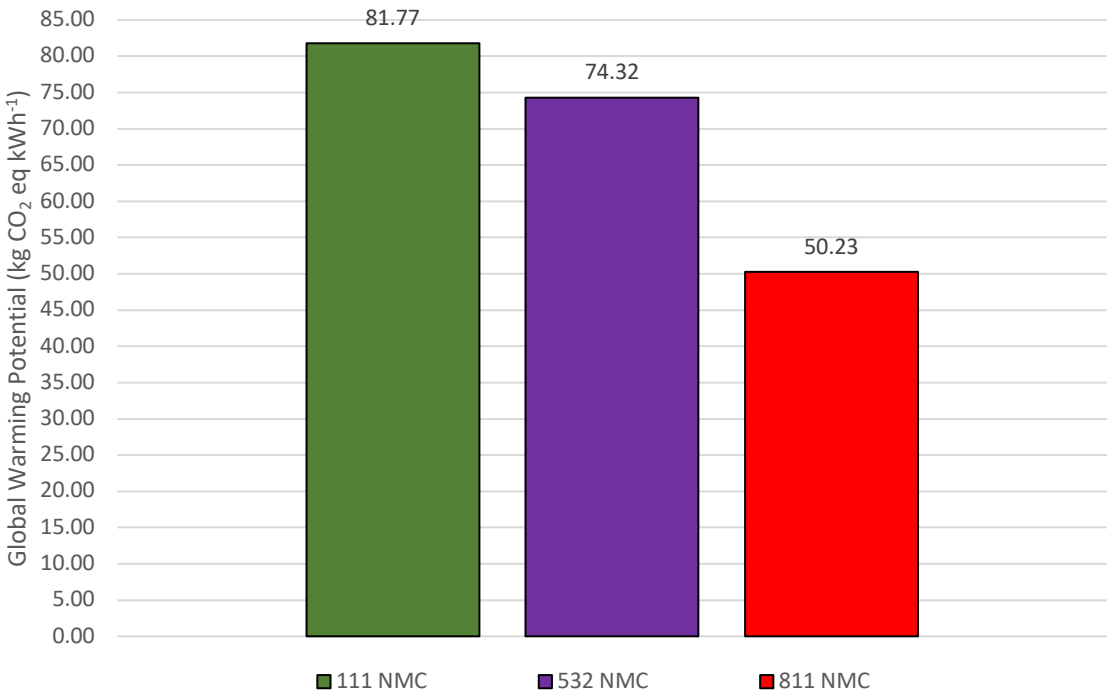

Figure 4.25: Graph of global warming potential impacts for each battery chemistry per kWh of battery capacity

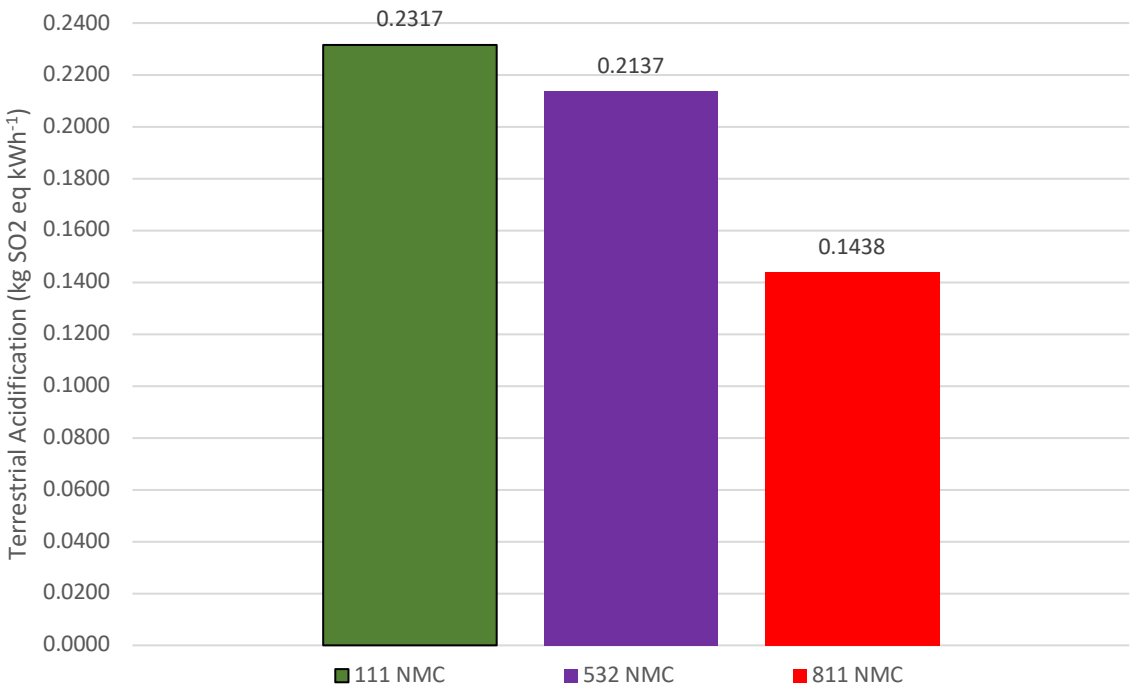

Figure 4.26: Graph of terrestrial acidification impacts for each battery chemistry per kWh of battery capacity

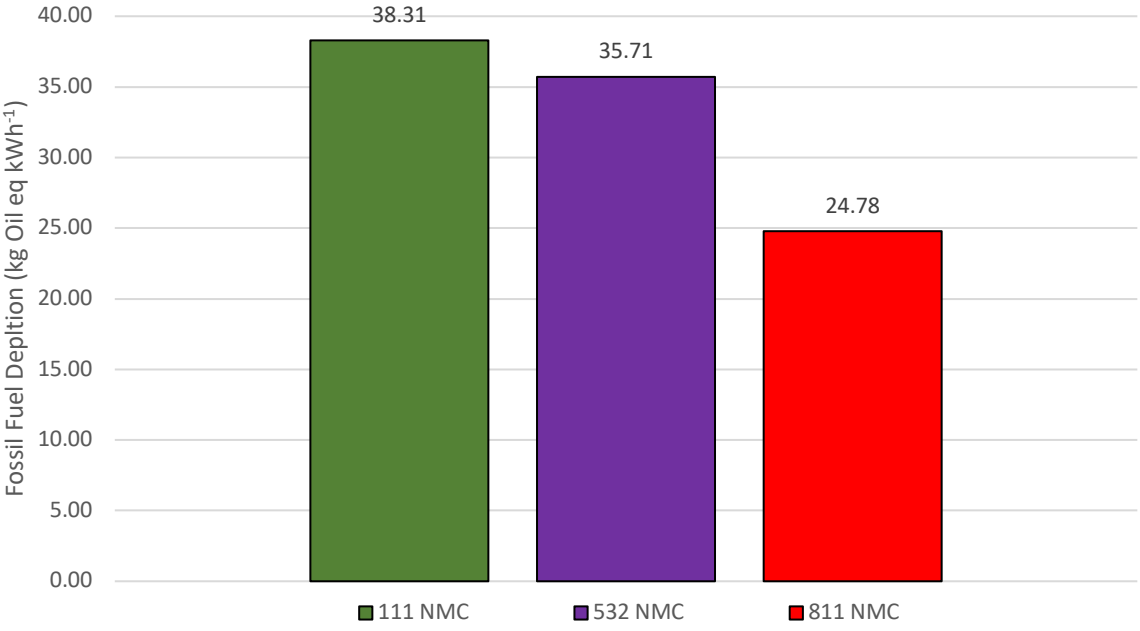

Figure 4.27: Graph of Fossil Fuel Depletion impacts for each battery chemistry per kWh of battery capacity

This comparison shows the decrease in environmental impacts that the changes from 111 LiNMC through to 811 LiNMC has. This is further re-enforced by changing the format of the comparison data to examine the percentile differences in the different chemistries and the number of modules each chemistry requires, with 532 LiNMC being used as the base line. This can be seen if table 4.5:

Table 4.5: Ratios of impacts and numbers of modules between different battery chemistries

Impact factor (as a % of the 532 NMC values)	111 LiNMC	532 LiNMC	811 LiNMC
Module numbers within pack	107.7	100.0	65.4
Global Warming Potential (kg CO_2 eq)	110.0	100.0	67.6
Terrestrial Acidification (kg SO_2 eq)	108.4	100.0	67.3
Fossil Fuel Depletion (kg Oil eq)	107.3	100.0	69.4

Table 4.5 does shows that the different module numbers, and therefore the material needed for each pack, seemed to be the major contributing factor. However, the differences between the module and impact ratios does show that the active material composition does have some influence over the impact the battery pack production has. The rapid production of this comparison, compared with having to manually change the necessary values within the model, does show how this tool can influence the code. The current tool is only compatible with the lithium-ion model, although this could be changed with further development to the tool.

4.5.3 Data presentation tool

To test the data presentation tool, several different sets of processes were selected in the control excel worksheet, to demonstrate the effectiveness of the tool. This included the global warming potential and terrestrial acidification of the production of the cathode active material of the lithium-ion pack, along with the same impacts for the production of aluminium foil within the model. Table 4.6, along with figures 4.28, 4.29, 4.31, and 4.32 display the data the tool produced for the cathode active material processes for an entire

battery pack, with few changes being made, such as presenting the impact values to 3 decimal places in table 4.6. All the data shown in this section was produced from running the tool once with the two sets of processes taking up two tables each, one for each impact category:

Table 4.6: Processes for 532 NMC Lithium-ion cathode active material production comparison

Process	**GLOBAL WARMING POTENTIAL** (kg CO_2-Eq)	terrestrial acidification (kg SO_2-Eq)
Ammonium hydroxide solution production	28.443	0.005
Cobalt Sulphate production	588.745	1.065
Electricity mix (cathode active material production) (process transmission)	39.531	0.083
Lithium carbonate production (ore based) (Active material production)	26.010	0.100
Manganese Sulphate production (from metal)	165.680	0.396
Nickel Sulphate production	950.654	2.014
Sodium Carbonate production (LiNMC active material)	103.845	0.224

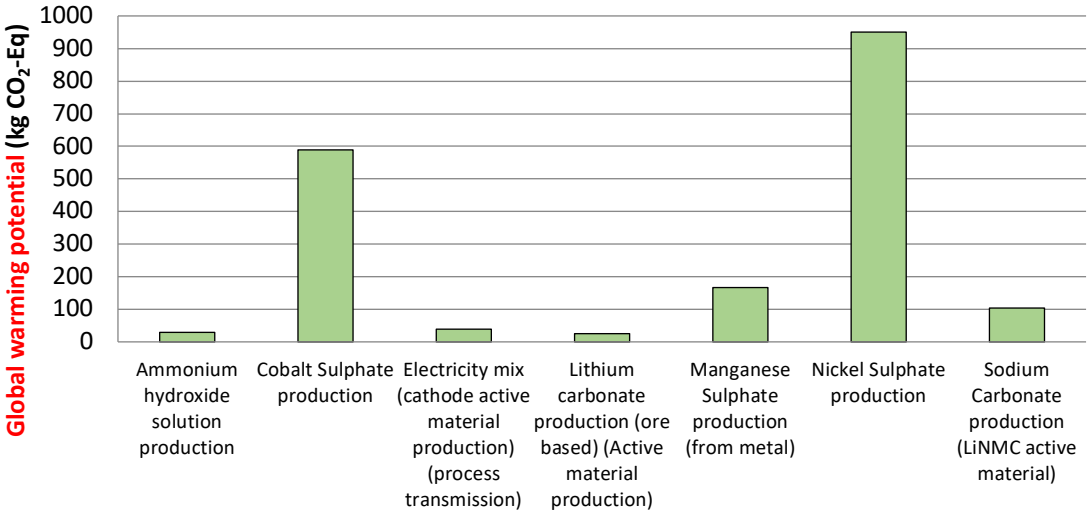

Figure 4.28: Processes for 532 NMC Lithium-ion active material production global warming potential bar chart

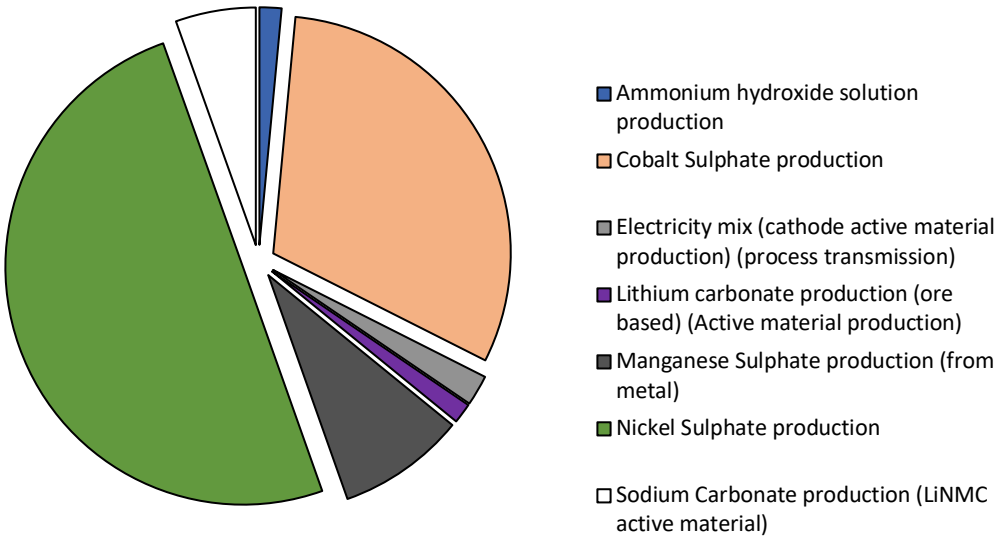

Figure 4.29: Processes for 532 NMC Lithium-ion active material production, pie chart on global warming potential impacts

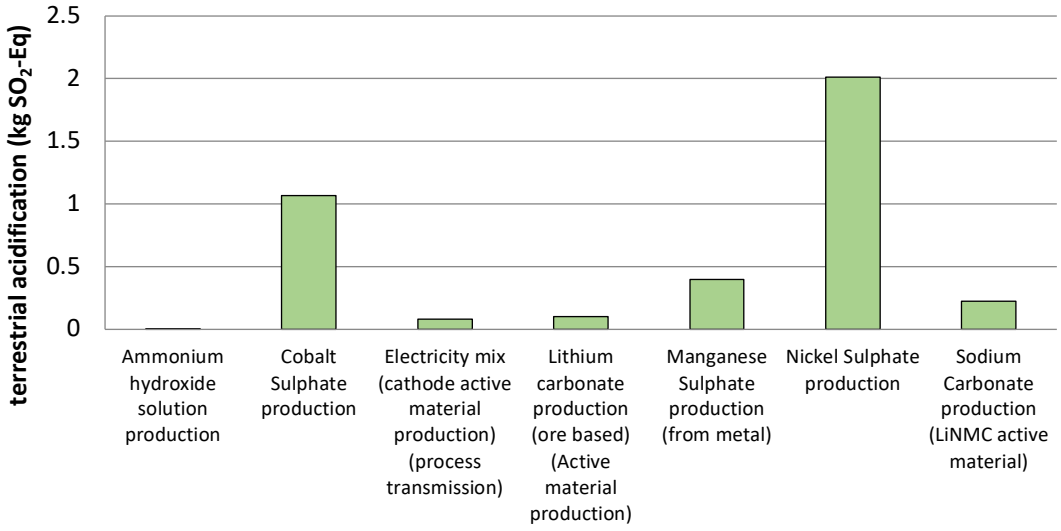

Figure 4.30: Processes for 532 NMC Lithium-ion active material production terrestrial acidification bar chart

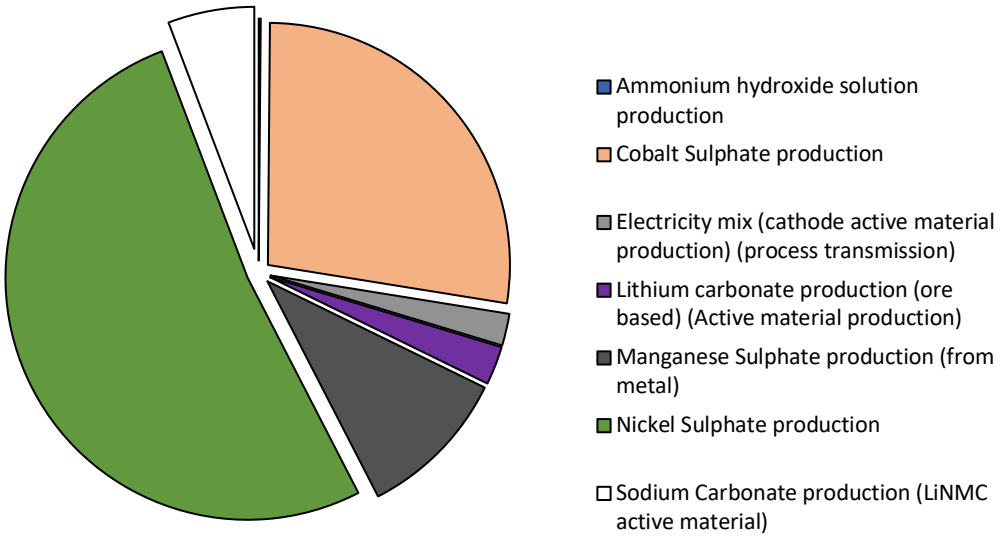

Figure 4.31: Processes for 532 NMC Lithium-ion active material production terrestrial acidification pie chart

As can be seen in figures 4.29 and 4.31, the metal sulphate productions contributed the most to the active materials emissions, with nickel sulphate being the larges with over 50% of the total emissions for both impact categories. This shows that valuable conclusions can

be drawn from the data processed by this tool, which can achieve it quicker than the process of manually searching the exported excel database.

For the aluminium production, table 4.7 displays the emissions produced the production of aluminium foil, with the data this time being displayed in produced line graphs to display the increases in impact each process contributes to, as seen in figure 4.32. Figure 4.33 displays the contribution each individual stage makes to the global warming impact:

Table 4.7: Process for aluminium production comparison

Process	**GLOBAL WARMING POTENTIAL** (kg CO_2-Eq)	terrestrial acidification (kg SO_2-Eq)
Bauxite Mining	0.200	0.001
Aluminium oxide production	127.803	1.007
Aluminium electrolysis	654.614	2.948
Aluminium Ingot casting	661.360	2.967
Aluminium foil production	806.325	3.532

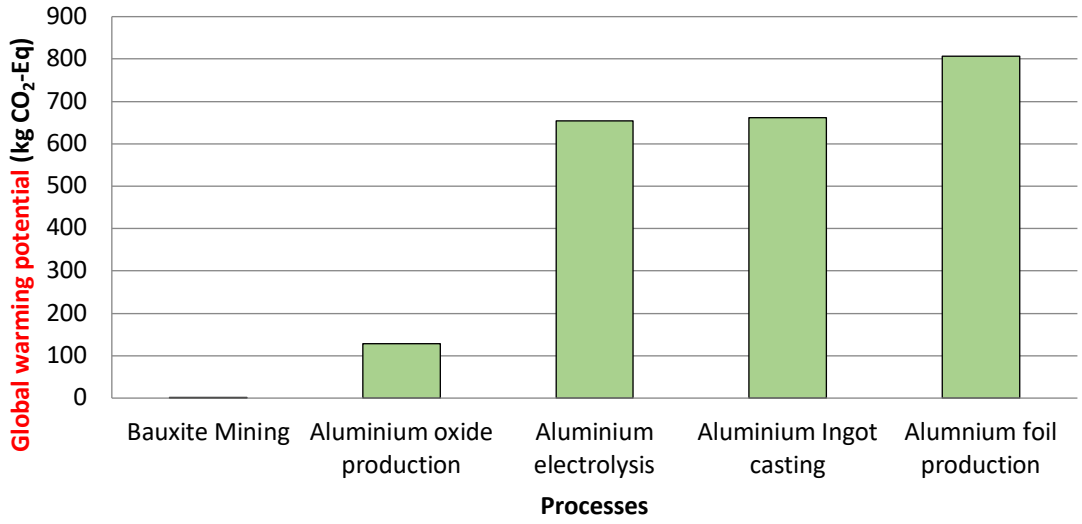

Figure 4.32: Cumulative processes for aluminium production global warming potential bar graph

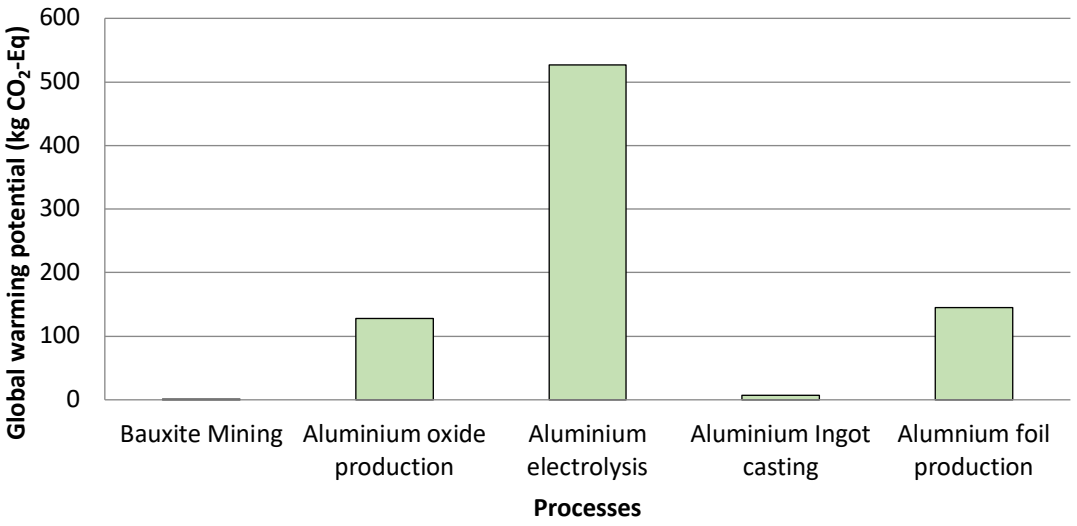

Figure 4.33: Individual processes for aluminium production global warming potential bar graph

Figures 4.32 and 4.33 show the massive contribution the electrolysis process makes to the emissions produced during this set of processes, as can be seen the steep decline as you move backwards through the processes. This can be contributed to not only to the large energy demand of the electrolysis, but also to the materials consumed by the process, such as carbon anodes. This example shows how the bar graph compliments the tools line up of graph options and offers a useful function to the user.

4.5.4 Conclusions derived from tool use

As can be seen from the examples listed in sections 4.5.1-4.5.3, a variety of conclusions can be derived from the modifications, and production of tables and graphs, the tools produce through their use. With the location modification tool, it can be seen how changing the location of a single input process, even one as impactful as aluminium production, has a relatively small change to the overall impacts of the battery pack. Meanwhile it also shows the effect of changing the manufacturing centre's location is dramatic, which can be attributed to the change in electricity mix within a high demand set of processes, as well as the change in distances needing for all the supply processes.

For the battery chemistry tool, the data derived from its modifications show the effect that changes in battery chemistries have. This can be shown with the 811 ratio of LiNMC benefiting from lower demands for high emission processes, such as the production of cobalt sulphate, as well as the reduced materials needed to achieve the desired 60 kWh capacity for the battery pack. The high impacts produced by cobalt sulphate manufacturing is reinforced with the data presented by the data presentation tool. This data supports this conclusion, as even at the 532 ratio of LiNMC, where cobalt has the lowest mass of the three metal sulphates, it is the second largest contributor to the GWP and terrestrial acidification over all the inputs in producing the LiNMC active material.

4.6 Innovation within the tools

These tools demonstrate the improvements that can be made to LCA software using programming languages and the skills needed to design and produce these programs. With life cycle assessment set to become more important within industry, as concerns on environmental wellbeing and desires to assess a businesses impact grow, these tools offer an excellent addition to working with LCA software. They offer improve interactions with the models, which will assist LCA practitioners, data analysists and other groups who need environmental data for their work, either by simplifying the process of changing the model or how they review and process the data from these models.

There were differences with how useful some of the tools are depending on what they were used for. The location modification tool showed that only changing one location had a minimal impact on the emissions of the overall production process, although with multiple changes, such as the relocation of the battery manufacturing plant, had a more substantial impact. This does show that the tool has beneficial effects when modifying the existing model and can be easily used by non-LCA practitioners to prepare data for their own use, such as building a report on the impacts that a planned battery plant may have on the environment. The battery chemistry tool offers the easy and quick comparison of different chemistries and how they affect the impacts the battery packs produce. The data presentation tool offers easy access to the data produced by nearly 300 different processes

within the openLCA lithium-ion model, as well to separate the desired data into a separate excel sheet for further analysis as the user wishes.

4.7 Summary – LCA tools

The tools produced by this work offer advantages to those using them with both speed and readability of changing a LCA model or examining the data produced from it. While the tools cannot replace the expertise of a life cycle assessment practitioner, as the model still needs to be produced, they offer enhanced functions in conjunction with the openLCA software for manipulating the model to produce data needed by the user. The tools currently only operate with the specified openLCA model used for testing but could easily be adapted for use with other models or even converted to operate with model constructed within other LCA software packages.

The data presentation tool offers a cleanly presented set of data, which can be searched for and assembled easily within the control spreadsheet in a user-friendly manner. The battery chemistry tool allows for the quick and repeatable comparison of different types of battery pack without having to build new models for each one, which can be a time-consuming process. The location modification tool allows a user to examine how different material sources within their supply chain affect their environmental impact, although how this affects the overall model appears to minor at best. However, even the smallest changes can be beneficial to the users on showing the environmental impact one location has over another, and that this can be achieved quickly and repeatably thanks to the user interface and the database of information.

5. Conclusion

5.1 Project output significance

Energy solutions for electric vehicles have made significant advances over the last decade but different aspects of the production of their batteries hold them back, whether it is due to impeded performance or how their production affects the environment. With many consumers choosing to purchase electric vehicles based on their environmentally friendly credentials, this poses a large issue, along with other consumers not purchasing due to the lower range the vehicles have compared with their petrol counterparts.

Examination of various supercapacitors raised queries of how different binders, mixing methodologies, and thicknesses of their electrodes affected their performance. This led to extensive testing of carbon-based button cell supercapacitors to examine different variations of these three variables. The testing showed that the CMC and SBR mix of binders offered better capacity for the button cell compared with the PVDF based binders common in other supercapacitors, while also showing that the mixing methodology influenced capacity as well. This is supported by the data from figure 2.4 and 2.5. The major conclusion from the comparison of electrode thicknesses however was with failure rates, with increasing failure rates for all the variations of the two largest electrode wet thicknesses examined. Examination of them, as seen in figures 2.8 and 2.9, indicated that binders were pooling on the surface, obstructing the electrodes active sites, which could have affected the capacity of the cell. This was along with contamination and cracks in the electrodes, such as the contamination seen in figure 2.10, which could have contributed to failures within the cells, such as poor electrode stability, alongside the binder pooling.

Alongside further development of energy storge solutions, there is definite industrial interest in examining the environmental impact of the production of batteries for electric vehicles, as well as the impacts for other energy storage solutions. Discussions with international groups under Ricardo PLC, from Italy and Malaysia, showed industrial interest in assessing the emissions of batteries for electric motorcycles, as well as for static energy storage for electricity grids. There have been many different examinations of the emissions a battery produces across its life cycle, although many that have been in the public eye have

focused on the use phase of the battery's life. Batteries still struggle to lower their emissions at their production phase, with a reliance on virgin materials being a critical issue.

A major issue that stands in LCA work is the difficulty of using some of the dedicated programs for producing LCA models. While many different software packages exist and offer a wealth of advantages, including databases of available data on a variety of processes, the software is often complex to use, inflexible, and required extensive training to produce the model industry wants. Many companies still rely on Microsoft Excel to produce LCA data, as while it requires more work as the equations and data must be build up manually, a process many dedicated software's automate, it is a simple software that many employees are already trained to use. Therefore, providing a means to improve and simplify the user experience of using the dedicated software would be beneficial, both for existing users and potential future users who may or may not be dedicated life cycle assessment practitioners.

The first stage of this work was to produce LCA models on electric vehicle batteries production. This gave an insight on how the production contributed to the overall emissions of the battery's production but also showed how the examined software, openLCA, worked and what could be done to improve the experience of using the software. This produced two models and sets of environmental impact data for a 60-kWh battery pack, one with a lithium-ion based chemistry and one with a sodium-ion chemistry, with details on these found in section 3. The results, found in figures 3.19, 3.20, 3.21, and 3.22, showed the sodium-ion chemistry emitted more pollution for the impact factors examined, with the larger number of cells needed to reach the desired capacity and the cell's higher reliance on aluminium being major factors that contributed to this. This was found on repeat calculations on the models and was mirrored by comparisons made to similar battery packs examined in literature, as seen in table 3.7. These impacts will improve as sodium-ion energy densities increase due to technological developments, as this would reduce the mass of materials needed to reach the desired capacity for battery packs, therefore reducing the impacts derived from producing the required materials.

The production of these models often required multiple iterations and changes to the data, as details about each process within the models were changed, with updated data or changes in design, such as changes in the supply location for a material. To assist in changing these values in the future, two Python based tools were created to make changes to the

lithium-ion battery model input flows for distance and electricity mix values, as well as to modify the battery chemistry and the other variable this impacts within the model. Another tool created processed the data from the model, collecting data requested by a user and arranging it in a clean and understandable format, in both tables and graphs for further use.

Details on all three of these tools can be found in section 4, with each of the tools proving their worth. While the tool to modify the distances had minimal impact outside of moving the battery assembly plant, it still proved the value of tools that allowed for easy modification of the model, without having the manually change the values within openLCA. That task can be difficult to achieve, especially if the model is unfamiliar to the user looking to make changes to gain appropriate data. The battery chemistry tool showed more differences and offer the opportunities for quick, easy, and repeatable comparison of equivalent battery packs with different battery chemistries. Both tools have the disadvantage that they are currently built specifically for use with a specific openLCA model but their foundation in Python means that they can be adapted to operate with multiple different models in the future. This is detailed more in sections 4.5.1 and 4.52. The data presentation tool worked well alongside these modification tools, providing desired data in a readable and rapid fashion. Small changes would also be needed to operate with the data from other models, but the current tool offers a solid basis for future tools.

A summary of how the aims of each of the projects detailed in this report were achieved and how they contributed to science and industry can be found below in table 5.1:

Table 5.1: Research aims and their contributions

Aim	Scientific contribution	Industrial contribution
Testing of the impact of changing different aspects of supercapacitor inks – comparison of different binders, mixing methodologies and wet thicknesses	1. Demonstrated the differences mixing methodologies have on the capacity of supercapacitors. 2. The surfaces of the supercapacitor electrodes had major issues when examined, such as binder pooling on the surface, cracks, and contaminants, which likely impeded performance.	1. Demonstrated the benefits of the CMC and SBR mix of binders over the PVDF within the specific ink mix. This could be used in support of using these binders in industrial production of supercapacitors.
Understanding the manufacturing process of a Lithium-ion battery pack – examination of the full manufacturing process and production of LCA model from that data	1. Identification of different parts of the battery manufacture process and the construction of a complete model. 2. Production of knowledge of the production process of lithium-ion battery packs.	1. Manufactured access to a complete and detailed model of battery pack production and the data derived from said model.
Compare the environmental impacts of two battery chemistries – achieved by comparison of lithium-ion and sodium-ion battery packs through the LCA	1. The lithium-ion chemistry battery pack examined produced lower emissions compared with its sodium-ion counterpart, with	1. Sodium-ion requires an increase in its specific capacity to compete with lithium-ion, as the large amount of material needed to reach desired

methodology	sodium-ion's increase being attributed to increased demand for material. 2. Sodium-ion holds the potential to be more environmentally friendly compared with lithium-ion, although more research and development needs to be conducted.	battery capacity would impact the performance of a vehicle and increase economic costs of production and use. 2. Further funding and work within this area are needed to improve the capacity of sodium-ion chemistries, which could lead to more jobs being required to achieve this.
Improve the use of LCA software – achieved by production of Python based tool to interact with models and process data	1. Showing the simplification of modifying and presentation data from LCA models.	1. Several tools that are beneficial for working with openLCA models and software. 2. Demonstration of the benefits of additional tools to using LCA software and how both Excel and Python can be used in producing them. 3. Demonstrated the versatility of LCA software and how changes can be made to it to further intended design goals. 4. Allows for the wider use of LCA models by non-LCA practitioners,

		increasing the social understanding of LCA from other STEM professions having use of the methodology.

5.2 Future work

5.2.1 LCA tools work

While the tools offer an excellent set of functions to assist in working with LCA models and data, there are several improvements that would help the tool in their function or in adding new ones:

1) Conversion of the location modification tool to operate with a user interface like that of the data presentation tool, given the tool can be slow when modifying multiple locations. The proposed interface would speed up this by removing ultimately unnecessary processing time inputting each change individually.
2) Implementation so that the tools can interact with other LCA models and exported data, for both openLCA based models and other LCA software models. This would expand the usability of the tool by applying to more models without forcing users to conform to the current LCA model.
3) Continued improvement of the data used in the models and the tools, with more processes that are not reliant on lab scale data. As with many different LCA models, this is almost always needed as the production processes changes with other innovations in battery production, such as improvements to energy efficicency.
4) A possible addition to the battery chemistry tool to allow for the modification of the capacity of the batteries, as well as a possible means to modify some of the design elements of the pack. This could include altering the number of cells present in a module or a means to change the type of cell within the battery pack.

5.2.2 LCA model work

From the work conducted with the two LCA models constructed for this work, some further work would need to be done. which could include some of the following:

LCA model improvements

1) Capturing data and production of another LCA report on the production of the O3 type active material, to more accurately capture where emissions are produced within its production, alongside examination of other sodium-ion cathode active materials. This would likely require contact with groups and companies examining theses active materials, such as Faradion and HiNa Battery (Zhao et al., 2022).
2) Continued updating and improvement of the data used in the models to ensure they stay up to date. This includes keeping up to date and accurate data on the extraction of key metals, such as nickel and aluminium, alongside other key materials, such as the production of battery grade graphite.
3) Examine how to make the models more flexible to examine other battery chemistries. This could include examination of LMO lithium-ion, LFP lithium-ion and P2 type sodium-ion batteries.

Industry improvements to battery design

1) Work to improve the battery cells within both lithium-ion and sodium-ion to increase their capacity per cell, to reduce the material needed which in turn would reduce the overall emissions of producing the pack.
2) Investigate means of reducing the role of or outright removing the organic solvents, such as the NMP, within the production processes of both battery packs. Currently, de-ionized water offers one alternative, with it is used in anode production, as seen in section 3.29.
3) Continued development of recycling methodologies to keep more materials within the battery market after use, given the high impacts the virgin materials that batteries currently rely on produce. Many methodologies for key battery materials are not economically or environmentally sustainable. This is compounded with many materials

leaving the battery industry due to concerns that recovered materials performance would be below that of virgin materials (Beaudet et al., 2020).

5.3 Sustainability importance

With ever growing concerns on the impact of climate change and other consequences of pollution it is essential that we work to reduce or eliminate our emissions within industry. The introduction of electric vehicles has taken a step in the right direction for the transport industry, although the impacts to produce their batteries are concerning, especially at the prospect of their ever-growing adoption worldwide.

Having the tools to effectively assess the emissions production, along with having viable energy storage solutions, such as supercapacitors, to replace or compliment the current battery technologies within electric vehicles is essential for the industry going forward. Within this report is detailed an overview of the production of useful models and data relating to the life cycle of battery packs, along with tools to make the use of these model more accessible and cost-effective for industry and academia. The availability of this information, whether for the models, their impact data or the mechanisms that power the tools described, offer a wide set of contributions to furthering sustainability within the automotive industry.

This not only comes from additional data on battery pack impacts helping to inform future developments, both in pursuing new battery designs and how to manufacture them, but also by making life cycle assessments more accessible. By allowing industry to improve their use of life cycle assessment software, they are more likely to adopted and expand on its use within their businesses. Wider adoption of life cycle assessment methodologies will work to improve the sustainability of the industry, by providing them with the information they need to make informed decisions on their business practices and hopefully work to reduce their impacts.

These solutions can be used in many other industries beside transport, given energy storage devices are increasingly being sort for different applications, such as static storage for electricity grids. Ensuring that they are available and can be proven to have beneficial

environmental impacts will be necessary to keep humanity progressing while combating the effects of our past errors with the environment.

6. References

Abdykirova, G.Zh., Tanekeeva, M.Sh., Sydykov, A.E. and Diosenova, S.B., 2016. Production of electrolytic manganese dioxide from purified solutions after the leaching of manganese-bearing slurry. *Steel in Translation* [Online], 46(5), pp.319–321. Available from: https://doi.org/10.3103/S0967091216050028.

Accardo, A., Dotelli, G., Musa, M.L. and Spessa, E., 2021. Life Cycle Assessment of an NMC Battery for Application to Electric Light-Duty Commercial Vehicles and Comparison with a Sodium-Nickel-Chloride Battery. *Applied Science* [Online], 11(3). Available from: https://doi.org/10.3390/app11031160.

Ahmed, S., Nelson, P.A., Gallagher, K.G., Susarla, N. and Dees, D.W., 2017. Cost and energy demand of producing nickel manganese cobalt cathode material for lithium ion batteries. *Journal of Power Sources* [Online], 342, pp.733–740. Available from: https://doi.org/10.1016/j.jpowsour.2016.12.069.

Alizadeh Asl, S., Mousavi, M. and Labbafi, M., 2017. Synthesis and Characterization of Carboxymethyl Cellulose from Sugarcane Bagasse. *Journal of Food Processing & Technology* [Online], 08(08). Available from: https://doi.org/10.4172/2157-7110.1000687.

Amnesty International, 2016. *Exposed: Child labour behind smart phone and electric car batteries*. *Amnesty.org* [Online]. Available from: https://www.amnesty.org/en/latest/news/2016/01/child-labour-behind-smart-phone-and-electric-car-batteries/ [Accessed 21 November 2018].

Atkins, P., Overton, T., Rourke, J., Weller, M., Armstrong, F. and Hagerman, M., 2010. *Shriver & Atkins' Inorganic Chemistry*. 5th ed. W.H Freemand and Company.

Augustyn, V., Simon, P. and Dunn, B., 2014. Pseudocapacitive oxide materials for high-rate electrochemical energy storage. *Energy & Environmental Science* [Online], 7(5), p.1597. Available from: https://doi.org/10.1039/c3ee44164d.

Azaïs, P., Duclaux, L., Florian, P., Massiot, D., Lillo-Rodenas, M.-A., Linares-Solano, A., Peres, J.-P., Jehoulet, C. and Béguin, F., 2007. Causes of supercapacitors ageing in organic electrolyte. *Journal of Power Sources* [Online], 171(2), pp.1046–1053. Available from: https://doi.org/10.1016/j.jpowsour.2007.07.001.

Baba, A.A., Ibrahim, L., Adekola, F.A., Bale, R.B., Ghosh, M.K., Sheik, A.R., Pradhan, S.R., Ayanda, O.S. and Folorunsho, I.O., 2014. Hydrometallurgical Processing of Manganese Ores: A Review. *Journal of Minerals and Materials Characterization and Engineering* [Online], 02(03), pp.230–247. Available from: https://doi.org/10.4236/jmmce.2014.23028.

Balasubramaniam, B., Singh, N., Verma, S. and Gupta, R.K., 2020. Recycling of Lithium From Li-ion Batteries. *Encyclopedia of Renewable and Sustainable Materials* [Online]. Elsevier, pp.546–554. Available from: https://doi.org/10.1016/B978-0-12-803581-8.10764-7.

Beaudet, A., Larouche, F., Amouzegar, K., Bouchard, P. and Zaghib, K., 2020. Key Challenges and Opportunities for Recycling Electric Vehicle Battery Materials. *Sustainability* [Online], 12(14), p.5837. Available from: https://doi.org/10.3390/su12145837.

Beheshti, R., Tabeshian, A. and Aune, R.E., 2017. *Lithium-Ion Battery Recycling Through Secondary Aluminum Production* [Online]. pp.267–274. Available from: https://doi.org/10.1007/978-3-319-52192-3_26.

Boulanger, N., Skrypnychuk, V., Nordenström, A., Moreno-Fernández, G., Granados-Moreno, M., Carriazo, D., Mysyk, R., Bracciale, G., Bondavalli, P. and Talyzin, A. V., 2021. Spray Deposition of Supercapacitor Electrodes using Environmentally Friendly Aqueous Activated Graphene and Activated Carbon Dispersions for Industrial Implementation. *ChemElectroChem* [Online], 8(7), pp.1349–1361. Available from: https://doi.org/10.1002/celc.202100235.

Boustead, 2005. *Purified Brine*. *Plastics Europe* [Online]. Available from: http://www.inference.org.uk/sustainable/LCA/elcd/external_docs/brn_311147f1-fabd-11da-974d-0800200c9a66.pdf [Accessed 21 December 2019].

Bresser, D., Buchholz, D., Moretti, A., Varzi, A. and Passerini, S., 2018. Alternative binders for sustainable electrochemical energy storage – the transition to aqueous electrode processing and bio-derived polymers. *Energy Environmental Science* [Online], 11, pp.3096–3127. Available from: https://doi.org/10.1039/C8EE00540G.

Bridgewater, G., Capener, M.J., Brandon, J., Lain, M.J., Copley, M. and Kendrick, E., 2021. A Comparison of Lithium-Ion Cell Performance across Three Different Cell Formats. *Batteries* [Online], 7(2), p.38. Available from: https://doi.org/10.3390/batteries7020038.

Chernysh, O., Khomenko, V., Makyeyeva, I. and Barsukov, V., 2019. Effect of binder's solvent on the electrochemical performance of electrodes for lithium-ion batteries and supercapacitors. *Materials Today: Proceedings* [Online], 6, pp.42–47. Available from: https://doi.org/10.1016/j.matpr.2018.10.073.

Curran, M.A., 2017. Overview of Goal and Scope Definition in Life Cycle Assessment. *Goal and Scope Definition in Life Cycle Assessment. LCA Compendium – The Complete World of Life Cycle Assessment* [Online]. pp.1–62. Available from: https://doi.org/10.1007/978-94-024-0855-3_1.

Dai, Q., Kelly, J. and Elgowainy, A., 2018. *Cobalt Life Cycle Analysis Update for the GREET Model*.

Dai, Q., Kelly, J.C., Dunn, J. and Benavides, P.T., 2018. *Update of Bill-of-materials and Cathode Materials Production for Lithium-ion Batteries in the GREET Model*.

Dai, Q, Kelly, J.C., Gaines, L. and Wang, M., 2019. Life Cycle Analysis of Lithium-Ion Batteries for Automotive Applications. *Batteries* [Online], 5(48). Available from: https://doi.org/https://doi.org/10.3390/batteries5020048.

Dai, Qiang, Kelly, J.C., Gaines, L. and Wang, M., 2019. Life Cycle Analysis of Lithium-Ion Batteries for Automotive Applications. *Batteries* [Online], 5(2), p.48. Available from: https://doi.org/10.3390/batteries5020048.

Dunn, J.B., Gaines, L., Barnes, M., Sullivan, J. and Wang, M., 2014. *Material and Energy Flows in the Materials Production, Assembly, and End-of-Life Stages of the Automotive Lithium-Ion Battery Life Cycle*.

Dunn, J.B., Gaines, L., Barnes, M., Wang, M. and Sullivan, J., 2012. *Material and energy flows in the materials production, assembly, and end-of-life stages of the automotive lithium-ion battery life cycle* [Online]. Argonne, IL (United States). Available from: https://doi.org/10.2172/1044525.

Dutta, A., Mitra, S., Basak, M. and Banerjee, T., 2022. A comprehensive review on batteries and supercapacitors: Development and challenges since their inception. *Energy Storage* [Online]. Available from: https://doi.org/10.1002/est2.339.

Ekvall, T., Tillman, A.M. and Molander, S., 2005. Normative ethics and methodology for life cycle assessment. *Journal of Cleaner Production* [Online], 13(13–14), pp.1225–1234. Available from: https://doi.org/10.1016/j.jclepro.2005.05.010.

Elkingson, J., 1997. *Cannibals with Forks: The Triple Bottom Line of 21st Century Business*. Oxford.

Ellingsen, L.A.W., Majeau-Bettez, G., Singh, B., Srivastava, A.K., Valøen, L.O. and Strømman, A.H., 2014. Life Cycle Assessment of a Lithium-Ion Battery Vehicle Pack. *Journal of Industrial Ecology* [Online], 18(1), pp.113–124. Available from: https://doi.org/10.1111/jiec.12072.

Ellingsen, L.A.-W., Majeau-Bettez, G., Singh, B., Srivastava, A.K., Valøen, L.O. and Strømman, A.H., 2014. Life Cycle Assessment of a Lithium-Ion Battery Vehicle Pack. *Journal of Industrial Ecology* [Online], 18(1), pp.113–124. Available from: https://doi.org/10.1111/jiec.12072.

ESU Services, 2021. *Life Cycle Inventory Data* [Online]. Available from: http://esu-services.ch/data/ [Accessed 29 September 2021].

European Aluminium Association, 2013. *Environmental Profile Report for the European Aluminium Industry*.

European Environment Agency, 2018. *Electric vehicles from life cycle and circular economy perspectives TERM 2018: Transport and Environment Reporting Mechanism (TERM) report* [Online]. Available from: https://doi.org/10.2800/77428.

European Environment Agency, 2019. *Regulation (EU) 2019/631*. *EEA.europa.eu* [Online]. Available from: https://www.eea.europa.eu/policy-documents/regulation-eu-2019-631#:~:text=Regulation (EU) 2019%2F631 of the European Parliament and,EU) No 510%2F2011. [Accessed 21 June 2022].

EWI, 2021. *Ultrasonic Metal Welding for Lithium-Ion Battery Cells* [Online]. Available from: https://ewi.org/ultrasonic-metal-welding-for-lithium-ion-battery-cells-2/.

Farjana, S.H., Huda, N., Mahmud, M.A.P. and Lang, C., 2019. A global life cycle assessment of manganese mining processes based on EcoInvent database. *Science of The Total Environment* [Online], 688, pp.1102–1111. Available from: https://doi.org/10.1016/j.scitotenv.2019.06.184.

Forghani, M. and Roberts, A.J., 2021. Application of step potential electrochemical spectroscopy in pouch cell prototype capacitors. *Electrochimica Acta* [Online], 390, p.138845. Available from: https://doi.org/10.1016/j.electacta.2021.138845.

Garakani, M.A., Bellani, S., Pellegrini, V., Oropesa-Nuñez, R., Castillo, A.E.D.R., Abouali, S., Najafi, L., Martín-García, B., Ansaldo, A., Bondavalli, P., Demirci, C., Romano, V., Mantero, E., Marasco, L., Prato, M., Bracciale, G. and Bonaccorso, F., 2021. Scalable spray-coated graphene-based electrodes for high-power electrochemical double-layer capacitors operating over a wide range of temperature. *Energy Storage Materials* [Online], 34, pp.1–11. Available from: https://doi.org/10.1016/j.ensm.2020.08.036.

Goedkoop, M., Heijungs, R., Huijbregts, M., Schryver, A.D. and Zelm, R. V, 2013. *ReCiPe 2008*.

González, A., Goikolea, E., Barrena, J.A. and Mysyk, R., 2016. Review on supercapacitors: Technologies and materials. *Renewable and Sustainable Energy Reviews* [Online], 58, pp.1189–1206. Available from: https://doi.org/10.1016/j.rser.2015.12.249.

Google, 2020. *GoogleMaps*.

GreenDelta, 2019. *OpenLCA* [Online]. Available from: http://www.openlca.org/ [Accessed 25 February 2019].

Hawkins, T.R., Singh, B., Majeau-Bettez, G. and Strømman, A.H., 2013. Comparative Environmental Life Cycle Assessment of Conventional and Electric Vehicles. *Journal of Industrial Ecology* [Online], 17(1), pp.53–64. Available from: https://doi.org/10.1111/j.1530-9290.2012.00532.x.

Heimböckel, R., Hoffmann, F. and Fröba, M., 2019. Insights into the influence of the pore size and surface area of activated carbons on the energy storage of electric double layer capacitors with a new potentially universally applicable capacitor model. *Physical Chemistry Chemical Physics* [Online], 21(6), pp.3122–3133. Available from: https://doi.org/10.1039/C8CP06443A.

Helmers, E., Dietz, J. and Weiss, M., 2020. Sensitivity Analysis in the Life-Cycle Assessment of Electric vs. Combustion Engine Cars under Approximate Real-World Conditions. *Sustainability* [Online], 12(3), p.1241. Available from: https://doi.org/10.3390/su12031241.

Helmers, E. and Marx, P., 2012. Electric cars: technical characteristics and environmental impacts. *Environmental Sciences Europe* [Online], 24(1), p.14. Available from: https://doi.org/10.1186/2190-4715-24-14.

Horn, M., MacLeod, J., Liu, M., Webb, J. and Motta, N., 2019. Supercapacitors: A new source of power for electric cars? *Economic Analysis and Policy* [Online], 61, pp.93–103. Available from: https://doi.org/10.1016/j.eap.2018.08.003.

Hu, G., Kang, J., Ng, L.W.T., Zhu, X., Howe, R.C.T., Jones, C.G., Hersam, M.C. and Hasan, T., 2018. Functional inks and printing of two-dimensional materials. *Chemical Society Reviews* [Online], 47(9), pp.3265–3300. Available from: https://doi.org/10.1039/C8CS00084K.

Huisman, J., Ciuta, T., Bobba, S. and Georgitzikis, K., 2020. *Raw Materials in the Battery Value Chain - Final content for the Raw Materials Information System – strategic value chains – batteries section* [Online]. Available from: https://doi.org/10.2760/239710.

International Energy Agency (IEA), 2020a. *Global car sales by key markets, 2005-2020*. *IEA* [Online]. Available from: https://www.iea.org/data-and-statistics/charts/global-car-sales-by-key-markets-2005-2020 [Accessed 18 January 2021].

International Energy Agency (IEA), 2020b. *Global EV outlook 2020*. *IEA* [Online]. Available from: https://www.iea.org/reports/global-ev-outlook-2020 [Accessed 2 November 2020].

International Energy Agency (IEA), 2021. *United Kingdom* [Online]. Available from: https://www.iea.org/countries/united-kingdom [Accessed 30 August 2021].

International Organization for Standardization, 2006. ISO 14044 - Environmental management — Life cycle assessment — Requirements and guidelines. *International Standard* [Online], 2006(7), pp.652–668. Available from: https://doi.org/10.1007/s11367-011-0297-3.

Jarosinski, A., Radomski, P., Lelek, L. and Kulczycka, J., 2020. New Production Route of Magnesium Hydroxide and Related Environmental Impact. *Sustainability* [Online], 12(21), p.8822. Available from: https://doi.org/10.3390/su12218822.

Jin, H., Wang, X., Gu, Z., Anderson, G. and Muthukumarappan, K., 2014. Distillers dried grains with soluble (DDGS) bio-char based activated carbon for supercapacitors with organic electrolyte tetraethylammonium tetrafluoroborate. *Journal of Environmental Chemical Engineering* [Online], 2(3), pp.1404–1409. Available from: https://doi.org/10.1016/j.jece.2014.05.019.

Johnson Matthey, 2021. *Battery materials* [Online]. Available from: https://matthey.com/en/products-and-services/battery-materials.

Jolliet, O., Margni, M., Charles, R., Humbert, S., Payet, J., Rebitzer, G. and Rosenbaum, R., 2003. IMPACT 2002+: A new life cycle impact assessment methodology. *The International Journal of Life Cycle Assessment* [Online], 8(6), pp.324–330. Available from: https://doi.org/10.1007/BF02978505.

Jørgensen, A., Dreyer, L.C. and Wangel, A., 2012. Addressing the effect of social life cycle assessments. *The International Journal of Life Cycle Assessment* [Online], 17(6), pp.828–839. Available from: https://doi.org/10.1007/s11367-012-0408-9.

Kanari, N., Menad, N.-E., Ostrosi, E., Shallari, S., Diot, F., Allain, E. and Yvon, J., 2018. Thermal Behavior of Hydrated Iron Sulfate in Various Atmospheres. *Metals* [Online], 8(12), p.1084. Available from: https://doi.org/10.3390/met8121084.

Kane, M., 2019. *Here is the Nissan LEAF e+ 62 kWh Battery* [Online]. Available from: https://insideevs.com/news/342009/here-is-the-nissan-leaf-e-62-kwh-battery-video/ [Accessed 21 September 2021].

Khoo, J.Z., Haque, N., Woodbridge, G., McDonald, R. and Bhattacharya, S., 2017. A life cycle assessment of a new laterite processing technology. *Journal of Cleaner Production* [Online], 142, pp.1765–1777. Available from: https://doi.org/10.1016/j.jclepro.2016.11.111.

Kirchherr, J., Reike, D. and Hekkert, M., 2017. Conceptualizing the circular economy: An analysis of 114 definitions. *Resources, Conservation and Recycling* [Online], 127, pp.221–232. Available from: https://doi.org/10.1016/j.resconrec.2017.09.005.

Koehler, L., 2015. Powder metallurgy Nickel and Nickel Alloys. *ASM Handbook*. p.pp 673-681.

Lammens, T.M., Potting, J., Sanders, J.P.M. and De Boer, I.J.M., 2011. Environmental comparison of biobased chemicals from glutamic acid with their petrochemical equivalents. *Environmental Science and Technology* [Online], 45(19), pp.8521–8528. Available from: https://doi.org/10.1021/es201869e.

Lehtimaki, S., 2017. *Printed supercapacitors for energy harvesting applications*. *Tampere University of Technology Publication* [Online]. Available from: https://tutcris.tut.fi/portal/files/10141460/lehtim_ki_1463.pdf.

Lewis, R.J., 1997. *Hawley's Condensed Chemical Dictionary*. 13th ed. John Wiley & Sons Ltd.

Listiyorini, E., 2022. *Why Indonesia Is Jolting Markets by Curbing Commodity Exports*. *Bloomberg UK* [Online]. Available from: https://www.bloomberg.com/news/articles/2022-01-19/why-indonesia-curbs-commodity-exports-jolts-markets-quicktake [Accessed 1 August 2022].

Liu, D., Chen, L.-C., Liu, T.-J., Fan, T., Tsou, E.-Y. and Tiu, C., 2014. An Effective Mixing for Lithium Ion Battery Slurries. *Advances in Chemical Engineering and Science* [Online], 04(04), pp.515–528. Available from: https://doi.org/10.4236/aces.2014.44053.

Lu, W. and Dai, L., 2010. Carbon Nanotube Supercapacitors. *Carbon Nanotubes* [Online]. InTech. Available from: https://doi.org/10.5772/39444.

Majeau-Bettez, G., Hawkins, T.R. and Strømman, A.H., 2011. Life Cycle Environmental Assessment of Lithium-Ion and Nickel Metal Hydride Batteries for Plug-In Hybrid and Battery Electric Vehicles. *Environmental Science & Technology* [Online], 45(12), pp.5454–5454. Available from: https://doi.org/10.1021/es2015082.

Marklines, 2018. *Nissan LEAF Teardown: Lithium-ion battery pack structure* [Online]. Available from: https://www.marklines.com/en/report_all/rep1786_201811 [Accessed 28 September 2021].

Martins-Rodrigues, M.C., Barbieri Da Rosa, L.A., Sousa, M.J. and Godoy, T.P., 2020. Recent Research Topics in Circular Economy. *International Journal of Economics and Management Systems*, 5, pp.1–13.

Masson-Delmotte, V.P., Zhai, A., Pirani, S.L., Connors, C., Pean, S., N, B., Caud, Y., Chen, L., Goldfarb, M.I., Gomis, M., Huang, K., Leitzell, E., Lonnoy, J.B.R., Mathews, T.K., Maycock, T., Waterfield, O., Yelekci, R., Zhou, Y. and Zhou, B., 2021. *Climate Change 2021: The Physical Science Basis. Contribution of Working Group I to the Sixth Assessment Report of the Intergovernmental Panel on Climate Change*.

McLaren, J., Miller, J., O'Shaughnessy, E., Wood, E. and Shapiro, E., 2016. *Emissions Associated with Electric Vehicle Charging: Impact of Electricity Generation Mix, Charging Infrastructure Availability, and Vehicle Type*.

Miao, Y., Hynan, P., von Jouanne, A. and Yokochi, A., 2019. Current Li-Ion Battery Technologies in Electric Vehicles and Opportunities for Advancements. *Energies* [Online], 12(6), p.1074. Available from: https://doi.org/10.3390/en12061074.

Middlemas, S., Fang, Z.Z. and Fan, P., 2015. Life cycle assessment comparison of emerging and traditional Titanium dioxide manufacturing processes. *Journal of Cleaner Production* [Online], 89, pp.137–147. Available from: https://doi.org/10.1016/j.jclepro.2014.11.019.

Mishra, A., Mehta, A., Basu, S., Malode, S.J., Shetti, N.P., Shukla, S.S., Nadagouda, M.N. and Aminabhavi, T.M., 2018. Electrode materials for lithium-ion batteries. *Materials Science for Energy Technologies*, 1(2), pp.182–187.

Moravcikova, K., Stefanikova, Ľ. and Rypakova, M., 2015. CSR Reporting as an Important Tool of CSR Communication. *Procedia Economics and Finance* [Online], 26, pp.332–338. Available from: https://doi.org/10.1016/S2212-5671(15)00861-8.

MTI Corporation, 2013. *Li-ion Battery Chemical Powders, Binders and Electrodes Sheet*. *MTI Corporation* [Online]. Available from: https://www.mtixtl.com/Li-ionBatteryChemicalPowdersBindersandElectrodesSheet.aspx [Accessed 27 February 2020].

Norgate, T. and Haque, N., 2010. Energy and greenhouse gas impacts of mining and mineral processing operations. *Journal of Cleaner Production* [Online], 18(3), pp.266–274. Available from: https://doi.org/10.1016/j.jclepro.2009.09.020.

O'Mahony, C., Haq, E.U., Sillien, C. and Tofail, S.A.M., 2019. Rheological Issues in Carbon-Based Inks for Additive Manufacturing. *Micromachines* [Online], 10(2), p.99. Available from: https://doi.org/10.3390/mi10020099.

O'Neil, M.J., Heckelman, P.E., Koch, C.B., Roman, K.J., Kenny, C.M. and D'Arecca, M.R., 2006. *The Merck Index – An Encyclopaedia of Chemicals, Drugs, and Biologicals*. Merck Research Laboratories.

OpenLCA, 2021. *ELCD* [Online]. Available from: https://nexus.openlca.org/database/ELCD [Accessed 29 September 2021].

Ott, D., Borukhova, S. and Hessel, V., 2016. Life cycle assessment of multi-step rufinamide synthesis – from isolated reactions in batch to continuous microreactor networks. *Green Chemistry* [Online], 18(4), pp.1096–1116. Available from: https://doi.org/10.1039/C5GC01932J.

Ozkan, E., Elginoz, N. and Germirli Babuna, F., 2018. Life cycle assessment of a printed circuit board manufacturing plant in Turkey. *Environmental Science and Pollution Research* [Online], 25(27), pp.26801–26808. Available from: https://doi.org/10.1007/s11356-017-0280-z.

Peters, J., Buchholz, D., Passerini, S. and Weil, M., 2016. Life cycle assessment of sodium-ion batteries. *Energy and Environmental Science* [Online], 9(5), pp.1744–1751. Available from: https://doi.org/10.1039/c6ee00640j.

Polymer Properties Database, 2015. *SBR - Styrene Butadiene Rubber* [Online]. Available from: http://polymerdatabase.com/Elastomers/SBR.html%0D [Accessed 19 December 2019].

Ricardo PLC, 2021. *Battery systems engineering* [Online]. Available from: https://automotive.ricardo.com/batteries.

Røynem, F. and Bolin, L., 2021. *Life Cycle assessment 2021: Carbon footprint of Polestar 2 variants*.

Ryu, H.-H., Sun, H.H., Myung, S.-T., Yoon, C.S. and Sun, Y.-K., 2021. Reducing cobalt from lithium-ion batteries for the electric vehicle era. *Energy & Environmental Science* [Online], 14(2), pp.844–852. Available from: https://doi.org/10.1039/D0EE03581E.

Samantara, A.K. and Ratha, S., 2018. Historical Background and Present Status of the Supercapacitors. *Materials Development for Active/Passive Components of a Supercapacitor* [Online]. pp.9–10. Available from: https://doi.org/10.1007/978-981-10-7263-5_2.

Schwarz, H.-G., 2004. Aluminum Production and Energy. *Encyclopedia of Energy* [Online]. Elsevier, pp.81–95. Available from: https://doi.org/10.1016/B0-12-176480-X/00372-7.

Sea-distances, 2020. *Sea-distances* [Online]. Available from: https://sea-distances.org/ [Accessed 21 June 2021].

Shahan, Z., 2015. *Electric car history (in depth)*. *CleanTechnica* [Online]. Available from: https://cleantechnica.com/2015/04/26/electric-car-history/ [[Accessed 4 January 2019].

Steinhauser, G., 2008. Cleaner production in the Solvay Process: general strategies and recent developments. *Journal of Cleaner Production* [Online], 16(7), pp.833–841. Available from: https://doi.org/10.1016/j.jclepro.2007.04.005.

Stoller, M.D., Stoller, S.A., Quarles, N., Suk, J.W., Murali, S., Zhu, Y., Zhu, X. and Ruoff, R.S., 2011. Using coin cells for ultracapacitor electrode material testing. *Journal of Applied Electrochemistry* [Online], 41(6), pp.681–686. Available from: https://doi.org/10.1007/s10800-011-0280-5.

Susarla, N. and Ahmed, S., 2019. Estimating Cost and Energy Demand in Producing Lithium Hexafluorophosphate for Li-Ion Battery Electrolyte. *Industrial & Engineering Chemistry Research* [Online], 58(9), pp.3754–3766. Available from: https://doi.org/10.1021/acs.iecr.8b03752.

Svens, P., Kjell, M., Tengstedt, C., Flodberg, G. and Lindbergh, G., 2013. Li-Ion Pouch Cells for Vehicle Applications — Studies of Water Transmission and Packing Materials. *Energies* [Online], 6(1), pp.400–410. Available from: https://doi.org/10.3390/en6010400.

Talens Peiró, L., Villalba Méndez, G. and Ayres, R.U., 2013a. Lithium: Sources, Production, Uses, and Recovery Outlook. *JOM* [Online], 65(8), pp.986–996. Available from: https://doi.org/10.1007/s11837-013-0666-4.

Talens Peiró, L., Villalba Méndez, G. and Ayres, R.U., 2013b. Lithium: Sources, Production, Uses, and Recovery Outlook. *JOM* [Online], 65(8), pp.986–996. Available from: https://doi.org/10.1007/s11837-013-0666-4.

The Aluminium Association, 2013. *The Environmental Footprint of Semi-Finished Aluminium Products in North America*.

The Essential Chemical Industry, 2017. *Phosphorus*. *essentialchemicalindustry.org* [Online]. Available from: https://www.essentialchemicalindustry.org/chemicals/phosphorus.html [Accessed 10 December 2020].

Thinkstep, 2020. *Life Cycle assessment LCA software: GaBi software*.

UK Battery Industrialisation Centre (UKBIC), 2021. *Module and Pack assembly line now operational at UKBIC*. *UKBIC* [Online]. Available from: https://www.ukbic.co.uk/module-and-pack-assembly-line-now-operational-at-ukbic/ [Accessed 19 February 2021].

UK Department of Transport, 2020. *CO2 emission performance standards for new passenger cars and light commercial vehicles*. *gov.uk* [Online]. Available from: https://www.gov.uk/government/consultations/regulating-co2-emission-standards-for-new-cars-and-vans-after-transition/co2-emission-performance-standards-for-new-passenger-cars-and-light-commercial-vehicles [Accessed 21 June 2022].

UK Government, 2019. *2018, UK Greenhouse gas emissions, provisional figures*. *National Statistics* [Online]. Available from: https://assets.publishing.service.gov.uk/government/uploads/system/uploads/attachment_data/file/790626/2018-provisional-emissions-statistics-report.pdf [Accessed 30 July 2020].

United Nations (UN), n.d. *Sustainability*. *un.org* [Online]. Available from: https://www.un.org/en/academic-impact/sustainability [Accessed 11 July 2022].

United Nations (UN), 2019. *The Paris Agreement*. *United Nations* [Online]. Available from: https://unfccc.int/process-and-meetings/the-paris-agreement/the-paris-agreement [Accessed 8 December 2019].

United Nations (UN), 2021. *Climate change lead to more extreme weather, but early warnings save lives*. *United Nations Framework Convention on Climate Change* [Online]. Available from: https://unfccc.int/news/climate-change-leads-to-more-extreme-weather-but-early-warnings-save-lives#:~:text=UN Climate Change News%2C 1,World Meteorological Organization (WMO).

United Nations (UN), 2022. *Sustainable Development*. *sdgs.un.org* [Online]. Available from: https://sdgs.un.org/goals [Accessed 28 July 2022].

US Department of Energy, 2000. *Energy and Environmental Profile of the U.S. Chemical Industry*.

US Geological Survey, 2022. *Mineral commodity summaries 2022* [Online]. Available from: https://doi.org/10.3133/mcs2022.

Wang, J., Dong, S., Ding, B., Wang, Y., Hao, X., Dou, H., Xia, Y. and Zhang, X., 2017. Pseudocapacitive materials for electrochemical capacitors: from rational synthesis to capacitance optimization. *National Science Review* [Online], 4(1), pp.71–90. Available from: https://doi.org/10.1093/nsr/nww072.

Weinstein, L. and Dash, R., 2013. Supercapacitor carbons. *Materials Today* [Online], 16(10), pp.356–357. Available from: https://doi.org/10.1016/j.mattod.2013.09.005.

Wu, K., Dou, X., Zhang, X. and Ouyang, C., 2022. The sodium-ion battery: An energy-storage technology for a carbon-neutral world. *Engineering* [Online]. Available from: https://doi.org/10.1016/j.eng.2022.04.011.

Wu, Z., Li, L., Yan, J. and Zhang, X., 2017. Materials Design and System Construction for Conventional and New-Concept Supercapacitors. *Advanced Science* [Online], 4(6), p.1600382. Available from: https://doi.org/10.1002/advs.201600382.

Wu, Z.-S., Feng, X. and Cheng, H.-M., 2014. Recent advances in graphene-based planar micro-supercapacitors for on-chip energy storage. *National Science Review* [Online], 1(2), pp.277–292. Available from: https://doi.org/10.1093/nsr/nwt003.

Xu, C., Dai, Q., Gaines, L., Hu, M., Tukker, A. and Steubing, B., 2020. Future material demand for automotive lithium-based batteries. *Communications Materials* [Online], 1(1), p.99. Available from: https://doi.org/10.1038/s43246-020-00095-x.

Yao, H.-R., Wang, P.-F., Gong, Y., Zhang, J., Yu, X., Gu, L., OuYang, C., Yin, Y.-X., Hu, E., Yang, X.-Q., Stavitski, E., Guo, Y.-G. and Wan, L.-J., 2017. Designing Air-Stable O3-Type Cathode Materials by Combined Structure Modulation for Na-Ion Batteries. *Journal of the American Chemical Society* [Online], 139(25), pp.8440–8443. Available from: https://doi.org/10.1021/jacs.7b05176.

Yoo, S. and Managi, S., 2022. Disclosure or action: Evaluating ESG behavior towards financial performance. *Finance Research Letters* [Online], 44, p.102108. Available from: https://doi.org/10.1016/j.frl.2021.102108.

Young-Saver, D., 2021. Gas or Electric? Thinking algebraically about car costs, emissiona and trade-offs. *New York Times*.

Yuan, C., Deng, Y., Li, T. and Yang, F., 2017a. Manufacturing energy analysis of lithium ion battery pack for electric vehicles. *CIRP Annals - Manufacturing Technology* [Online], 66(1), pp.53–56. Available from: https://doi.org/10.1016/j.cirp.2017.04.109.

Yuan, C., Deng, Y., Li, T. and Yang, F., 2017b. Manufacturing energy analysis of lithium ion battery pack for electric vehicles. *CIRP Annals* [Online], 66(1), pp.53–56. Available from: https://doi.org/10.1016/j.cirp.2017.04.109.

Yue, J.-L., Zhou, Y.-N., Yu, X., Bak, S.-M., Yang, X.-Q. and Fu, Z.-W., 2015. O3-type layered transition metal oxide Na(NiCoFeTi) 1/4 O 2 as a high rate and long cycle life cathode material for sodium ion batteries. *Journal of Materials Chemistry A* [Online], 3(46), pp.23261–23267. Available from: https://doi.org/10.1039/C5TA05769H.

Zackrisson, M., 2017. *Life cycle assessment of long life lithium electrode for electric vehicle batteries – cells for Leaf, Tesla and Volvo bus*.

Zhao, L., Zhang, T., Li, W., Li, T., Zhang, L., Zhang, X. and Wang, Z., 2022. Engineering of sodium-ion batteries: Opportunities and challenges. *Engineering* [Online]. Available from: https://doi.org/10.1016/j.eng.2021.08.032.

Appendix A: List of literature sources for LCA data

Table A.1: Lithium-ion cell processes data sources

Process	Process coverage	Reference
N-Methyl-2-Pyrollodine (NMP) production	Cradle to gate	(Lammens et al., 2011)
Polyvinylidene fluoride (PVDF) production	Gate to gate	(Dunn et al., 2012)
Styrene Butadiene Rubber (SBR) production	Gate to gate	(US Department of Energy, 2000) (Polymer Properties Database, 2015)
Carboxymethyl cellulose (CMC) production	Gate to gate	(Alizadeh Asl, Mousavi and Labbafi, 2017)
Graphite production	Gate to gate	(Dunn *et al.*, 2014) (Augustyn, Simon and Dunn, 2014)
Carbon Black production	Gate to gate	(Dunn et al., 2014)
Li-NMC production	Gate to gate	(Ahmed et al., 2017)
Aluminium foil production	Gate to gate	(European Aluminium Association, 2013)
Copper foil production	Gate to gate	(European Aluminium Association, 2013)
$LiPF_6$ Electrolyte production	Gate to gate	(Dunn et al., 2014)
$LiPF_6$ production	Gate to gate	(Dunn et al., 2014)
PCL_5 production	Gate to gate	(Dunn et al., 2014)
Ethylene Carbonate Production	Gate to gate	(Dunn et al., 2014)
Polymer separator production	Gate to gate	(Yuan et al., 2017b)
Cell casing production	Gate to gate	(Svens et al., 2013)
Li-ion anode production	Gate to gate	(Yuan et al., 2017b)
Li-ion cathode production	Gate to gate	(Yuan et al., 2017b)
Li-ion cell assembly	Gate to gate	(Yuan et al., 2017b)

Table A.2: Sodium-ion cell processes data sources

Process	Process coverage	Reference
Polyacrylic Acid (PAA) production	Gate to gate	(Dunn et al., 2014)
Propylene carbonate production	Gate to gate	(Ott, Borukhova and Hessel, 2016)
O3 type cathode material production	Gate to gate	(Yue et al., 2015)
Na-ion anode production	Gate to gate	(Yuan et al., 2017b)
Na-ion cathode production	Gate to gate	(Yuan et al., 2017b)
$NaPF_6$ production	Gate to gate	(Dunn et al., 2014)
$NaPF_6$ electrolyte production	Gate to gate	(Dunn et al., 2014)
Na-ion cell assembly	Gate to gate	(Yuan et al., 2017b)

Table A.3: Raw material production processes data sources

Process	Process coverage	Reference
Aluminium processing	Gate to gate	(The Aluminium Association, 2013)
Bauxite mining	Cradle to gate	(The Aluminium Association, 2013)
Mining of ores	Cradle to gate	(Dai, Kelly and Elgowainy, 2018)
Copper production	Cradle to gate	(Thinkstep, 2020)
Steel production	Cradle to gate	(GreenDelta, 2019)
Cobalt sulphate production	Gate to gate	(Dai, Kelly and Elgowainy, 2018)
Manganese sulphate production	Gate to gate	(Dai, Kelly and Elgowainy, 2018) (Farjana et al., 2019) (Thinkstep, 2020)
Nickel sulphate production	Gate to gate	(Dai, Kelly and Elgowainy, 2018) (Khoo et al., 2017) (Thinkstep, 2020)
Ammonium bicarbonate production	Gate to gate	(Dai, Kelly and Elgowainy, 2018)
Lithium carbonate production	Gate to gate	(Talens Peiró, Villalba Méndez and Ayres, 2013b)
Sodium carbonate production	Gate to gate	(Steinhauser, 2008)
Sodium chloride brine production	Cradle to gate	(Boustead, 2005)
Lithium fluoride production	Cradle to gate	(Susarla and Ahmed, 2019)
Phosphorus production	Cradle to gate	(The Essential Chemical Industry, 2017) (Atkins et al., 2010)
Nickel metal production	Cradle to gate	(Khoo et al., 2017)
Nickel oxide production	Gate to gate	(Dai, Kelly and Elgowainy, 2018)
Manganese (IV) dioxide production	Gate to gate	(Dai, Kelly and Elgowainy, 2018)
Iron (III) oxide	Gate to gate	(Norgate and Haque, 2010)

Table A.4: Battery pack component processes data sources

Process	Process coverage	Reference
Battery cooling system	Gate to gate	(Hawkins et al., 2013)
Battery management system (BMS)	Gate to gate	(Majeau-Bettez, Hawkins and Strømman, 2011)
Battery module assembly	Gate to gate	(Dai, Kelly and Elgowainy, 2018)
Battery packaging production	Gate to gate	(Zackrisson, 2017)
Electric circuits production	Cradle to gate	(Ozkan, Elginoz and Germirli Babuna, 2018)
Battery pack assembly	Gate to gate	(L.A.W. Ellingsen et al., 2014)